Electronic Thesis and Dissertation Repository

5-30-2018 10:00 AM

Modelling the thermal transport of a thawing permafrost plateau

Joelle E. Langford
The University of Western Ontario

Supervisor
Schincariol, Robert A.
The University of Western Ontario

Graduate Program in Geology

A thesis submitted in partial fulfillment of the requirements for the degree in Master of Science

© Joelle E. Langford 2018

MODELLING THE THERMAL TRANSPORT OF A THAWING PERMAFROST PLATEAU

Abstract

Permafrost covers approximately 24% of the Northern Hemisphere and is in a state of decay which has large implications. To characterize the processes involved in the transitional period of permafrost decay, a three-dimensional finite element numerical model is developed. The model is based on the Scotty Creek Research Basin in the Northwest Territories, Canada (61°18'N, 121°18'W). FEFLOW groundwater flow and heat transport modelling software is used in conjunction with the piFreeze plug-in, to account for phase changes between ice and water. As transiently simulating actual permafrost evolution would require 100's of years of climate variations over an evolving landscape, whose geomorphic features are unknown, a steady-state developed permafrost bulb is used as an initial condition for a transient model run. The steady-state developed permafrost was generated by the application of freezing surface temperatures. The transient approach applies daily climatic data over the current plateau; the Simultaneous Heat and Water model (SHAW) is used to calculate ground temperatures and infiltration rates. It was found that a transient model with "unsteady-state" applied temperatures that include an unfrozen layer between the supra-permafrost table and ground surface yields better results than with steady-state permafrost initial conditions. Modelling permafrost will allow for the testing of remedial measures, such as mulching and borehole heat exchangers, to stabilize permafrost in high value infrastructure environments.

Keywords: permafrost aggradation, permafrost degradation, thermal transport, wetland hydrogeology.

Acknowledgments

I am so grateful for the continuous support and knowledge that Dr. Rob Schincariol has provided me with. Thank-you Rob for taking me on as a student who knew nothing about hydrogeological modelling and providing me with such an excellent opportunity to learn and grow. Your ability to constantly tie my thesis work to industry examples has helped to prepare me for a career in hydrogeology. Thank-you for always making time for a meeting when I needed one, I always felt more confident in my work after leaving a meeting with you. I am grateful that I had a supervisor that was so flexible and understood what I wanted to take away from a master's degree.

I would also like to thank Dr. Bill Quinton and the entire team at Scotty Creek. Bill thank-you for bringing me up to experience Scotty Creek in all its glory. I would also like to thank Bill for inviting me to take part in 'Scotty Days' at Wilfred Laurier University where I got to discuss my project with a knowledgeable group of cold regions research scientists. Not only did attending these meetings helped to deepen my understanding of cold region hydrology, modelling and chemistry but it also provided a much-needed sense of community. A big thank-you goes out to the Scotty Creek Research team, you have all amazed me with your Scotty Creek knowledge and passion.

A very special thanks to Dr. Ranjeet Nagare for your remarkable modelling guidance. Thank-you for always picking up the phone, no matter the time of day and providing me with indispensable advice. Not only did you provide me with modelling knowledge but also some great career advice and I am so grateful. Thank-you for guiding me through the many modelling challenges I faced in this thesis. I hope you continue to work with research students and think you will make an excellent supervisor or professor if that is the path you choose to take.

Aaron Mohammed, thank-you so much for your SHAW modelling knowledge and taking the time while you are working to complete your Ph.D.to develop SHAW models for my project.

Mom and Dad, thank-you for your never-ending support throughout my degree. Thank-you for not only putting a roof over my head and food on my plate but also for always believing that I am capable of achieving whatever I put my focus on. Thank-you to my brother and sister, Craig and Coryn, for always being there for me when I needed

Table of Contents

List of Tables

List of Figures

Chapter 1

1   Introduction

Approximately 24% of the land mass in the Northern hemisphere is underlain by permafrost (Zhang et al. 1999; Zhang et al. 2003). Permafrost is thermally defined as ground that maintains a temperature below 0˚C for at least two consecutive years (Dobinski 2011). Under modern day climate, permafrost in many regions is degrading, which has caused infrastructure failures and ecosystem shifts. The most rapid permafrost decay is occurring along the southern fringe of permafrost covered land, in what is defined as the discontinuous-sporadic permafrost zone. The discontinuous-sporadic permafrost zone of North America stretches across the middle of Canada (Heginbottom et al. 1995) (Figure 1-1). Over the last century, close to 50% of the permafrost located at study sites in the discontinuous permafrost region has decayed (Beilman and Robinson 2003). A warming of approximately 0.3ºC per decade of the shallow permafrost in the northern and central Mackenzie region of the Northwest Territories (NWT) has taken place since the 1980s which is tied to an increase in the mean annual air temperature (Beilman & Robinson 2003; Smith et al. 2005). Recent studies show that the rate of permafrost decay has increased in the approximate last twenty years (Quinton et al. 2011) (Figure 1-2). A study by Lawrence and Slater (2005) has predicted that by the end of the 21st century there will be a 90% loss of shallow permafrost within the Northern hemisphere.
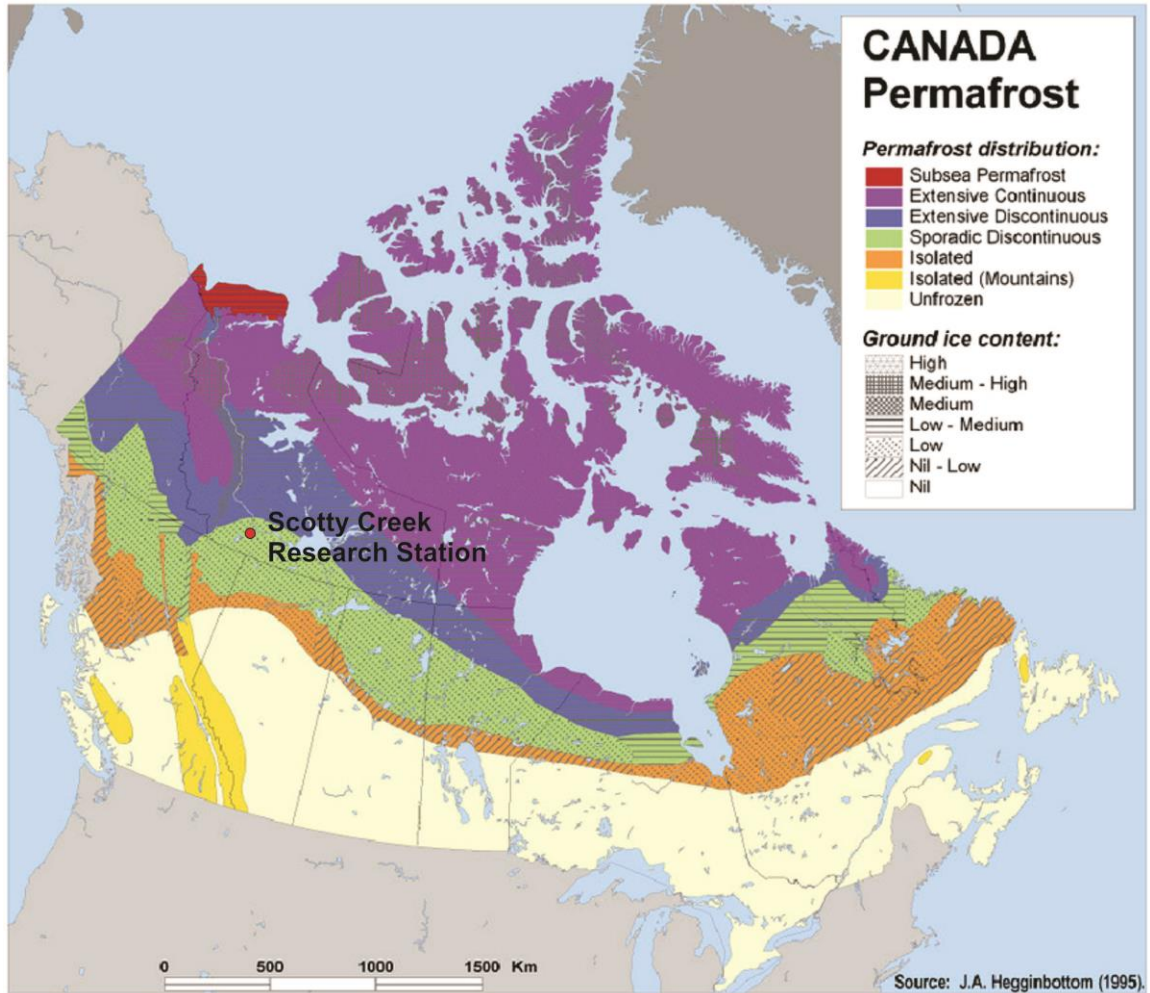
Figure 1-1: Permafrost distribution zonation in Canada; Location of the Scotty Creek Research Basin (Heginbottom et al. 1995).

Permafrost decay has many implications including change in hydrological regime such as increase in basin run off, which has already been observed in some northern basins (Connon et al. 2014), release of stored carbon (Donnell et al. 2012), subsidence of the forested permafrost plateaus and complete alteration of the boreal ecosystem (Jorgenson et al. 2001; Jorgenson and Osterkamp 2005). Landscapes are transforming from discontinuous-sporadic permafrost to expansive wetlands (Figure 1-2). The southern fringe of permafrost is composed of discontinuous (50-90%) to sporadic (10-50%) permafrost (Zhang et al. 2003). This region of permafrost is at the highest risk of

thaw because the thin permafrost bodies are isolated and are vulnerable to both vertical and horizontal thermal fluxes (McClymont et al. 2013). Studies have shown that the stability of a permafrost plateau is related to the size and shape of the permafrost plateau (Beilman and Robinson 2003). Once the permafrost reaches a tipping point or a certain geometry, thaw occurs at more rapid rates until it disappears entirely. The permafrost of the discontinuous region is relatively warm and thin in relation to continuous permafrost, with temperatures often greater than -2ºC and thicknesses nearing 10 m (Burgess and Smith 2001). When permafrost reaches a temperature close to 0 ºC, thawing pauses and the permafrost stabilizes for a period of time due to the latent heat required for phase change (Smith et al. 2010). Due to this phenomenon, the southern fringe of permafrost in the northern hemisphere may be preserved for a slightly longer period than if thaw continued at the same rate.
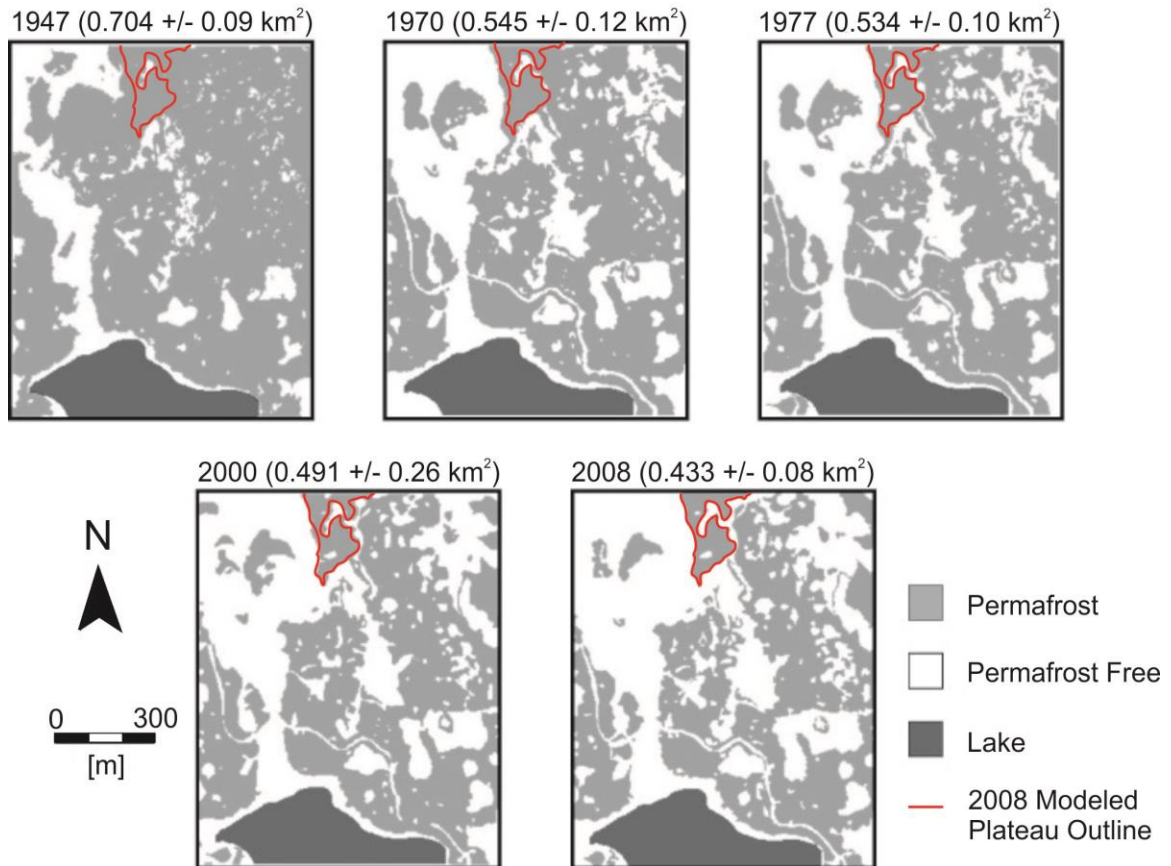
Figure 1-2: Historical 1 km² subsets of a plateau-wetland complex in Scotty Creek, NTW. The plateau being modelled is outlined in red. This figure was sourced from Quinton et al. (2011).

Thawing ice-rich permafrost plateaus are found in the lower Liard River valley of NWT, Canada. This is part of the discontinuous permafrost region, currently covered in approximately 40% permafrost (Quinton et al. 2011). This region is overlain by an extensive layer of peat and is part of Canada's boreal forest (Aylsworth and Kettles 2000). These peatlands are made up of slightly elevated permafrost plateaus, which are elevated approximately 1 m above the surrounding bogs and fens (Quinton et al. 2010) (Figure 1-3). The permafrost below the plateaus is being sustained by the vegetation and insulative peat overlying it, this is referred to as an ecosystem-protected permafrost region (Jorgenson et al. 2010).

Modelling has been a useful tool in characterizing the hydrology and climate of these complex systems. There are hemisphere-scale predictive models generated to predict the continued rate of permafrost degradation in the northern hemisphere (Doven et al. 2013). There are also smaller scale models of one- and two-dimensions (eg. Gao et al. 2016; Johansson et al. 2015; Williams et al. 2015; Nagare 2012) and three-dimensions (Kurylyk et al. 2016) used to study freeze-thaw processes and permafrost thaw on a local scale. A three-dimensional model of a permafrost plateau that includes the supra-permafrost (variably saturated) zone and surrounding wetlands has not yet been developed. Further advancement of permafrost models will lead towards development of improved permafrost protection methods and permafrost decay predictions.

1.1   Study objectives

The purpose of this study is to develop a model, and characterize the thermal transport processes of a typical degrading permafrost plateau found in the discontinuous permafrost fringe of Canada's boreal forest. The specific region being modelled is in the Scotty Creek basin (61°18'N, 121°18'W) (Figure 1-1), where data collection began in 1994, starting with snow measurements. Scotty Creek Research Station has developed into an all-season research camp at which scientific interest includes hydrology, ecology, forest fires and their relation to permafrost. Though the model includes multiple plateaus, the plateau of focus is approximately 600m long and 160m wide with an area of just over 0.06 km^2 (Figure 1-2). The plateau elevation is approximately 1 meter above the surrounding wetland (Figure 1-3), with a fen to the west and connected bogs to the east. Observations of this plateau over the last decade have documented rapid permafrost thaw, particularly on the thin southern portion of the plateau.
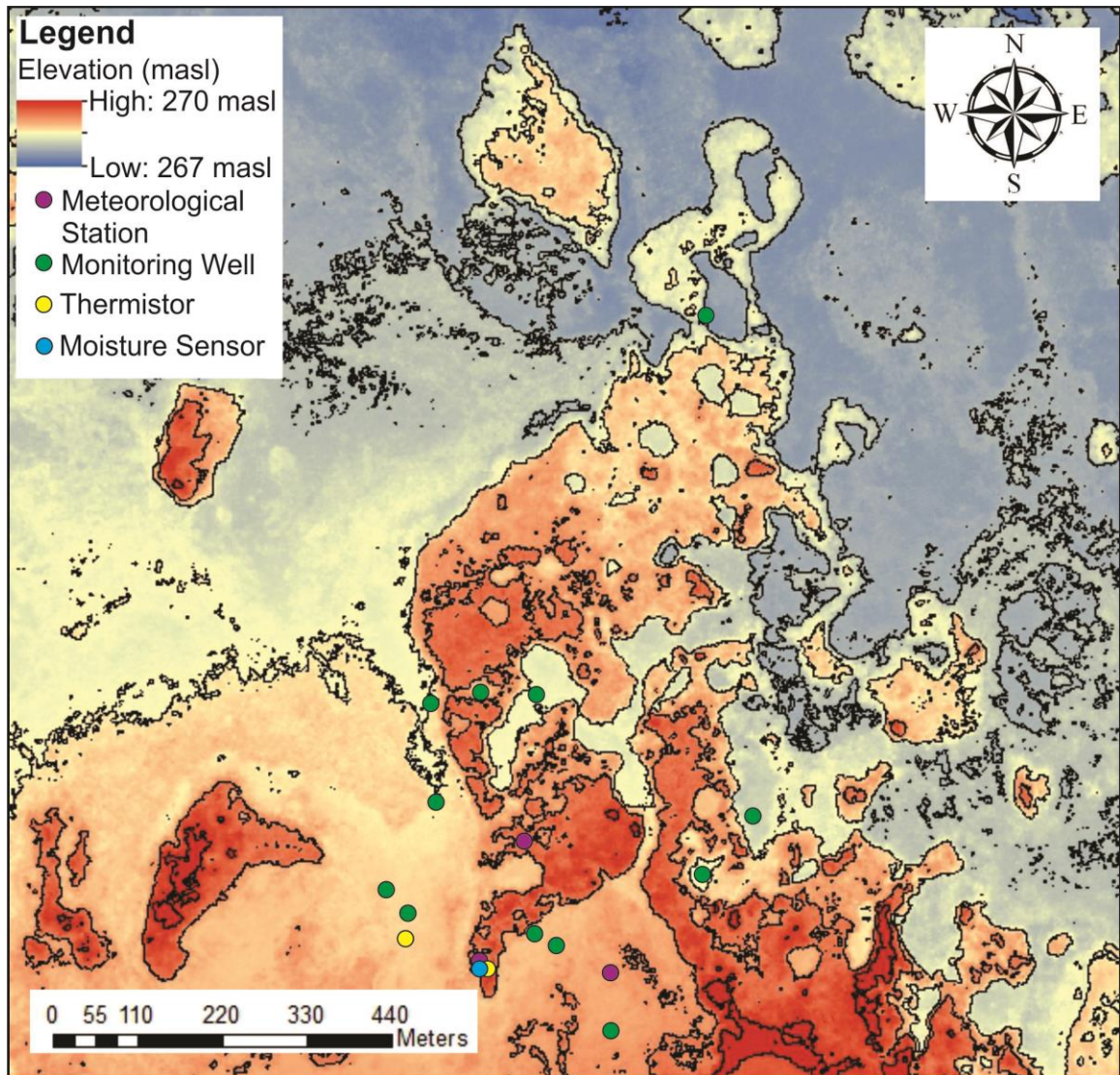
Figure 1-3: Aerial map of the plateau-wetland complex, including locations of meteorological stations, monitoring wells, thermistors and moisture sensors in the region.

FEFLOW (Finite Element subsurface FLOW and transport system) is the modelling software being used to build the three-dimensional coupled hydrogeological thermal transport model of the degrading permafrost plateau. FEFLOW is a finite-element hydrogeological modelling program used to model subsurface flow, mass transport and thermal transport. A FEFLOW plug-in called piFreeze which allows for modelling of freeze-thaw processes has recently been developed, making this project

possible. PiFreeze includes the latent heat effects of phase change, and the alteration of hydraulic conductivity and porosity due to ice formation in thermal transport and groundwater flow calculations. Because FEFLOW is a finite element modelling program, the meshing is flexible, allowing for accurate representation of topography. This is important because the water table is close to the surface, usually within 20 cm and variations in micro-topography cause variations in thermal transport across the plateau.

FEFLOW is a subsurface modelling program and another program, the Simultaneous Heat and Water modelling program (SHAW), is used to calculate the ground surface boundary inputs. SHAW is used to calculate ground temperatures and infiltration rates with climate input developed from trends applied to historical climate data before 1898, Fort Simpson climate data for 1898-2005 and data recorded in Scotty Creek for 2005-2015. These SHAW average monthly ground temperatures and daily infiltration rates are used as an upper bound of the FEFLOW model.

The goal of this project is to further advance the modelling of cold regions, including the development of proper methods to represent the thawing of permafrost and the annual freeze-thaw processes that occur in the active layer. The active layer is the ground that overlies permafrost and annually freezes and thaws which has not yet been included in a three-dimensional permafrost model. The data collected in the Scotty Creek research basin over the last 20 years is used to build and calibrate the model and previous models of the area and similar regions will be used as rough guidelines. Through developing a three-dimensional hydrogeological permafrost model, a stronger understanding of the thermal transport processes taking place in a plateau-wetland complex will be developed. This will allow for a more accurate representation of permafrost dynamics in future studies. Properly representing permafrost decay in a

three-dimensional model will demonstrate its sensitivities to multiple variables and provide a method to test permafrost protection and remediation techniques.

1.2   Thesis organization

This thesis is organized into five chapters. The first chapter serves as an introduction and literature review. The second chapter outlines the methods of model development used in this thesis including data collection, SHAW modelling and FEFLOW modelling as well as describes the various equations used in these two modelling programs. The third chapter reveals and discusses the results and performance of the models. The fourth chapter provides a further discussion of the model results. The final chapter concludes the thesis and provides suggestions for further work.

1.3   Declaration of Work Undertaken by Others

The SHAW calibration and model development was completed by Aaron Mohammed. To develop this model ground surface inputs were required and there were provided by Aaron. Aaron has worked with SHAW on previous projects and has a strong understanding of the physical processes involved in creating a one-dimensional SHAW model. I collected climate data and provided input files for Aaron to run in SHAW, as well as organized ground temperature and moisture data for the models to be calibrated against. Aaron then developed a wetland model and plateau model, both calibrated to measurements taken in Scotty Creek. Aaron ran the models through 140 year times series, each, and provided me with the output water balances and ground temperatures.

A large amount of data provided by Dr. Bill Quinton and the Scotty Creek Research team made this project possible. To develop the wetland properties of the

model I used results from groundwater pump tests completed by Brenden Christensen and tracer tests by Dr. Masaki Hayashi. Many years of ground temperatures in the fen and the plateau were provided by Dr. Quinton and were of great use to compare model results. Another excellent resource provided by Dr. Quinton is well Scotty Creek water level data and plateau moisture content data. The LiDAR data provided by Dr. Quinton was used to develop various maps and the surface topography of the model. This data has been collected over years by a large team of research scientists at Scotty Creek and without their hard work this project would not have been possible.

Chapter 2

2 Background information and literature review

2.1 Permafrost

Permafrost developed under the cold climate regimes of recent ice ages and became unstable under a subsequent warming climate. Permafrost is being warmed by multiple processes including thermal transport through the overlying supra-permafrost layer, which is dominated by conduction, lateral advective and conductive heat transfer via groundwater flow, and conductive heat transport from the underlying geothermal flux (Jorgenson et al. 2010). The active layer has been defined as ground overlying permafrost that freezes and thaws annually (Bonnaventure and Lamoureux 2013). The active layer acts as a thermal buffer between the atmosphere and permafrost (Kane et al. 2001) and therefore the active layer thermal properties are critical to the thermal state of underlying permafrost. The energy balance, which is governed by the contributions of latent heat, sensible heat, radiation and turbulent flux on the ground surface controls the ground surface temperature (Hayashi 2013). The ground surface temperature develops the thermal gradient between the ground surface and the permafrost table, which is below 0 °C. Vegetation acts as a thermal buffer between the permafrost and climate, but permafrost is in direct contact with groundwater and surface water which flow laterally along permafrost plateaus (Jorgenson et al. 2010).

Climate change is a large contributor to the recent permafrost degradation in Northwestern Canada. Trends are demonstrating increased mean annual air temperatures with longer summers and short winters in the Northwest Territories (NWT) (MSC 2017). Temperature is not the only climatic factor which determines the condition of the permafrost; throughout the winter, snow pack acts as an insulator of the ground,

10

preventing the ground from being directly exposed to the cold mid-winter temperatures (Hinkel and Hurd 2006; Osterkamp 2007). A year with a greater amount of snowfall will lead to decreased ground cooling. Increased precipitation before the winter will cause increased levels of saturation and therefore greater amounts of latent heat released during phase change in winter (Iijima et al. 2010).

Micro-topography of the permafrost table plays a critical role in the degradation of a permafrost plateau (Hayashi 2013; Woo 1986; Wright et al. 2009). The micro-topography of the permafrost table determines the regions that are most highly saturated because lateral flow along the permafrost table gradient allows water to pool in micro-depressions. This produces regions of increased moisture content and therefore dissimilar thermal conditions in depressions and ridges (Wright et al. 2009; Nagare et al. 2012; Hayashi 2013). The moisture content and distribution in peat has a large effect on the materials thermal properties and thus freeze-thaw characteristics. Saturated peat has a higher thermal conductivity than dry peat; therefore, the rate of thaw is enhanced in the saturated micro-depressions on the permafrost table, leading to increased thaw depths (Wright et al. 2009). This is a positive feedback system that relatively quickly leads to the expansion of the depression, until the permafrost has been entirely degraded (Wright et al. 2009; Jorgenson et al. 2010). A positive feedback cycle is also induced along the edges of thawing permafrost plateaus. As the permafrost decays and the ground subsides and becomes saturated, the trees become waterlogged and die, no longer providing shade for the plateau (Jorgenson and Osterkamp 2005; McClymont et al. 2013). The death of vegetation and decreased shading are referred to as edge effects.

In the NWT, summers are becoming longer and winters shorter. The climate largely determines the moisture content of the ground and thus the thermal

characteristics. The current climate cycle is causing the thaw depth of the supra-permafrost layer to increase, resulting in decay of the permafrost (Walvoord and Kurylyk 2016). As the thaw depth deepens, the annual freeze may no longer reach the permafrost table open during the winter, leaving an open channel of unfrozen ground called a talik (Figure 1-4). Taliks provide a route for year-round groundwater flow and increased thermal transport, leading to further deepening of the permafrost table (Zhang et al. 2008; Connon et al. 2018). Field studies have observed an increase in size and number of taliks (Zhang et al. 2008; Connon et al. 2018).

Permafrost degradation is occurring at the most rapid rate in the discontinuous-sporadic permafrost region of Northwestern Canada. This portion of the world is being exposed to the most rapidly warming climate. The mechanisms of positive feedback cycles in micro-depressions, edge effects, lateral thermal transport by groundwater as well as year-round thermal transport in taliks, are all contributing factors that are leading to the complete alteration of discontinuous-sporadic permafrost to wetlands. It is important to develop a strong understanding of these processes, including how they develop and what their long-term effects are.

2.2   Hydrogeology in the Scotty Creek plateau-wetland complex

The clay-silt material underlying the thick (approximately 3 m) layer of organic peat has very low permeability, providing a no-flow base condition required for a wetland to develop. Permafrost plateaus are isolated islands amongst wetland features such as fens and bogs. Permafrost plateaus have been described as runoff generators (Quinton and Hayashi 2005) because they are elevated (approximately 1 m) and have a gradient for water from precipitation, snow melt or ground ice thaw to flow down along the supra-permafrost table and feed into surrounding wetlands (Figures 1-3 and 1-4). The ice-rich permafrost in the region is relatively impermeable because ice fills the pores of the peat.

The impermeability of the permafrost causes plateaus to become runoff generators because infiltrating water cannot infiltrate to deep groundwater. The slope of the supra-permafrost table, which is the upper surface of the permafrost, determines the direction of subsurface runoff. The supra-permafrost gradient guides water to lower-lying permafrost locals and surrounding permafrost free regions. Because the peat becomes less hydraulically conductive with depth (Quinton et al. 2009; Nagare et al. 2013) as the frost table deepens during spring that, the supra-permafrost table flow slows (Figure 1-3).

There is localized flow in the region, most of which occurs in fens. Fens are the dominant flow pathways from wetlands to basin outlets. This flow is very slow due to the low gradient in the region; flow is highest during the spring freshet. Connected bogs feed into each other via a fill and spill method, in which a higher elevation bog fills and spills over into a lower elevation bog. Isolated bogs are purely fed by precipitation and drained by evapotranspiration. Studies in the region have found that some bogs are connected through groundwater routes in addition to the fill and spill routes. As permafrost plateaus decay and become wetland, connections between bogs and fens become larger and more continuous.
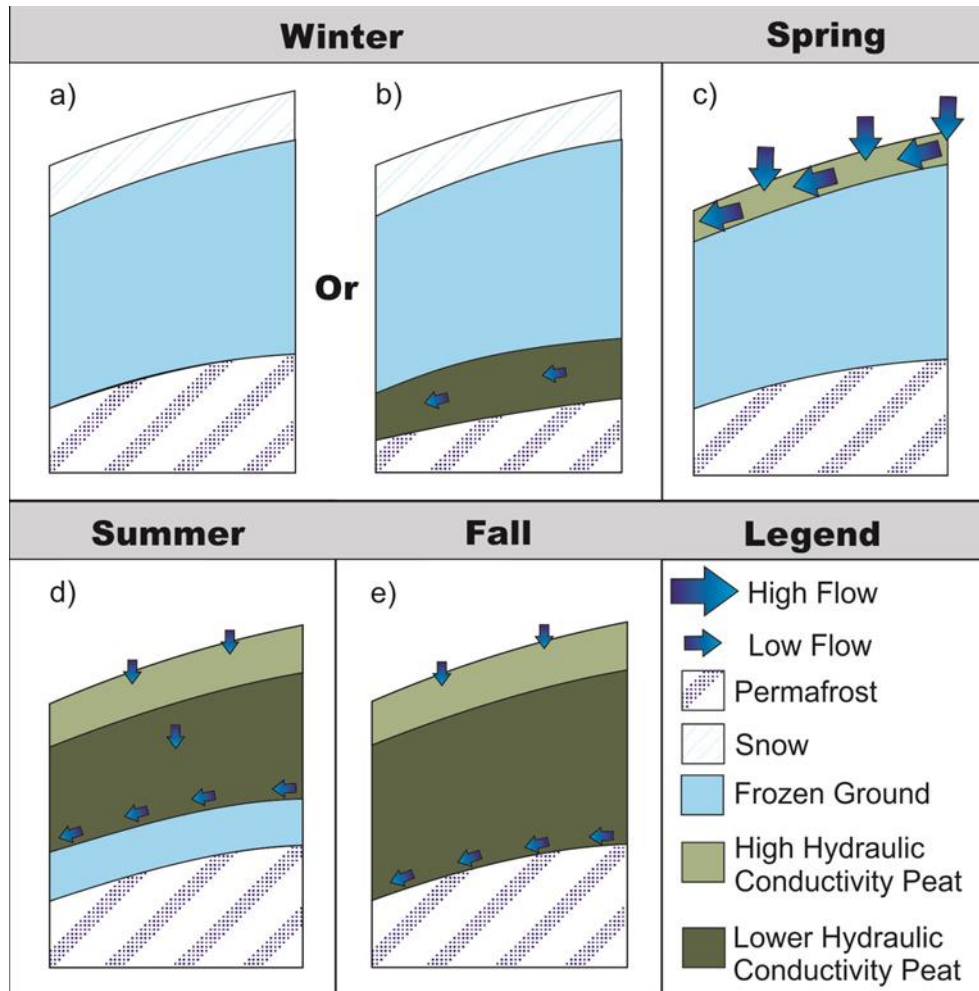
Figure 2-1: Diagrams of the subsurface flow on a permafrost plateau during (a) winter when the freezing front extends to the permafrost table; (b) winter when the frost table does not extend deep enough to meet the permafrost and a talik exists; (c) spring when the ground starts to thaw and water can infiltrate and flow along the supra-permafrost table; (d) Summer when the thaw front has extended deeper into the plateau and water can infiltrate deeper into the relatively less porous peat; and (e) fall when the entire active layer has thawed.

2.3 Cold regions subsurface thermal transport numerical modelling

Cold regions are particularly difficult portions of the world to accurately represent in a numerical model due to the complex physics of annual freeze-thaw. In a permafrost model that includes the unsaturated zone, there is ground that is continually frozen, never frozen and annually frozen, and all contribute to the hydrology and thermal

transport in the model in different ways. Both finite element and finite difference modelling programs have been used to represent this system. Finite difference models locate nodes based on rectangular grids and finite element models locate nodes based on coordinates in a mesh, allowing for more flexible meshes (Anderson et al. 2015). Early finite element and finite difference models of cold region processes were one-dimensional columns, used to study the vertical heat transport processes occurring through ground freeze-thaw cycles (eg. Riseborough et al. 2008; Zhang et al. 2003; 2008). Though one-dimensional models are excellent tools for narrowing down the processes occurring vertically, they are simplifications of large complex three-dimensional system. Later, authors such as (Frampton et al. 2013; Ge et al. 2011) extended cold region modelling to two-dimensions using the finite element saturated and unsaturated subsurface modelling program SUTRA. A three-dimensional model more accurately represents groundwater flow, meaning better representation of thermal transport, as thermal and groundwater flow are closely tied. Modelling in three-dimensions inherently involves a larger computational effort and more complex calculations.

One of the earliest three-dimensional thermal transport and groundwater flow modelling studies was done by Noetzli et al. (2007). Their study, using the finite element program FRACTURE, focused on the effects of climate change in alpine topography using basic high gradient alpine-type geometries. The first three-dimensional model of a permafrost bulb in a flat wetland environment, similar to this study, was completed by Kurylyk et al. (2016) using SUTRA-ICE. This coupled three-dimensional model simulated a half of a permafrost plateau, with the assumption the other half of the plateau mirrors its behavior. This model did not include the unsaturated zone (accounted for by using a coupled one-dimensional surface model NEST) or topography.

An important use of modelling in Northern Canada is for characterization of flow systems to predict basin discharge. Prediction of basin discharge based on climate is useful because these regions have low population density and stream gauge maintenance is challenging in remote areas. Hydrological Response Unit (HRU) modelling simplifies large basins into characteristically similar hydrological units (such as plateaus or bogs) (Pomeroy et al. 2007). This is an approach used to generate basin scale hydrologic models. An important modelling program developed for this purpose is the Cold Regions Hydrological Model (CRHM). The CRHM platform was developed based on field studies in Canadian cold regions and includes the algorithms that represent the various hydrological processes that are challenging to measure such as snow redistribution and interception, groundwater flow and infiltration (Pomeroy et al. 2007).

There are multiple transient modelling programs that are used to output ground surface boundary conditions of subsurface models based on climatic data and ground surface properties. The Northern Ecosystem Soil Temperature (NEST) and the Simultaneous Heat and Water Transfer (SHAW) programs are commonly used to generate ground surface properties in cold region modelling. It is common practice to use a one-dimensional model such as NEST or SHAW to determine a three-dimensional model transient surface boundary condition because a three-dimensional model that includes surficial and subsurface processes requires a large amount of computational power.

2.3   Scotty Creek Research Station

2.3.1   Study region

The permafrost plateau being modelled is in the Scotty Creek research basin, which is approximately 50 km south of Fort Simpson (61°18'N, 121°18'W) in the Northwest Territories of Canada. This basin falls within the greater Liard Valley which is part of the sporadic-discontinuous permafrost region of Canada. The Scotty Creek basin itself is covered by approximately 43% shallow, ice-rich permafrost peat plateaus, surrounded by fens (approximately 21%), connected and isolated bogs (approximately 26.7%) and lakes (approximately 9.3%) (Quinton et al. 2010). Geophysical studies in the region by McClymont et al. (2013) found the thickness of the permafrost plateaus in the region to range from 5-13m, meaning it protrudes into the glacial clay-rich till underlying the peat.
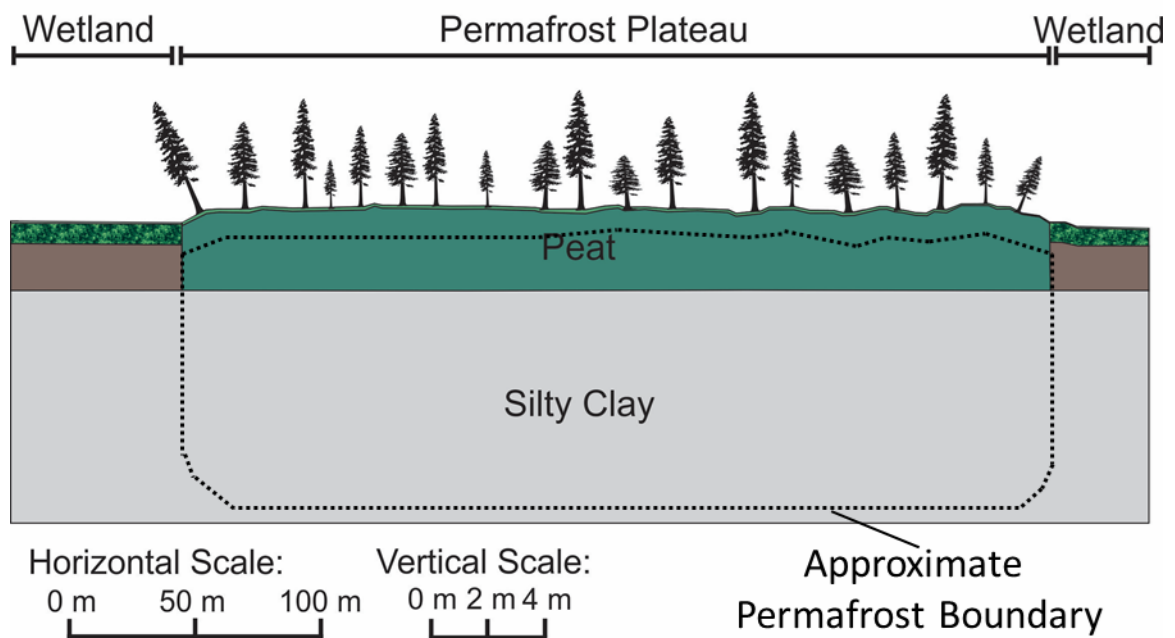
Figure 2-2: Cross section of a characteristic plateau-wetland complex in Scotty Creek, NWT.

Stratigraphically, Scotty Creek is underlain by glacially deposited silt and clay. This layer has a low hydraulic conductivity. This thick layer of silt and clay is overlain by a thin silt-sand layer (Aylsworth and Kettles 2000). Above these glacial deposits is an extensive layer of organic peat which ranges in thickness from about 2 to 4 m (Aylsworth and Kettles 2000). The state of decomposition of the peat affects the hydraulic properties (Grover and Baldock 2013). The peat may be subcategorized into two layers with an abrupt transitional layer: an upper organic layer (0-0.2 m) that has a lower bulk density and higher porosity and a lower layer (0.2-3 m) which has been further decomposed, leading to a higher bulk density and lower porosity (Quinton at al. 2008). Studies by Quinton et al. (2008) show that the upper layer is more hydraulically conductive than the lower more decomposed layer, with an abrupt transition zone.

The thin warm permafrost region is being sustained under rising mean annual air temperatures because peat acts as thermal insulation between the atmosphere and frozen ground. The vegetation of the peat plateaus in the region is composed of black spruce trees, as well as small shrubs, lichens and mosses, all of which protect the permafrost from climatic factors (Quinton et al. 2010). A vegetative mat composed of sedges floats approximately 5-20 cm below the water surface of the fens (Quinton et al. 2003) in the region, moving up and down with the water level (Garon-Labrecque et al. 2015).

The climate pattern of this region is dry continental, meaning it receives long cold winters and short hot and dry summers (MSC 2017). The average evapotranspiration rate in the region has been estimated by Hayashi et al. (2004) and Quinton and Hayashi (2005) to be approximately 270 mm a year. The average annual rainfall in Scotty Creek is 369 mm, of which just under half falls as snow (MSC 2017). By November, the precipitation in the area is snow. Snow pack peaks in March then rapidly ablates and

melts creating the spring freshet. Basin drainage is transported through connected fens and bogs, rivers and connected lakes. Connected bogs transport water via a 'fill and spill' mechanism (during times of high water levels the topographically higher plateau spills some of its water into the next connected bog). Plateaus act as runoff generators in Scotty Creek and in similar basins in the discontinuous permafrost fringe (Quinton et al. 2010).

2.3.2 Data Collection

The data used in this project has been collected at Scotty Creek since 1994, beginning on the southern tip of this study's plateau. The collection of this data was performed by Dr. William Quinton and his research team at Wilfred Laurier University and in conjunction with the Cold Regions Research Network. Since this research has been established, vegetation, basin drainage, climate, permafrost and forest fires have been monitored by an entire team of research scientists.

Various instruments have been installed throughout Scotty Creek in various ground cover types. There has been a network of water level recorders (Solinst Levelogger Gold, Hobo U20L-04) installed in various plateaus, fens and bogs (Figure 1-2). The annual freeze thaw of the peat presents a challenge in properly installing wells and water level recorders because of processes such as mire breathing in which the surface elevation of a bog moves up and down daily due to changes in water storage. To overcome this, black iron pipe wells were pounded into the sturdier underlying silty clay and the water level recorders were placed in them.

Permafrost depths and frost depths have been physically monitored along multiple transects with a 1.3 m frost probe. There were three meteorological stations installed on and around this studies plateau. Two meteorological stations were installed

in 2004, one on the southern decaying tip of the plateau (plateau tower) and one in the adjacent south-east bog (bog tower) (Figure 1-3). Another meteorological station was installed in 2009 in a more tree dense location on the plateau (dense tower). These meteorological stations have recorded half-hourly air temperature and relative humidity (HMP45C, Temperature and Relative Humidity Probe, Vaisala Inc, Helsinki, Finland), as well as incoming and outgoing radiation (CNR1, Net Radiometer, Campbell Scientific, Logan, UT, USA) and wind speed (031A, Met One Wind Speed Sensor, Campbell Scientific, Logan, UT). A precipitation gauge (Geonor T-200B) was installed south of the plateau along the edge of a lake with no overhead canopy in August 2008. This gauge recorded the total hourly precipitation. A stream gauge was installed to monitor the Scotty Creek Basin discharge in 1996 and data has been logged here since 1999. The data at each of these stations has been carefully downloaded by a large team of research scientists in the cold regions research network.

Chapter 3

3 Methods

3.1 Numerical modelling

The numerical models used to represent the plateau-wetland complex in Scotty Creek are the Simultaneous Heat and Water flow model (SHAW) and FEFLOW. SHAW was chosen as the ground surface modeling program for this thesis because of its robust physical basis. FEFLOW was selected as the three-dimensional modeling program because of its flexible meshing capabilities and freeze-thaw plug-in called piFreeze. SHAW modeling outputs provide FEFLOW modeling inputs (Figure 3-1). This section describes the basic equations used to describe the surficial (SHAW) and sub-surficial (FEFLOW) water flow and thermal transport processes.
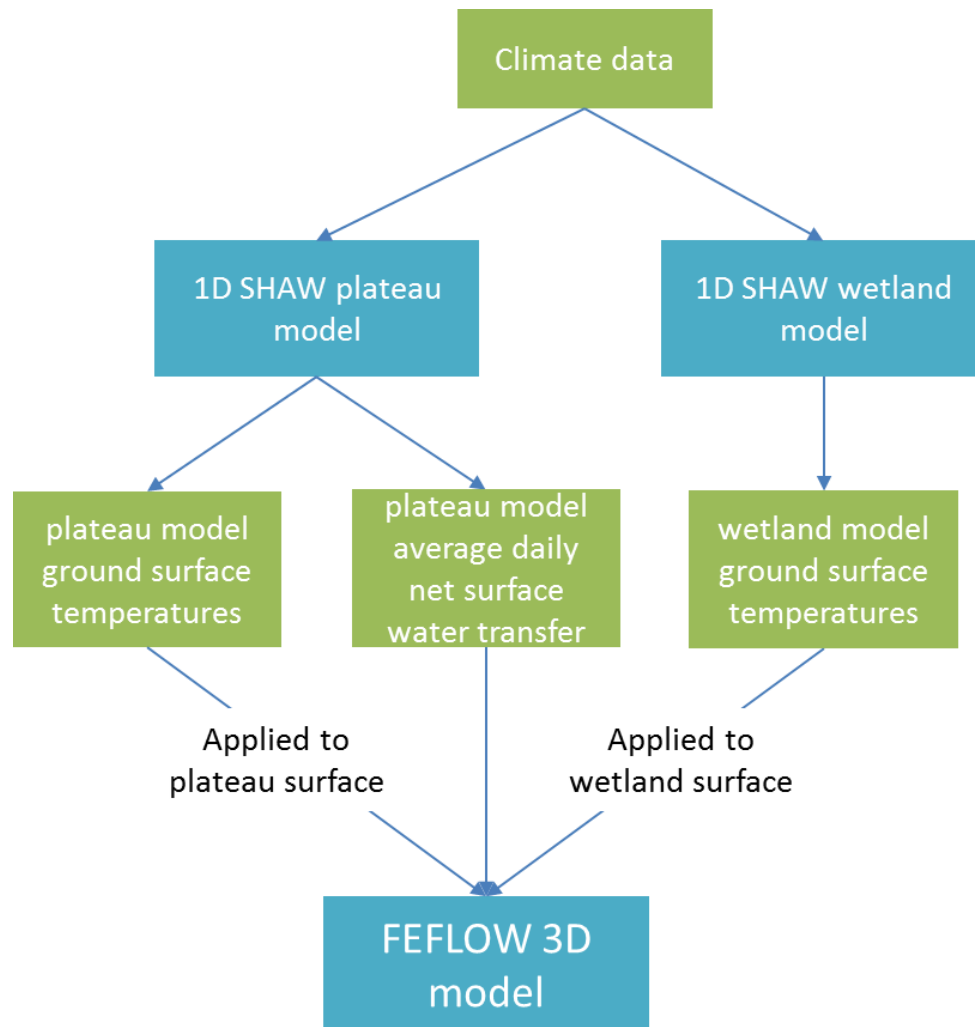
Figure 3-1: A flow chart demonstrating the data flow from initial climate data to the final FEFLOW model.

3.1.1 FEFLOW

Multiple hydrogeological modelling programs have been improved to more accurately model freeze-thaw processes and couple groundwater and thermal flow (Kurylyk and Watanabe 2013). FEFLOW is the hydrogeological flow modelling program that is being used in this thesis. The finite element mesh generation in FEFLOW is flexible, allowing models to replicate complicated topography and geologic layers in two- or three-dimensions. FEFLOW can simulate variably saturated groundwater flow and

heat transport processes. The numerical model SUTRA, a code used to predict water, heat and solute transport in variably saturated flow, now includes SUTRA-Ice. SUTRA-Ice couples groundwater and thermal flow of the fully saturated subsurface in cold regions and includes coding that calculate the development and decay of ice in the subsurface (McKenzie et al. 2007).

FEFLOW offers a plug-in piFreeze that provides coding to account for phase change processes during ground freeze-thaw in variably saturated media. PiFreeze introduces ice as a temperature dependent phase (DHI-WASY 2016; Clausnitzer and Mirnyy 2016). PiFreeze includes the effects of latent heat, alterations of hydraulic conductivities, porosities and thermal transport properties in freeze-thaw cycle calculations (DHI-WASY 2016). These code additions are required to develop a model that represents ice-rich permafrost in a peatland because there the formation and thawing of ice completely alters the way water and heat move through the media.

3.1.1.1   FEFLOW Unsaturated flow

FEFLOW is a process-based numerical model, meaning it uses physically based equations to determine groundwater flow within a specified model domain (Anderson et al. 2015). Combinations of governing equations are used to compute the groundwater flow and thermal transport in the system. Initial and boundary conditions are used in the governing equations to calculate the hydraulic head distribution and thermal distribution. Governing equations that account for variable saturation are employed to account for vadose zone processes. The Darcy equation (Equation 2.1), in which saturation is assumed to be one, is used to calculated groundwater flow in fully saturated models.

$$q = -K_r(s)K(\nabla h + \chi \mathrm{e}) = -K_x(s)K[\nabla \psi + (1 + \chi)\mathrm{e}] \qquad (2.1)$$

$K_r(s)$ = relative hydraulic conductivity (m s^{-1})

h $=$ ψ + z; hydraulic (piezometric)head (m)

χ $=$ buoyancy

e $=$ gravitational unit vector

      Darcy's equation (Equation 2.1) is too simplified to use in variably saturated

media. The hydraulic conductivity of a material in the vadose zone is a function of its

saturation. FEFLOW uses a variation of Richard's equation (Richards 1931) (Equation

2.2), which includes the Darcy flux term. The Darcy flux is calculated using the Darcy

equation (equation 2.1). The Richard's equation (Equation 2.2) is used to calculate flow

through variably saturated media (Dhi-Wasy GmbH 2009).

$$S_0 \cdot s(\psi)\frac{\partial \psi}{\partial t} + \varepsilon \frac{\partial s(\psi)}{\partial t} + \nabla \cdot q = Q \tag{2.2}$$

$S_0 = \varepsilon\gamma + (1-\varepsilon)Y$; specific storage due to fluid medium compressibility (m^{-1})

$s(\psi)$ $=$ saturation

ψ $=$ pressure head (m)

ε $=$ porosity

q $=$ Darcy flux vector $(m\ s^{-1})$

Q $=$ Specific mass supply $(m\ s^{-1})$

      Richard's equation (Richards 1931) can only solve for pressure (ψ) or saturation

(s), it relies on material characteristic curves to determine a relationship between soil

moisture, pressure and hydraulic conductivity (Anderson et al. 2015). This equation is

further complicated with the introduction of freezing and thawing because ice alters the

porosity. The FEFLOW plug-in piFreeze alters Richard's equation to account for the

changes in porosity that occur when ice develops and thaws (Clausnitzer et al. 2016;

DHI-WASY 2016). A term that accounts for the change in mass balance caused by

freezing (Q_f) is added to Richard's equation (Equation 2.3). This term represents the new

source of water due to freezing and thawing in pores and when the pore is not fully saturated this term goes to zero. This is because it is assumed ice will occupy the previously air-filled portion of the pore, not altering the porosity. If the pore is fully saturated, however, ice must occupy a portion of the pore that was previously occupied by liquid, therefore decreasing the porosity (Equation 2.4).

$$S_0 \cdot s(\psi) \frac{\partial \psi}{\partial t} + \varepsilon \frac{\partial s(\psi)}{\partial t} + \nabla \cdot q = Q + Q_f \qquad (2.3)$$

$$Q_f = -\frac{\partial \varphi}{\partial T} \frac{\partial T}{\partial t} \left[\frac{\rho_i}{\rho_l} \frac{\partial \varepsilon_i}{\partial \varphi} + \frac{\partial \varepsilon_l}{\partial \varphi} \right] \; for \; s = 1 \qquad (2.4)$$

$Q_f = 0 \; for \; s < 1$

$\varphi = \dfrac{\varepsilon_l \rho_l}{\varepsilon_l \rho_l + \varepsilon_i \rho_i} ; the \; freezing \; function$

$T = temperature \; (^{\circ}C)$

$\varepsilon_i = volumetric \; bulk \; fraction \; of \; ice \; (m^3 \; m^{-3})$

$\partial \varepsilon_l = volumetric \; bulk \; fraction \; of \; water \; (m^3 \; m^{-3})$

FEFLOW Thermal transport

The thermal properties of the various ground materials are input into FEFLOW and thermal boundary conditions are applied. To determine how heat moves from the boundary conditions, and through the model, FEFLOW uses various heat transport equations. The Fourier Law of heat conduction is used to determine the heat flux from one node to another (Equation 2.5; Banks 2008). The rate of heat transfer (Q_T) directly relates to the bulk thermal conductivity (λ) and the thermal gradient.

$$Q_T = \lambda \cdot A \cdot \frac{\partial T}{\partial x} \qquad (2.5)$$

$Q_T = rate \; of \; heat \; transfer \; (W)$

$\lambda = effective\ thermal\ conductivity\ (W\ m^{-1}K^{-1})$

$A = surface\ area\ (m^2)$

$\dfrac{\partial T}{\partial x} = temperature\ gradient\ (^{\circ}C\ m^{-1})$

PiFreeze changes the FEFLOW thermal governing summation equations of effective thermal conductivity and heat capacity of the media to account for ice content and the latent heat of phase change. PiFreeze accomplishes this by adding an ice term, with preset characteristics associated with ice, to the thermal conductivity equation (Equation 2.6) and heat capacity equation (Equation 2.7). A term to define the latent heat of phase change is also added to the heat capacity equation (Clausnitzer et al. 2016; DHI-WASY 2016).

$$\lambda = \varepsilon_l\lambda_l + \varepsilon_s\lambda_s + \varepsilon_i\lambda_i \tag{2.6}$$

$\lambda = effective\ thermal\ conductivity\ (W\ m^{-1}K^{-1})$

$\varepsilon_l = bulk\ volume\ of\ liquid\ (m^3\ m^{-3})$

$\lambda_l = liquid\ thermal\ conductivity\ (W\ m^{-1}K^{-1})$

$\varepsilon_s = bulk\ volume\ of\ solid\ (m^3\ m^{-3})$

$\lambda_s = solid\ thermal\ conductivity\ (W\ m^{-1}K^{-1})$

$\varepsilon_i = bulk\ volume\ of\ ice\ (m^3\ m^{-3})$

$\lambda_i = ice\ thermal\ conductivity\ (W\ m^{-1}K^{-1})$

$$C = \varepsilon_l C_l + \varepsilon_s C_s + \varepsilon_i C - L_f \rho_i \dfrac{\partial \varepsilon_i}{\partial \varphi}\dfrac{\partial \varphi}{\partial T} \tag{2.7}$$

$C = effective\ heat\ capacity\ (J\ kg^{-1}K^{-1})$

$L_f = latent\ heat\ of\ phase\ change\ (Jkg^{-1})$

3.1.2 Simultaneous Heat and Water Transport Model (SHAW)
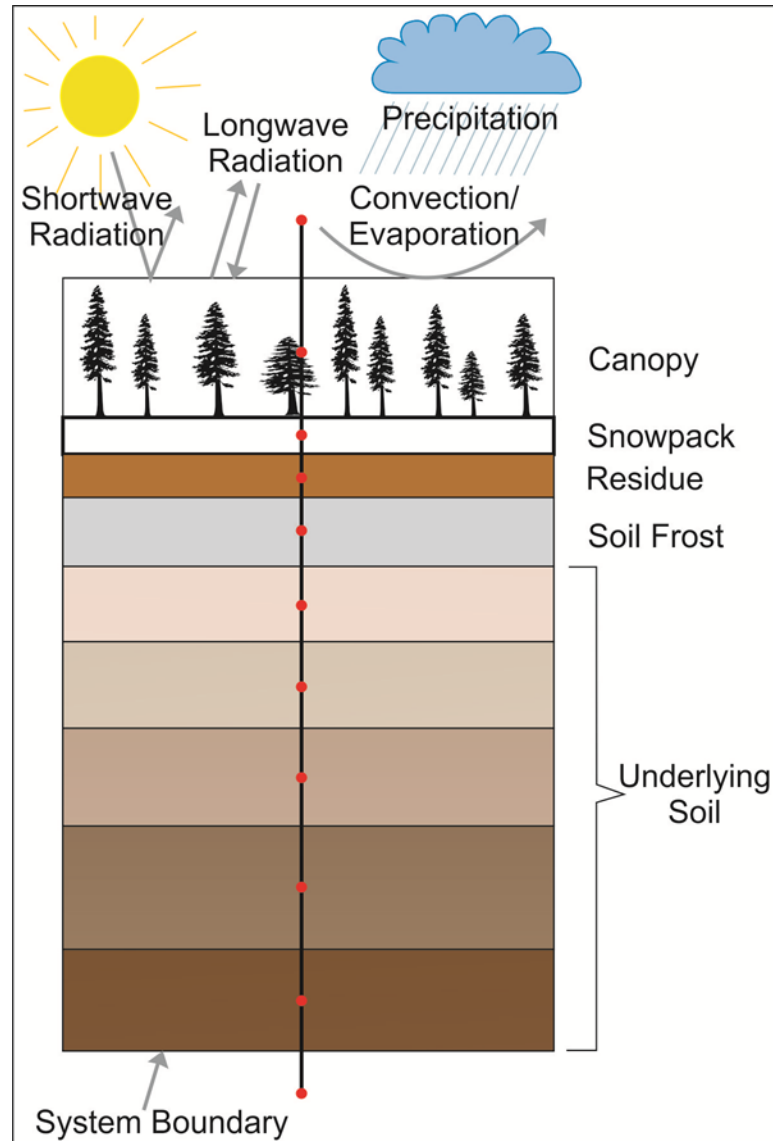
Figure 3-2: SHAW conceptual model with nodes overlaying the layers they represent in one-dimension (image is based on Flerchinger 2017).

The simultaneous heat and water (SHAW) model (Flerchinger 2000) is used to compute ground surface temperatures to be applied in the FEFLOW model. SHAW is a one-dimensional modelling program that simulates the flow of heat, water and solute as well as freeze thaw processes. A detailed description of SHAW assumptions and calculations can be found in Flerchinger (2000, 2017). SHAW uses various weather

inputs (Figure 2-1) to determine the heat and water fluxes occurring at ground surface (Flerchinger 2017). The surface energy balance in SHAW is calculated using the following equation (Equation 2.8).

$$R_n + H + L_v E + G = 0 \tag{2.8}$$

$R_n = net\ all-wave\ radiation\ (W\ m^{-2})$

$H = sensible\ heat\ flux\ (W\ m^{-2})$

$L_v = latent\ heat\ of\ evaporation\ (J\ kg^{-1})$

$E = total\ evapotranspiration\ (kg\ m^{-2}\ s^{-1})$

$G = soil\ or\ ground\ heat\ flux\ (W\ m^{-2})$

Energy fluxes are computed at each layer starting at the tree canopy and moving down through snow, ground residue (decaying organic matter such as fallen leaves) and into the subsurface. At the end of every time-step the energy balance is saved in a finite-difference form. This includes the ground surface temperature, which may be directly applied in FEFLOW. Water fluxes are computed in a similar top-down fashion, beginning with vapor transfer processes in the canopy. The water transfer through the overlying residue is computed using Equation 2.9 in SHAW (Flerchinger 2017).

$$\frac{\partial \rho_v}{\partial t} = \frac{\partial}{\partial z}\left(K_v \frac{\partial \rho_v}{\partial z}\right) + \frac{\partial}{\partial z}\left(\frac{(h_r \rho'_{vs} - \rho_v)}{r_h}\right) \tag{2.9}$$

$\rho_v = vapor\ density\ (kg\ m^{-3})$

$K_v = convective\ vapor\ transfer\ coefficient\ within\ the\ residue\ (m\ s^{-2})$

$h_r = relative\ humidity$

$\rho'_{vs} = saturated\ vapor\ density$

$r_h = resistance\ to\ vapor\ transfer\ between\ residue\ elements\ and\ air\ voids\ (s\ m^{-1})$

Once the water flux of the overlying residue is computed the water flux through the underlying soil layer is computed using equation 2.10.

$$\frac{\partial \theta_l}{\partial t} + \frac{\rho_i}{\rho_l}\frac{\partial \theta_i}{\partial t} = \frac{\partial}{\partial z}\left[K\left(\frac{\partial \psi}{\partial z} + 1\right)\right] + \frac{1}{\rho_l}\frac{\partial q_v}{\partial z} + U \tag{2.10}$$

$\theta_l = volumetric\ moisture\ content\ (m^3 m^{-3})$

$\theta_i = volumetric\ ice\ content\ (m^3 m^{-3})$

$K = unsaturated\ hydraulic\ conductivity\ (m\ s^{-1})$

$\psi = volumetric\ water\ content\ (m^3 m^{-3})$

$q_v = volumetric\ vapor\ content (m^3 m^{-3})$

$U = source/sink\ term\ for\ water\ extracted\ by\ roots$

Each time step calculation starts with heat and water fluxes. After the flux calculations have been completed precipitation and infiltration are computed based on weather data, snow and ponded water accumulation and the interception by canopy and residue. The infiltration into soil is determined using the Green-Ampt approach for a multi-layered soil (Equation 2.11; Green and Ampt 1911) .

$$f = \frac{dF'_m}{dt'} = \frac{F'_m/\Delta\theta_l + \psi_f + \sum \Delta z_k}{\frac{F'_m}{\Delta\theta_l K_{e,m}} + \sum \frac{\Delta z_k}{K_{e,k}}} \tag{2.11}$$

$f = infiltration\ rate\ (m\ s^{-1})$

$K_{e,k} = effective\ hydraulic\ conductivity\ of\ layer\ k\ (m\ s^{-1})$

$\psi_f = suction\ head\ (m)$

$\theta_l = volumetric\ liquid\ content$

$F'_m = accumulated\ infiltration\ (m)$

The latest version of SHAW (SHAW 3.0) includes subsurface runoff, which occurs in highly porous media such as peat. Water infiltrates through the ground surface

but cannot infiltrate deep enough to reach groundwater because of the impermeable properties of frozen ground. This water flows along the surface of the frost table. Subsurface runoff is the dominant form of runoff on permafrost plateaus. This update allows for more representative modelling of the peat's saturation. The moisture content of ground material affects the thermal properties, meaning this updated version of SHAW will predict ground temperatures more accurately.

3.2   Model design and application

3.2.1 FEFLOW model domain

The first step in determining where to place model boundaries was to review the regions topography. A topographic map was developed from LiDAR which was flown in 2008. A plateau was selected as the focus of the study. This decision was made based on the available field data and the distance from potential model boundaries and groundwater divides. The boundaries were selected surrounding the plateau based on their alignment with the physical and hydraulic features that are assumed to remain stable throughout the models projected time frame. Previous studies have demonstrated that there are localized flow patterns in the region that may be characterized based on topography (Christensen et al. 2010; Hayashi et al. 2004; Quinton et al. 2010). Following these studies, the elongate eastern and western boundaries of the model have been assumed to align with the direction of flow in the fen and no groundwater flow crosses through these boundaries (Figure 2-2). These boundaries intercept smaller surrounding plateaus because following through the fen brings the boundaries too close to the plateau. The consequence of boundaries being too close to the plateau is coarse dispersion of the boundary thermal conditions interacting with the plateau. It was determined through testing on subset models that the boundary needs to be at least 5-

10 m away from the plateau for the plateau to have independent thermal properties. These boundaries cross the smaller plateaus through the topographic highs, even though this is a low relief region there is still small amounts of flow on the plateaus, therefore the boundary cuts through the approximate groundwater divides.

The northern and southern boundaries were selected to be at a distance large enough to prevent boundary thermal interaction with the plateau. This was particularly important along the southern boundary, where water is feeding into the model. Groundwater flows out of the model at the northern boundary. The northern and southern boundaries were selected to be perpendicular to fen water flow, thus along a topographic isoline.

3.2.2   Boundary conditions and conceptual model

In a steady state model, the boundary conditions should be representative of average conditions of the region being modelled. In this case, though the water level rises and falls in the fen, the hydraulic head was assumed to be at approximately the ground surface to develop the steady state hydraulic head solution. The northern and southern boundaries were set as constant head boundaries equal to the surface elevation at these points (Figures 2-2 and 2-3). The elongated edge boundaries were assumed to be no-flow boundaries (Figure 2-2). As shown in the conceptual model water will flow into the model at the southern relatively higher elevation boundary and flow north along either side of the elevated plateau to leave the model at the northern boundary (Figure 2-3). This boundary condition was applied on all layers down to the top of the clay, which is relatively impermeable.
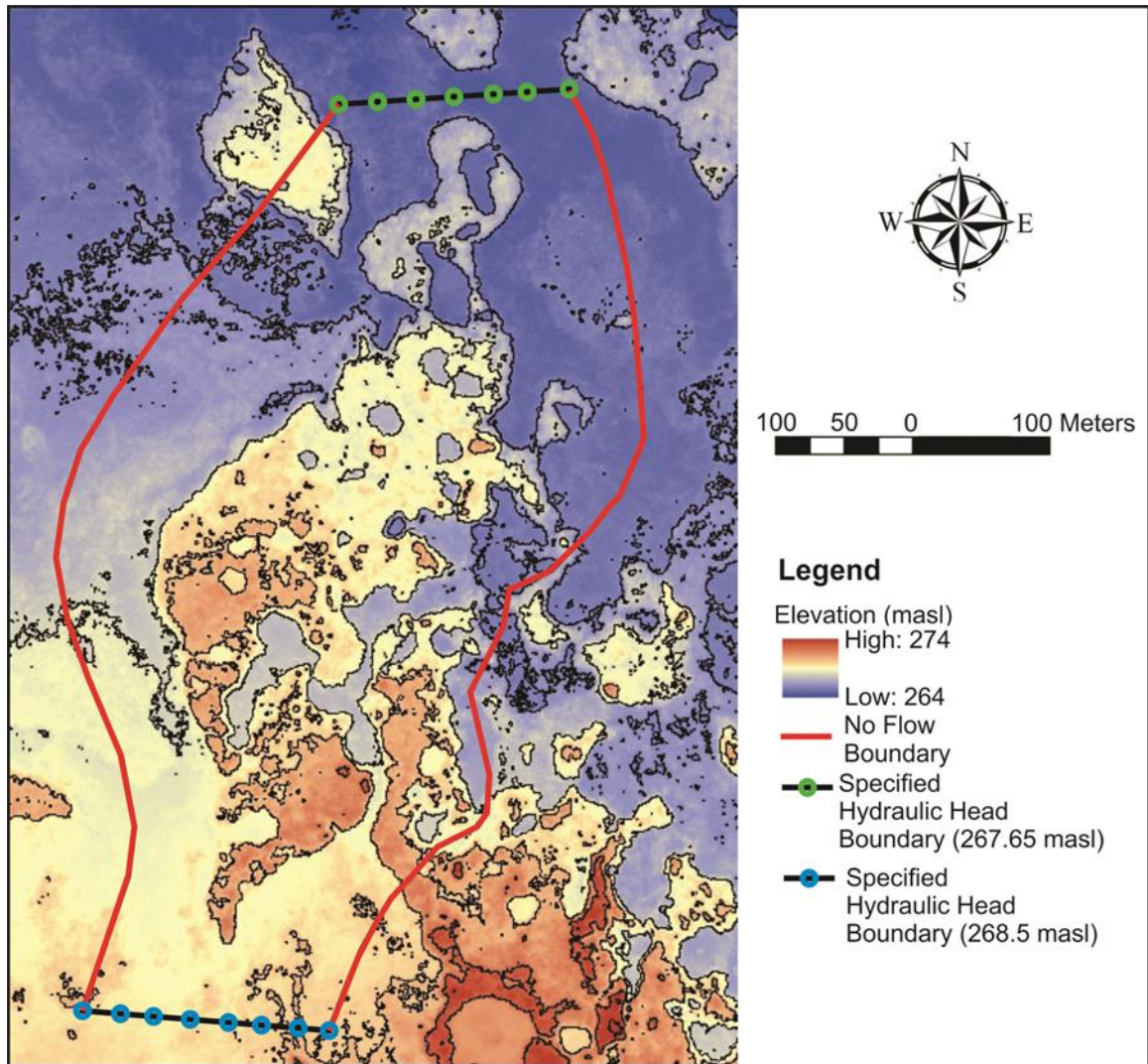
Figure 3-3: The applied FEFLOW boundary conditions displayed on the horizontal model domain.

A steady state model in which permafrost is developed was generated. In order to develop permafrost, thermal boundary conditions were based on a similar study by Kurylyk et al. (2016). A constant temperature of -2.5°C was applied over the modern-day permafrost plateau, 1.3°C over the modern-day wetlands and 1.5°C as a basal temperature. Transient SHAW average monthly ground surface temperatures (1875-1925) were then applied to the permafrost bulb and surrounding wetlands. The

temperature of the basal boundary is an estimated temperature based on subsurface temperature gradients in the region (Figure 2-3) (Smith et al. 2005).

Once steady-state permafrost has been developed, these will be used as initial conditions for a transient model run. The daily net water transfer at ground surface calculated from the SHAW plateau water balance was applied to the model surface. This transient data required a daily time-step because average monthly precipitation removes the precipitation events and smooths them out over a month. This means water would constantly be entering the ground surface and the peat would not dry out in the summer months between precipitation events. This was demonstrated through early model testing of monthly inputs which resulted in an overly saturated vadose zone. Dry peat is an excellent insulator and if it is not properly represented in the model the permafrost thaw rate would be accelerated.

Throughout the transient run, constant hydraulic head boundaries are applied at the northern and southern boundary, as done in the steady state simulations (Figure 2-3). Thus, during the transient run, the hydraulic head boundaries will not represent the rise and fall of the water level throughout the year. The average range of water levels in the Scotty Creek wetlands is 0.5 m. The largest effect of this will be demonstrated in the wetlands where the water level rise and fall determines the flow rates. This will, however, have a negligible effect on the plateau because majority of the groundwater flow occurring on plateaus is subsurface runoff from infiltrated precipitation, which is being represented in this model. In the transient conceptual flow model this model is designed after, water enters the model at the southern boundary and flows north around the plateau and out the northern boundary (Figure 2-3). Water also enters and exits the model on the surface boundary according to an applied daily net water transfer (Figure 2-3).
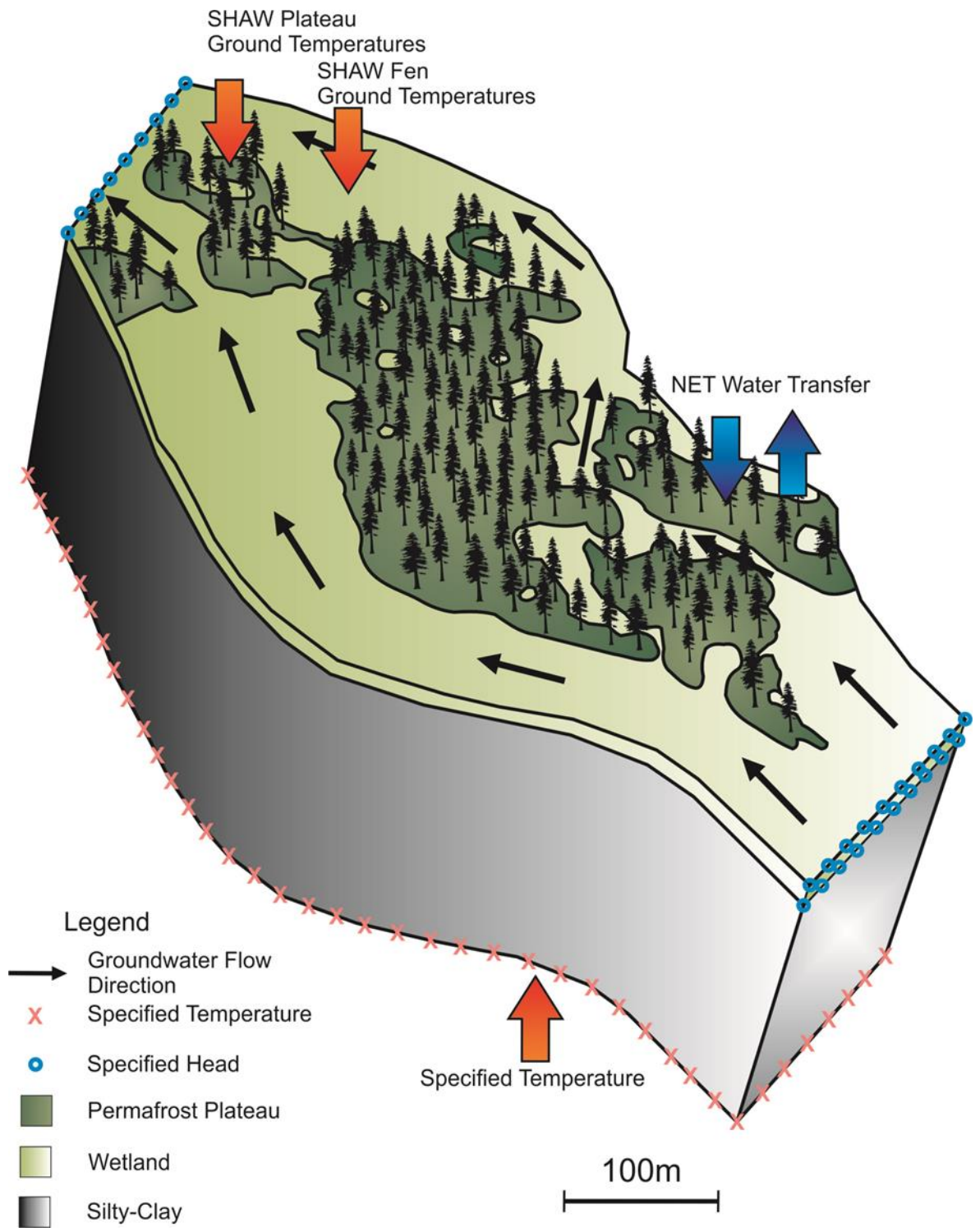
Figure 3-4: The FEFLOW conceptual model.

3.2.3 Model discretization

3.2.3.1   SHAW discretization

A SHAW one-dimensional model consists of multiple nodes that represent different layers of the environment from the canopy to the subsurface (Figure 2-1). Each node is typically assigned properties to represent a different layer. In the SHAW plateau model there is a steep temperature gradient that occurs between the atmosphere and the near 0 ˚C permafrost. To increase accuracy in this high thermal gradient environment the SHAW model was more finely discretized and used multiple nodes within each layer of peat. The nodes in the plateau were spaced ranging from 0.01 m in the shallow peat to 0.25 m in the deeper peat. The SHAW wetland model does not require such a fine discretization because it has a lower thermal gradient than the plateau. The SHAW wetland model has a nodal spacing of 0.01 m in the top 0.1 m and a larger nodal spacing of 1.0 m at the base of the 7.0 m deep model.

3.2.3.2   FEFLOW discretization

Mesh generation in a finite element model is important because the number of nodes in the model regulates and affects the accuracy of the solution as well as the computational time necessary for the solution to be completed. A balance between computational time and model accuracy needs to be determined; this is done by focusing on the main goals of the model (Anderson et al. 2015). The focus of this project is the thermal transport within a degrading permafrost plateau; therefore, the horizontal discretization is denser on the plateau of interest (elements ~1-3 m) and coarser on the surrounding plateaus and fens (elements ~3-5 m). With a model domain of approximately 50 m in width and 700 m in length, this discretization resulted in 47089 elements and 23793 nodes per layer (Figure 2-4).
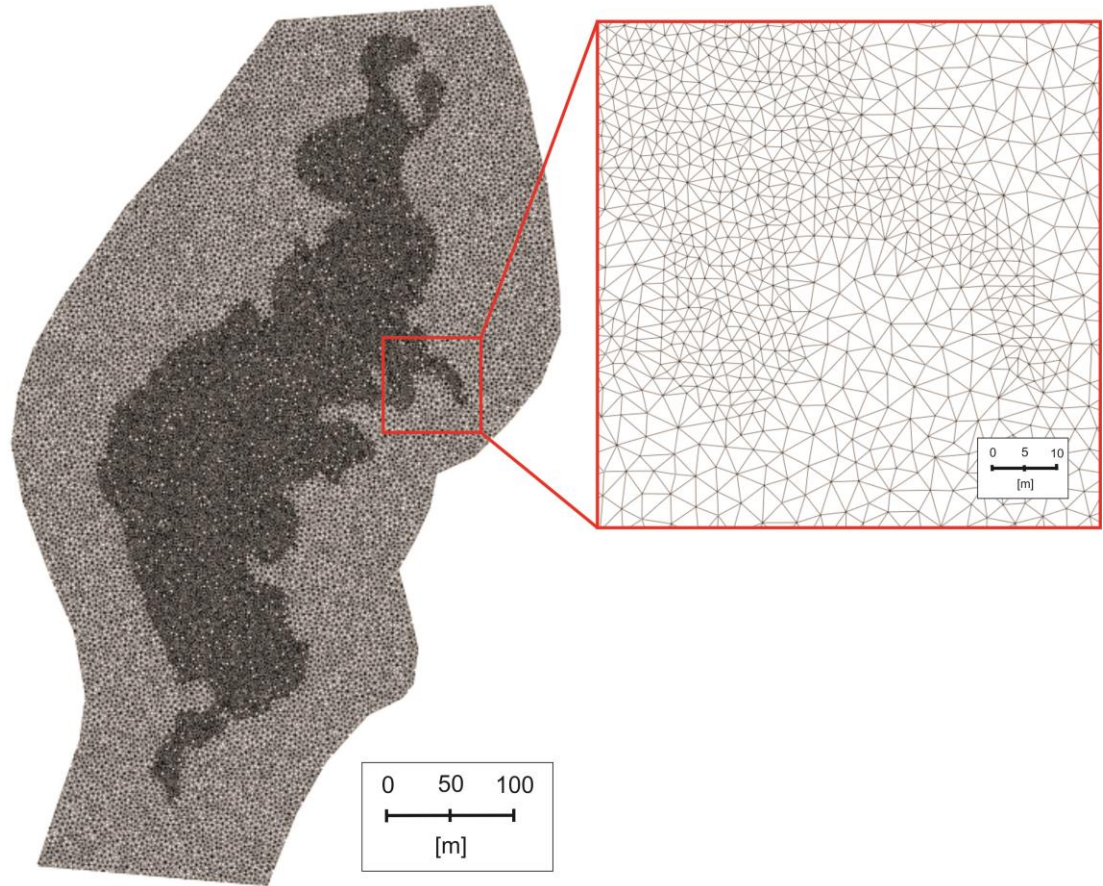
Figure 3-5: Horizontal discretization of FEFLOW model.

FEFLOW offers multiple mesh generators that allow different mesh specifications to be carried out such as forcing Delaunay criterion, building out elements from lines or points of a shape file or evenly distribution of elements. The mesh builder triangle was used to generate the mesh because it allows local refinement, which was used on the plateau as well as allows the modeler to specify maximum element sizes and minimum angles (Figure 2-4). When generating a mesh using the triangle mesh builder the option to force Delaunay criterion to be met was used. Forcing the Delaunay criteria to be met during mesh generation avoids development of elongated sliver triangles by maximizing the smallest angles possible of all triangles. Delaunay criterion is important to be met to ensure a quality mesh without elongated elements with obtuse angles.

Table 3-1: Vertical discretization of FEFLOW model.

Slices	Layer Thickness [m]	Depth [m]
1 - 11	0.01	0 - 0.1
12 - 19	0.025	0.1 - 0.3
20 - 27	0.05	0.3 - 0.7
28 - 48	0.1	0.7 - 3.02
49 - 50	0.25	3.02 - 3.52
51 - 52	0.5	3.52 - 4.52
53 - 97	0.925	4.52 - 47.07
98 - 99	0.5	47.07 - 47.57
99 - 100	0.25	47.57 - 47.82

Once the mesh was developed and checked to follow the Delaunay criterion, this discretized layer was copied down to a depth of approximately 50 m (Table 2-1). The discretization in the vertical direction is determined based on the distance between layers. To determine the spacing required between layers, multiple sensitivity tests were run on a sub model. It was found that a finer discretization (0.1 m nodal spacing) is necessary within a large thermal gradient which is developed between permafrost and warmer summer ground temperatures. Therefore, layers need to be denser surrounding the thermal boundaries, in this case along the top and bottom of the model. Because the focus of the model is in the peat plateau, which is only in the top 3-4 m of the model, this section is the most densely vertically discretized (Table 2-4; Figure 2-5). The base of the model is only discretized enough to transfer the heat accurately from the base geothermal flux (Table 2-4; Figure 2-5). This discretization resulted in a total node count of 2,379,300 and element count of 4,661,811.
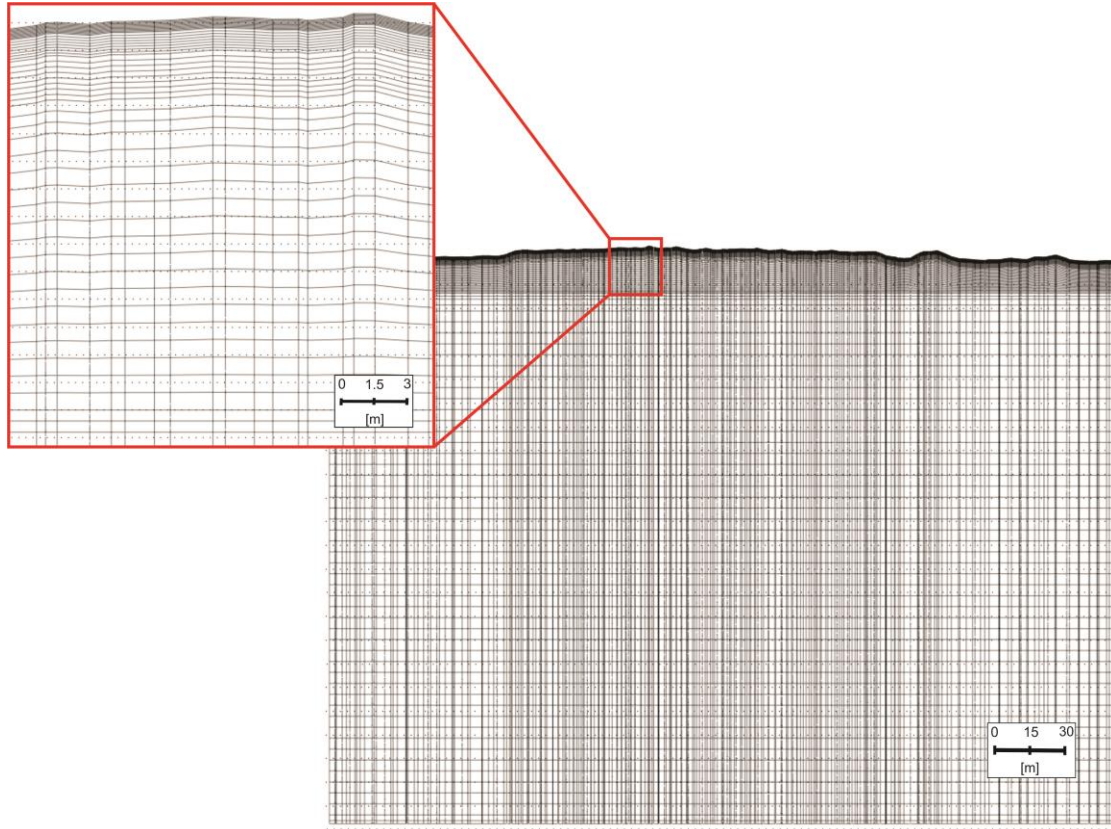
Figure 3-6: A cross section depiction of the vertical discretization of FEFLOW model.

3.2.4 Model properties

3.2.4.1 SHAW model properties

There were two SHAW models developed, one to represent a typical permafrost plateau and one to represent wetland. The ground properties used in the SHAW models are shown in Tables 2.2 and 2.3. SHAW requires the ground material to be broken down using five defined fractions: organic, sand, silt, clay and rock. Only the wetland SHAW model goes deep enough to include the clay found in Scotty Creek. The plateau model has a 1.5 m depth, which is the approximate average supra-permafrost table depth. The plateau model required both vertical (K_{sv}) and horizontal (K_{sh}) saturated hydraulic

38

conductivity because it included subsurface horizontal groundwater flow. Even though SHAW is a one-dimensional model, horizontal hydraulic conductivity has been added to act as a sink term. The wetland model did not include horizontal flow and only required the vertical saturated hydraulic conductivity (K_{sv}).

Table 3-2: SHAW model plateau properties.

Parameter	Values used at soil nodes in the SHAW model										
Depth [m]	0.0 - 0.05	0.05 - 0.1	0.1 - 0.3	0.3 - 0.4	0.4 - 0.5	0.5 - 0.6	0.6 - 0.7	0.7 - 0.8	0.8 - 1.0	1.0 - 1.25	1.25 - 1.50
Texture	peat	peat	peat	peat	peat	peat	peat	peat	peat	peat	peat
Organic fraction [%]	97	97	97	97	97	97	97	97	97	97	97
Sand fraction [%]	1	1	1	1	1	1	1	1	1	1	1
Silt fraction [%]	1	1	1	1	1	1	1	1	1	1	1
Clay fraction [%]	1	1	1	1	1	1	1	1	1	1	1
Rock fraction [%]	0	0	0	0	0	0	0	0	0	0	0
ρ_b [kg m^{-3}]	88	88	93	134	156	180	203	225	248	248	248
Porosity [-]	0.9	0.9	0.88	0.85	0.8	0.8	0.78	0.75	0.75	0.72	0.7
Air entry pressure [Pa]	-0.01	-0.01	-0.05	-0.05	-0.05	-0.05	-0.05	-0.05	-0.05	-0.05	-0.05
b [-]	5.3	5.3	5.6	5.6	5.6	5.6	5.6	5.6	5.6	5.6	5.6
K_{sv} [m s^{-1}]	2.78×10^{-4}	1.39×10^{-4}	2.78×10^{-5}	1.39×10^{-5}	6.94×10^{-6}	1.39×10^{-6}	1.39×10^{-6}	2.78×10^{-7}	2.78×10^{-7}	2.78×10^{-7}	2.78×10^{-7}
K_{sh} [m s^{-1}]	5.56×10^{-4}	2.78×10^{-4}	5.56×10^{-5}	2.78×10^{-5}	1.39×10^{-5}	2.78×10^{-6}	2.78×10^{-6}	5.56×10^{-7}	5.56×10^{-7}	5.56×10^{-7}	5.56×10^{-7}

Table 3-3: SHAW model wetland properties.

Parameter	Values used at nodes in the SHAW model											
Depth [m]	0.0 - 0.01	0.1 - 0.3	0.3 - 0.4	0.4 - 0.5	0.5 - 0.6	0.6 - 0.7	0.7 - 0.8	0.8 - 1.3	1.3 - 1.6	1.6 - 2.0	2.0 - 3.0	3.0 - 7.0
Texture	peat	peat	peat	peat	peat	peat	peat	peat	peat	peat	peat	clay till
Organic fraction [%]	97	97	97	97	97	97	97	97	97	97	97	0
Sand fraction [%]	1	1	1	1	1	1	1	1	1	1	1	10
Silt fraction [%]	1	1	1	1	1	1	1	1	1	1	1	60
Clay fraction [%]	1	1	1	1	1	1	1	1	1	1	1	30
Rock fraction [%]	0	0	0	0	0	0	0	0	0	0	0	0
ρ_b [kg m^{-3}]	88	93	134	156	180	203	225	248	248	248	248	1300
Porosity [-]	0.85	0.85	0.8	0.8	0.78	0.78	0.78	0.75	0.72	0.7	0.6	0.5
Air entry pressure [m]	-0.01	-0.05	-0.05	-0.05	-0.05	-0.05	-0.05	-0.05	-0.05	-0.05	-0.05	-0.36
b [-]	5.3	5.3	5.6	5.6	5.6	5.6	5.6	5.6	5.6	5.6	5.6	7.75
K_{sv} [m s^{-1}]	2.78×10^{-4}	1.39×10^{-4}	2.78×10^{-5}	1.39×10^{-5}	6.94×10^{-6}	1.39×10^{-6}	1.39×10^{-6}	2.78×10^{-7}	2.78×10^{-7}	2.78×10^{-7}	2.78×10^{-7}	2.78×10^{-9}

3.2.4.2   FEFLOW model properties

The ground properties (Figure 2-6 and Table 2-4) used in the FEFLOW model were based on measurements and studies done in the Scotty Creek Research Basin. The model was divided into three ground classifications: peat plateau, wetland and clay. The divisions between these ground types are straight and non-gradational, even though there is a transitional zone between wetland to peat in Scotty Creek (Figure 3-7).

However, there are not enough measurements recorded in the plateau-wetland transitional zone to accurately represent it. The plateau-wetland transitional zone is small and the material difference between plateau and wetland is also small, therefore it is appropriate to not include this zone in the model. On a typical permafrost peat plateau in Scotty Creek, the upper 0.2 m has a higher porosity and hydraulic conductivity as it is less decomposed and consolidated relative to the deeper peat. Table 2-4 lists the various parameters applied in the model, broken down into the three categories peat, wetland and clay. The different ground properties are visually laid out in a cross section of a typical plateau-wetland complex in figure 2-6.

Table 3-4: FEFLOW model properties. Superscripts denote the term sources, equate 'a' to Kurylyk et al. 2016; 'b' to McClymont et al. 2013 and 'c' to Zhang et al. 2010.

Parameter:	Plateau	Wetland	Clay
Porosity	Upper: 0.92[c]	Layer 1: 0.85	0.55 [c]
	Lower: 0.83[c]	Layer 2: 0.6	
		Layer 3: 0.8	
Saturated Hydraulic Conductivity [m/s]	Upper: 1×10^{-3}	Layer 1: 1×10^{-1}	6×10^{-10} [a]
	Lower: 1×10^{-5}	Layer 2: 1×10^{-2}	
		Layer 3: 1×10^{-5}	
Thermal Conductivity [W m^{-1} K^{-1}]	0.25[b]	0.25 [b]	1.62 [b]
Heat Capacity [MJ m^{-3} K^{-1}]	2.6[a]	2.6 [a]	2 [a]
Θ_s [m^{3}m^{-3}]	Upper: 0.85[c]	0.85 [c]	0.5 [c]
	Lower: 0.8[c]		
Θ_r [m^{3}m^{-3}]	Upper: 0.18 [c]	0.18 [c]	0.18 [c]
	Lower: 0.2 [c]		
α [m^{-1}]	Upper: 50 [c]	50 [c]	2.8 [c]
	Lower: 10 [c]		
n	Upper: 1.45 [c]	1.45	1.28 [c]
	Lower: 1.35 [c]		
m	Upper: 0.31	0.31	0.22 [c]
	Lower: 0.26		
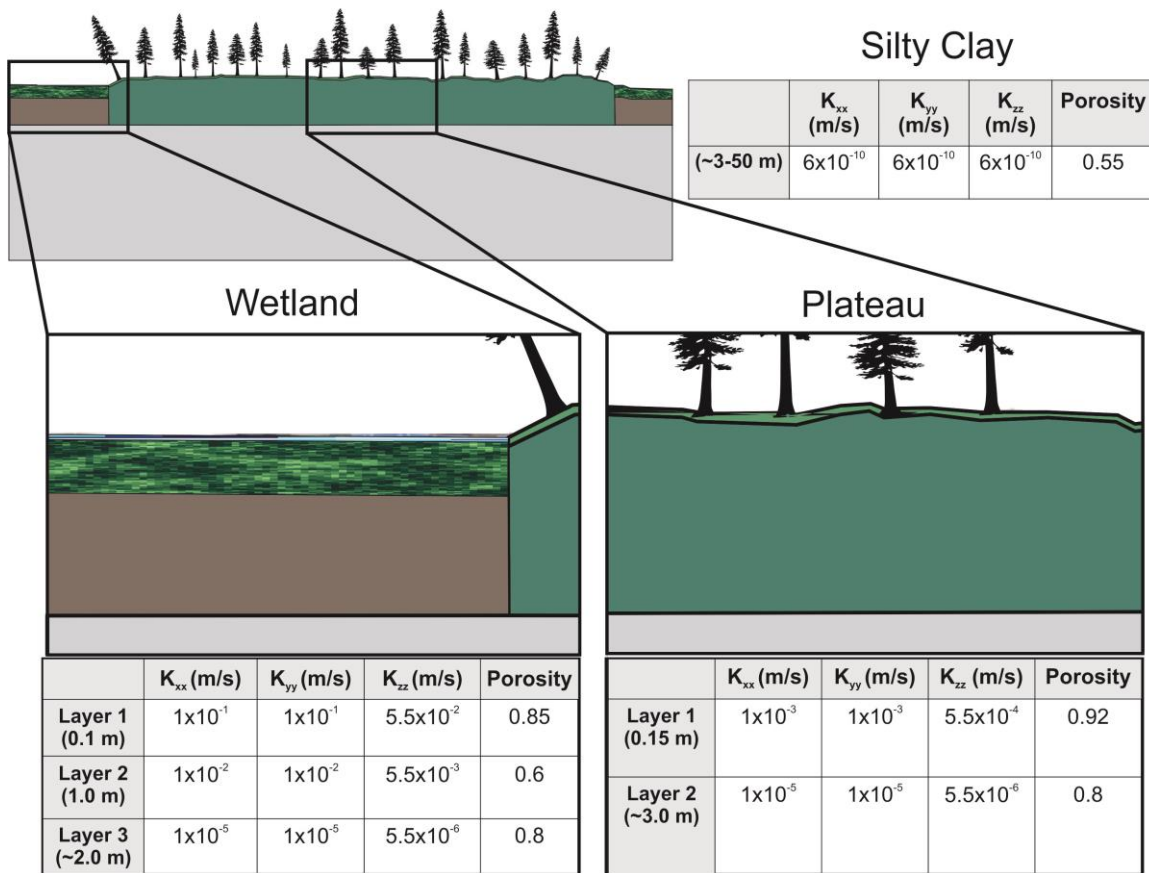
Figure 3-7: Cross section display of model properties.

The material properties of the wetlands surrounding permafrost plateaus in Scotty Creek have not been characterized very thoroughly and there is no published work on this. Therefore, the fen properties used in the model were developed based on few previously completed field tracer tests in Scotty Creek by Dr. Quinton, Dr. Hayashi, Brendan Christensen and other students, as well as model sensitivity tests completed in FEFLOW and literature of similar regions (Sjoberg et al. 2016). The fen was broken down into three hydrogeologic layers. The upper 0.2 m layer was defined as a highly hydraulically conductive layer with a high porosity with a porosity of 0.85. This small layer is most active in the spring during the freshet when the water table rises. Below this layer is a 1 m thick less porous material made up of sedges that grow in fen

environments. This layer is referred to as a 'floating mat' of vegetation. Below the 'floating mat' is a layer that has been referred to as 'muck.' This is a high porosity, highly-saturated portion of the fen. Due to the extremely low hydraulic gradient in the area, the water in the lower portion of the fen is relatively stagnant. Most of the water that is transported in the fen moves through the highly conductive upper layer during the spring freshet.

The thick peat in Scotty Creek overlays a glacial till mineral soil deposit composed of dominantly of clay and clay-silt (Aylsworth and Kettles 2000). The clay has very low permeability (Table 2-2) and is assumed to continue to the base of the model (approximately 45 m). The material properties of the glacial till were sourced from published studies by Kurylyk et al. (2016) and Zhang et al. (2010).

The thermal properties of water, both liquid and ice, were assigned in FEFLOW (Table 2-5). The thermal conductivity of ice is over three times greater than the thermal conductivity of liquid water, thus when ice develops in pore space the bulk thermal conductivity is greatly increased. The heat capacity of liquid water is just over double that of ice, meaning it can absorb more heat before changing temperature than ice.

Table 3-5: The thermal properties of water applied in the FEFLOW model. Superscripts denote the term sources, equate 'a' to Kurylyk et al. 2016 and 'b' to Williams and Smith (1989).

Phase	Thermal Conductivity [W/m˚C]	Heat Capacity [J/m³˚C]
Liquid	6.00×10^{-1}[a]	4.18×10^{6}[a]
Ice	2.14×10^{0}[b]	1.86×10^{6}[b]

3.2.5 Model input

3.2.5.1   SHAW model input

SHAW requires various weather inputs including maximum and minimum air temperature, dew point temperature, precipitation, radiation and wind run. Meteorological data has been collected half hourly at the Scotty Creek Research Station. The Fort Simpson climate station has been recording weather since 1898, including maximum and minimum air temperatures and precipitation. Fort Simpson average daily air temperatures were used as SHAW inputs between 1898 and 2004 (Figure 2-8). Data collected in Scotty Creek was used as SHAW input between 2005 and 2015 (Figure 2-7). Any gaps within the datasets of less than 3 days were filled using linear interpolation. Gaps longer than 3 days were filled using data from the most recent complete year. The air temperature trends have been clearly defined in the region (McClymont et al. 2013) and a trend of 0.015 ˚C/year was applied to the 1900 to 1910 average air temperature to estimate air temperatures between 1875 and 1900 (Figure 2-7).
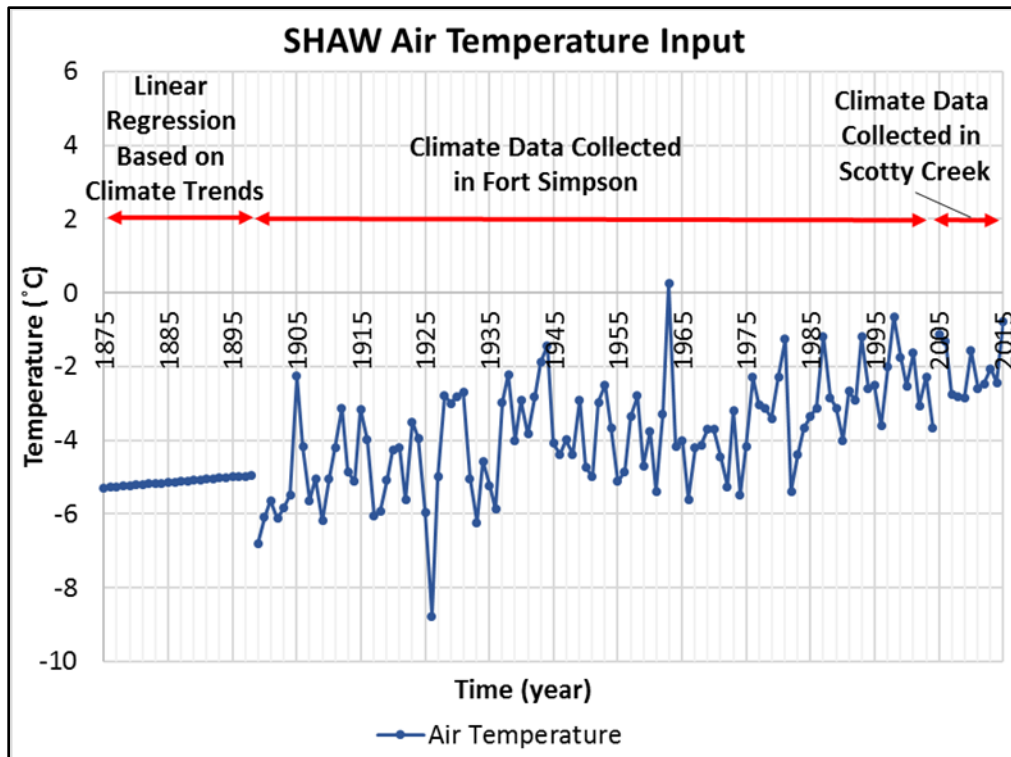
Figure 3-8: SHAW input air temperature.

Daily precipitation totals taken at Fort Simpson in 1898 to 2008 and Scotty Creek precipitation data between 2008 and 2015 were used as SHAW precipitation inputs (Figure 2-8). There is no available precipitation data in the Scotty Creek region between 1875 and 1898. Therefore, it was assumed that precipitation had not changed significantly between 1875 and 1925 and Fort Simpson precipitation data between 1898 and 1923 was used to fill the data gap (Figure 2-8). Some climate studies have found that precipitation in the Northwest Territories increased between 1900 and 1998 (Zhang et al. 2000). However this increase in precipitation coincides with an increase in air temperature, thus an increase in evapotranspiration (Zhang et al. 2000). Other studies have found that there were not enough active data sampling sites to prove that precipitation has increased (Smith et al. 2007). It is assumed that precipitation did not

significantly change between 1875 and 1923. The 1875-1898 gap in precipitation data was filled by repeating the 1900-1923 precipitation data.
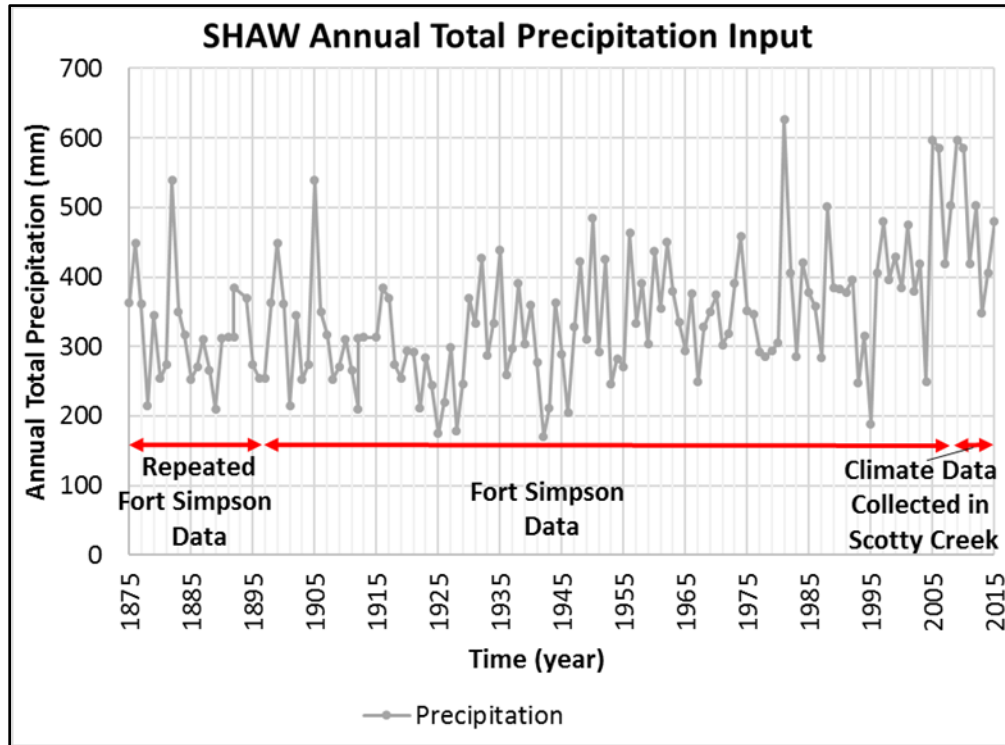
Figure 3-9: Annual totals of the daily precipitations used as SHAW input.

It was assumed that the radiation and wind in Scotty Creek have not changed significantly over the last one-hundred years. The Scotty Creek 2005-2015 radiation and wind data were used repetitively to fill in the 1875-2004 gap (Figures 2-9 and 2-10). Radiation and wind are two climatic variables that differentiate plateau and wetland weather. Due to the occurrence of trees above permafrost plateaus, plateaus are generally protected from strong winds and shaded from radiation (Figure 2-9 and 2-10). Wind run is the distance of wind traveled over a point. This was calculated using the daily recorded wind speeds on the Scotty Creek wetland and plateau meteorological stations.
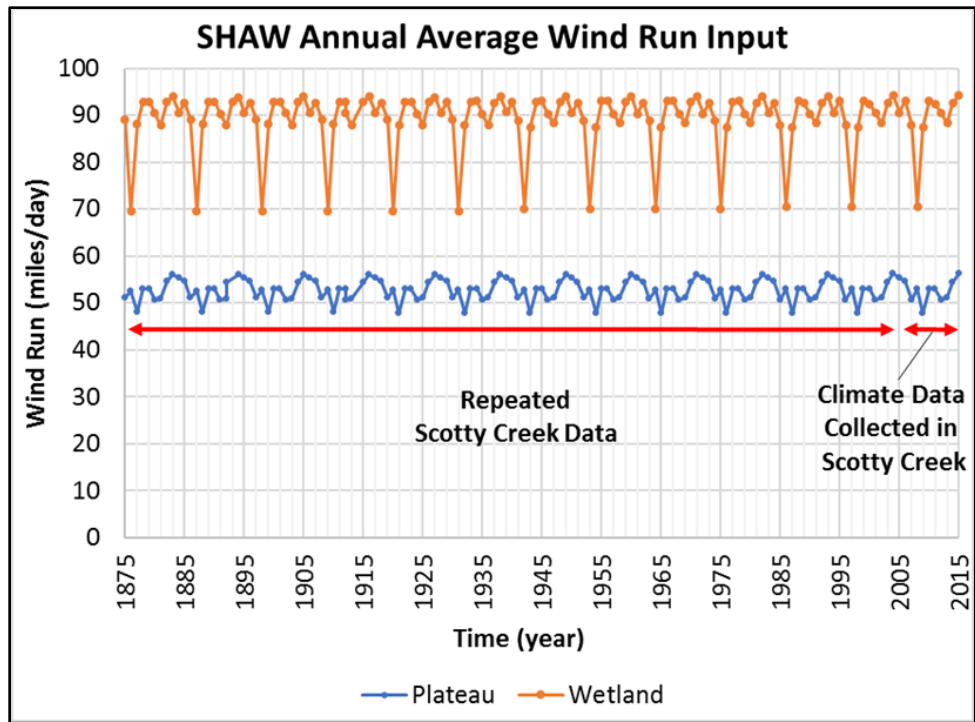
Figure 3-10: SHAW average annual plateau and wetland wind run inputs.
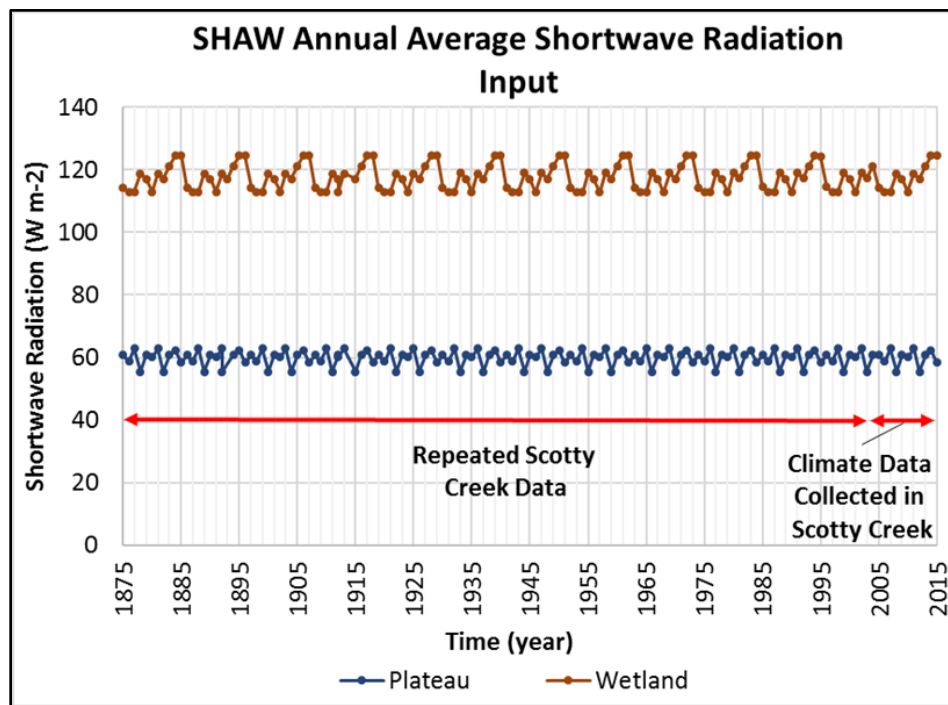
Figure 3-11: SHAW average annual plateau and wetland shortwave radiation inputs.

3.2.5.2 FEFLOW model input

There are two phases of FEFLOW modelling, one steady state phase in which a permafrost bulb is developed followed by transient runs in which the permafrost bulb is exposed to representative SHAW ground temperatures. There were two transient runs, one with SHAW climate data from 1875 to 1925 and one from 1999 to 2015. There have been studies published in which permafrost bulbs have been represented in two and three-dimensions (Christensen et al. 2010; McClymont et al. 2013; Kurylyk et al. 2016). These studies were used as references to the approximate size of the permafrost bulb. There are no measurements of the permafrost bulb as far back as 1875 so the 2008 permafrost bulb geometry was assigned. To develop the permafrost bulb in steady state under the modern-day topography, a temperature of -2.5 °C and 1.3 °C were applied on the ground surface overlying the plateau and the wetland respectively (Kurylyk, 2016).

Applying a constant temperature below 0 °C in steady state develops an ice-rich, continuous permafrost bulb underlying the freezing boundary condition. This smooth continuous permafrost bulb does not match what is found in today's discontinuous permafrost environment and cannot be expected to behave in a similar manner when modern day temperatures are applied to it. Transient monthly average temperatures and daily net infiltration were applied to the continuous permafrost bulb to thaw the bulb in a realistic way that includes talik development and differential thaw caused by variable moisture distribution in the supra-permafrost layer.

Chapter 4

4   Results

4.1   SHAW

4.1.1   Ground temperature

The ground temperatures derived from SHAW modelling are being used as transient boundary input for the FEFLOW model. The SHAW models are calibrated to represent the ground surface temperatures found at Scotty Creek. Half hourly ground temperature data in Scotty Creek has been collected since 2005 and half hourly plateau moisture content has been collected since 2006. The temperatures used for calibration and the temperatures used for comparison were both collected on the southern tip of the plateau (Figure 1-5). The year of 2011 was selected as a calibration year for the permafrost plateau model because it had consistent ground temperature and moisture content measurements. The year of 2006 was used as a calibration year for the wetland climate because it had consistent thermistor data and moisture content is irrelevant because wetlands are assumed to continuously be fully saturated. The resulting modelled plateau and wetland temperatures average approximately 6.1 ˚C and 6.8 ˚C respectively warmer than the measured air temperatures (Figure 3-1).
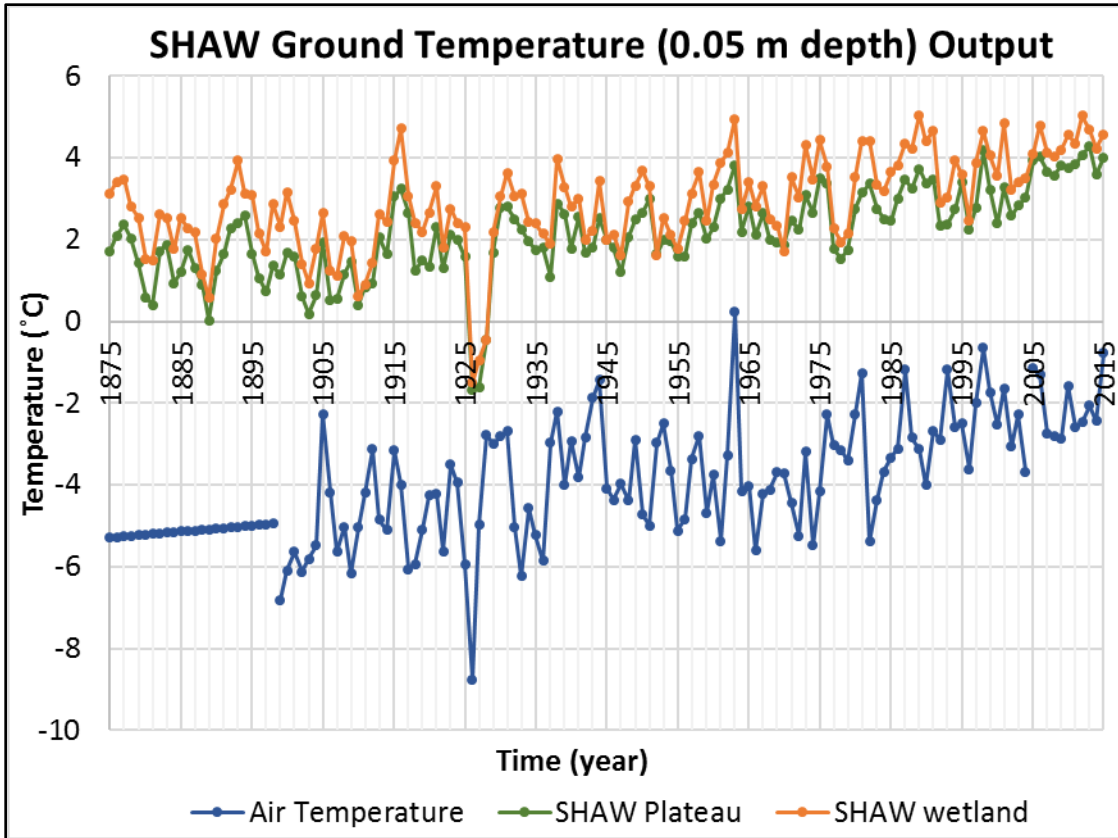
Figure 4-1: Air temperature inputs and SHAW ground temperature outputs for wetland and plateau.

The SHAW modelled ground temperatures of the plateau and the wetland were compared to plateau and fen temperatures measured in Scotty Creek (locations 'Plateau South' and Fen Middle' on Figure 3-2). Plateau temperatures have been collected since 2005, the years 2006 to 2012 are plotted for comparison (Figures 3-3 and 3-4). To compare modelled and measured values in this thesis the Mean Absolute Error (MAE), Mean Squared Error (MSE), Standard Deviation (SD) and Standard Error (SE) have been calculated and displayed under each one-to-one plot. The MSE, SD and SE demonstrate how well the data is fitting the trend of the measured data. The MAE demonstrates the average model accuracy. There are no specifically set error goals for this model other than determining modelling methods that minimize error. The SHAW plateau model results have a MSE of 0.70 ˚C, and MAE of 0.24 ˚C, a SD of 0.84 ˚C and

a SE of 0.01 ˚C (Figure 3-4). The SHAW plateau ground temperatures match well with the spring, summer and fall temperatures. The SHAW model performs most poorly in the winter months. The winter SHAW temperatures lack the frigid event-based low temperatures that are measured in Scotty Creek (Figures 3-3 and 3-4). This difference only occurs for brief periods of times and the temperature difference ranges from 1 ˚C to 5 ˚C. This is demonstrated in a one-to-one plot where data trends towards warmer modelled and colder measured temperatures below 0 ˚C (Figure 3-4). There are periods of winter in which SHAW temperatures are underestimated, which helps to balance out the overestimated values. The relatively even distribution surrounding the trend line in the one-to-one plot demonstrates the modelling error, and any measurement errors.

The fact that most of the error occurs in the winter periods suggests that a cold weather process is being misrepresented in the model. The cause of the SHAW plateau modelled and measured temperature differences is likely a miscalculation of snow pack. SHAW is a one-dimensional model and does not account for the complexities of snow distribution. Snow pack in SHAW is a balance of accumulated below 0 ˚C precipitation, and thawed above 0 ˚C precipitation. An overestimation in snowpack on the plateau would act as an insulator, protecting the peat from the cold events, as seen in these results (Figures 3-3 and 3-4). Snowpack is typically larger on the plateaus than on open wetland because wind redistribution is minimized by the trees (Quinton et al. 2010). However, the ground temperatures were taken on the southern tip of the permafrost plateau, where the plateau and thus tree cover is thinner ('Plateau South' on Figure 3-2). This likely led to increased snow redistribution on this portion of the plateau, relative to a location more central on the plateau, for example at 'Plateau Middle' in Figure 3-2. Increased snow redistribution causes lower snow pack and less insulation, thus colder

measured winter ground temperatures. The SHAW model is more representative of the

central plateau.
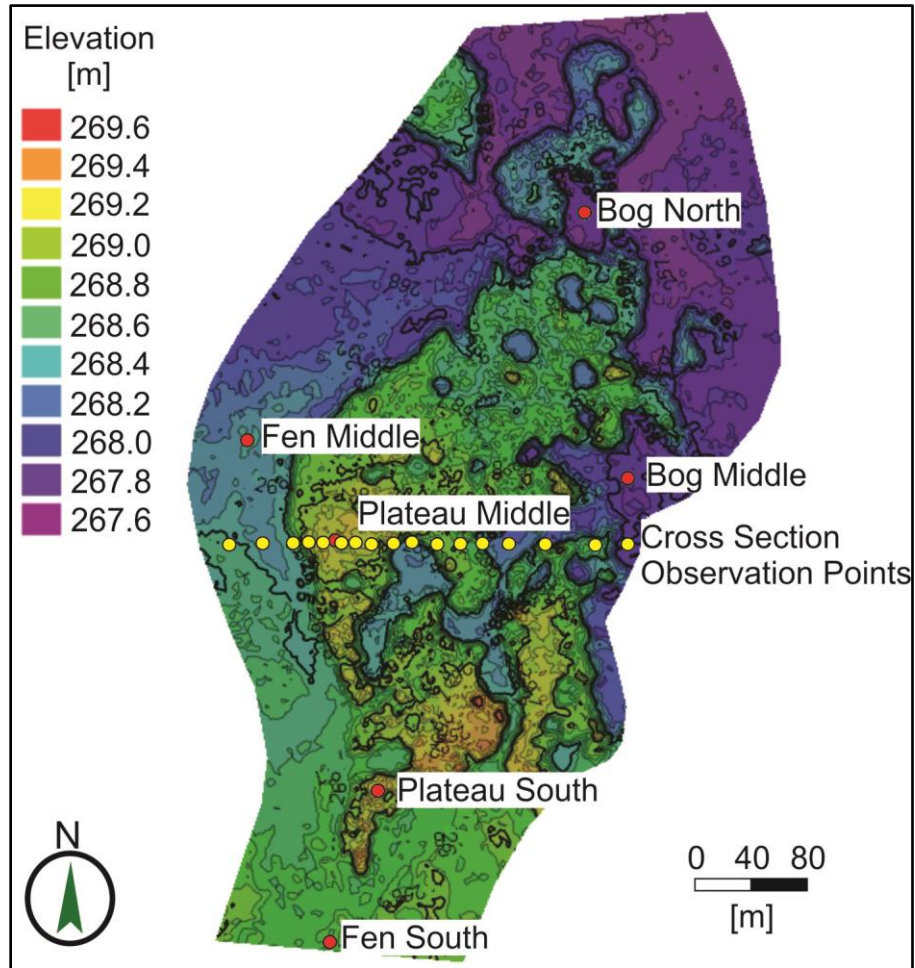
Figure 4-2: A map of the locations of the various data observation points where the nodal temperature, hydraulic head, moisture content, saturation and pressure are recorded at every time step.
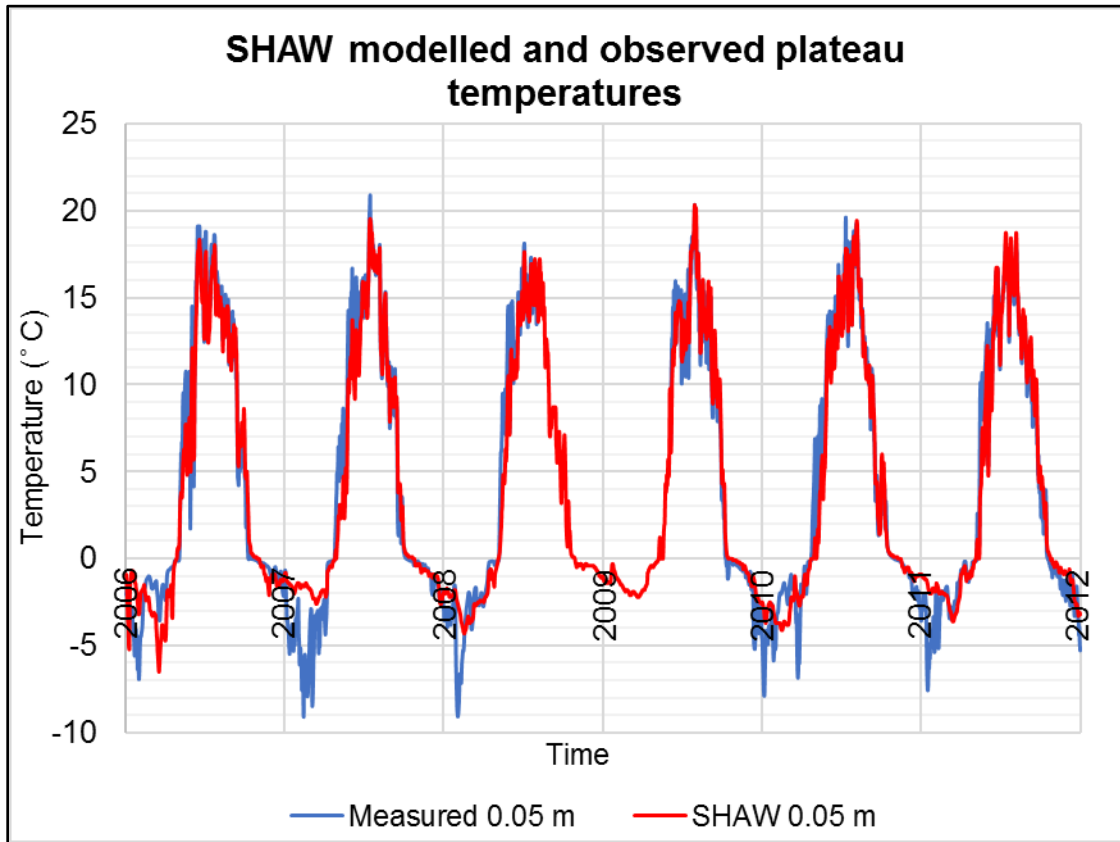
Figure 4-3: Measured ground temperatures and SHAW modelled ground temperatures at 0.05 m depth below surface elevation, between 2006 and 2012. **Sensor failure occurred between August 2008 and May 2009.
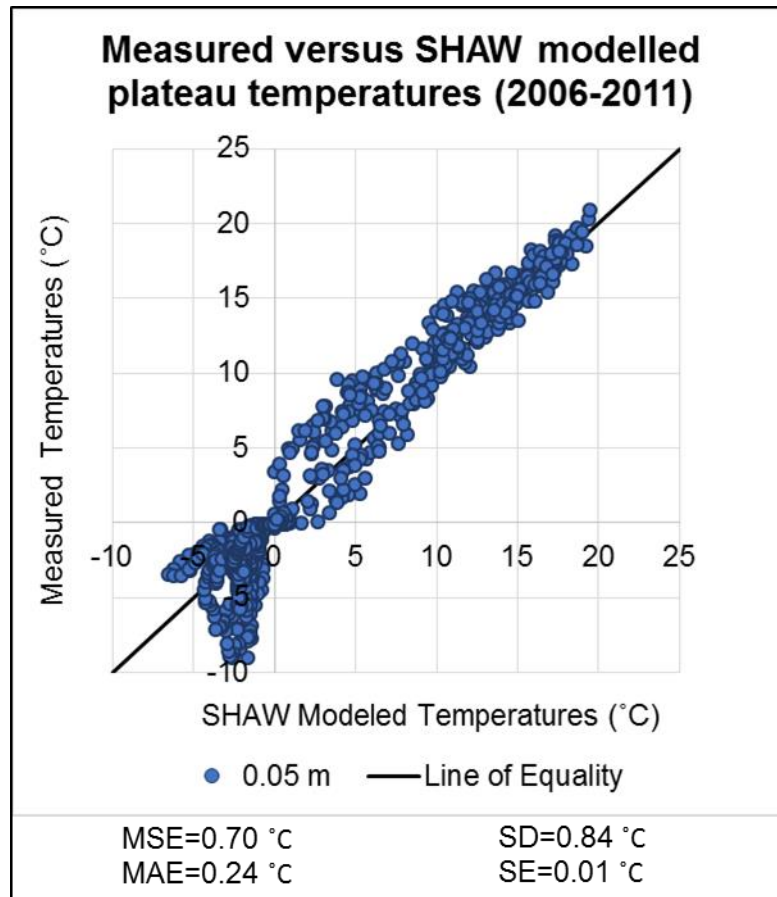
Figure 4-4: One-to-one plot of the Scotty Creek measured versus the SHAW modelled plateau ground temperatures at 0.05 m depth below surface elevation. Model statistics are displayed below the plot.

Wetland temperatures were taken in Scotty Creek between 2005 and 2008 at four wells directly west of the plateau. The exact depths and locations of these thermistors are regarded as approximate. One thermistor (DW) was selected as the fen temperature reference and it is located near the center of the fen, further from the plateau than other fen thermistors. This is approximately 100 m south of the 'fen middle' observation point location (Figure 3-2). The shallowest approximate wetland depth at which a thermistor was placed is 0.1 m. The modelled SHAW 0.1 m temperatures were compared to the measured 0.1 m Scotty Creek temperatures to test the SHAW model performance (Figures 3-5 and 3-6). The 0.05 m SHAW temperatures were used as

FEFLOW input and are not plotted here because there are no measurements for comparison. The SHAW wetland model temperatures have an MSE of 1.78 ˚C, MAE of 0.33 ˚C, SD of 1.34 ˚C and SE of 0.02 ˚C, which are all higher than the SHAW plateau model. Like in the plateau SHAW model, performance is less accurate in the winter months; however, unlike the plateau model, the winter temperatures are colder than the measured. The modelled winter temperatures are consistently lower than the measured by a maximum of approximately 3 ˚C. Measured wetland temperatures maintain a temperature close to 0 ˚C throughout winter. This is demonstrated in the one-to-one plot by a cluster of data points that collect along the measured 0 ˚C line (Figure 3-6).
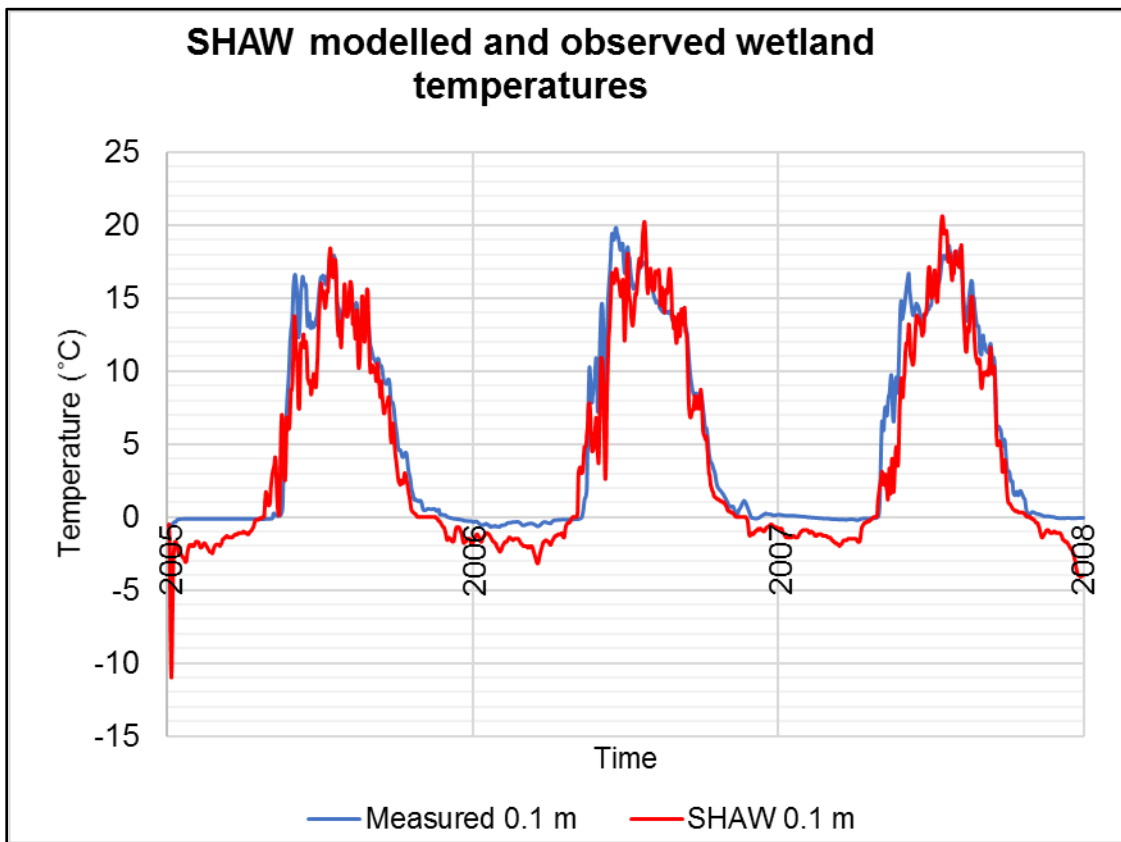
Figure 4-5: Measured wetland temperatures and SHAW modelled wetland temperatures (0.10 m depth) from 2005 to 2008.
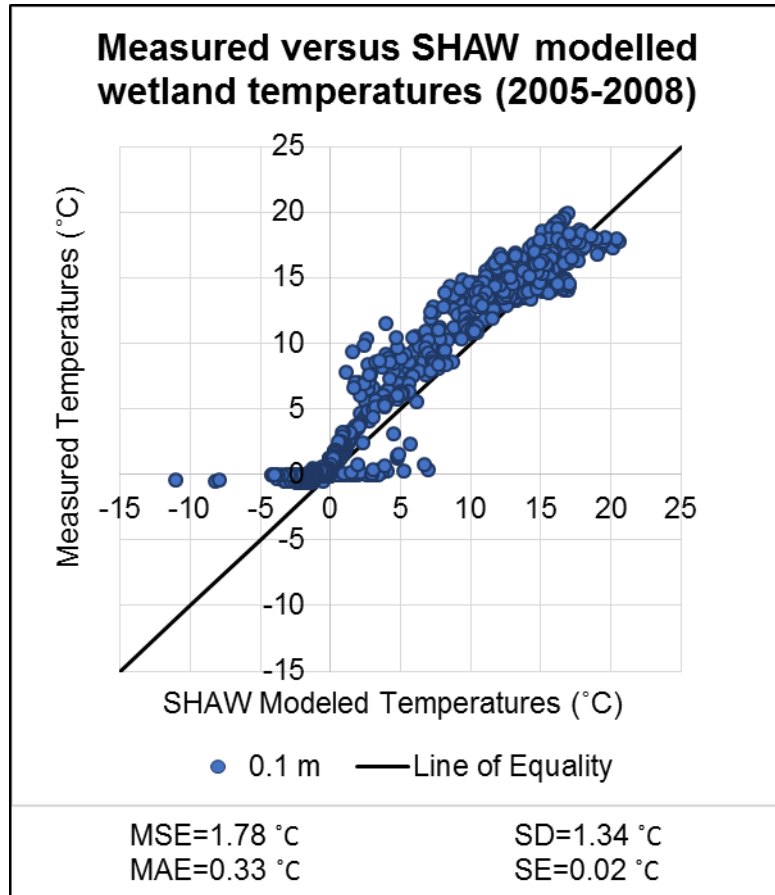
Figure 4-6: One-to-one plot of the Scotty Creek measured versus the SHAW modelled wetland temperatures at 0.1 m depth below ground surface. Model statistics are displayed below the plot.

These consistent winter temperature differences between wetland measured and modelled are likely a result of the SHAW model's oversimplification of a three-dimensional thermal transport and groundwater flow system. The wetland SHAW model is 7.0 m in depth and extends into the underlying clay, however, the only boundary driving temperatures in the model is the surface boundary. In reality, the fen freezes to a depth of approximately 1.0 m and below this depth is unfrozen relatively warm (approximately 2 ˚C) slowly flowing water. This three-dimensional flow system cannot be properly represented in a one-dimensional model and this difference is likely the cause of the winter temperature differences between the wetland measured and SHAW modelled values.

4.1.2 Water

The SHAW model outputs a daily water balance, and from this water balance the ground surface net infiltration is calculated. The calculated net infiltration was used as the ground surface daily input for the FEFLOW transient model. The first plateau model was run using the earliest version of SHAW 3.0, which did not include subsurface runoff. Permafrost plateaus are referred to as runoff generators because of their relatively higher relief; because of the high porosity of peat, the dominant form of runoff is sub-surficial along the impermeable supra-permafrost table. The only time of the year when surficial runoff occurs is in the early spring when the frost table is at ground surface. As the frost table thaws and moves deeper, the runoff becomes increasingly deeper.

As the earliest SHAW plateau model did not include subsurface runoff, over time the column filled with water as the base was frozen and relatively impermeable. This caused an overestimation of runoff during summer and fall when surficial runoff should be negligent (Figure 3-7). A new plateau SHAW model was made in an upgraded version of SHAW 3.0 that included sub-surficial runoff with an input of a plateau representative average gradient of 0.025. This is still a one-dimensional model, with the addition of subsurface runoff as a pathway for water to leave the column, preventing the column from filling and throwing off the water balance. The new plateau SHAW model, like observed runoff in Scotty Creek, has surficial runoff during the spring only (Figure 3-7).
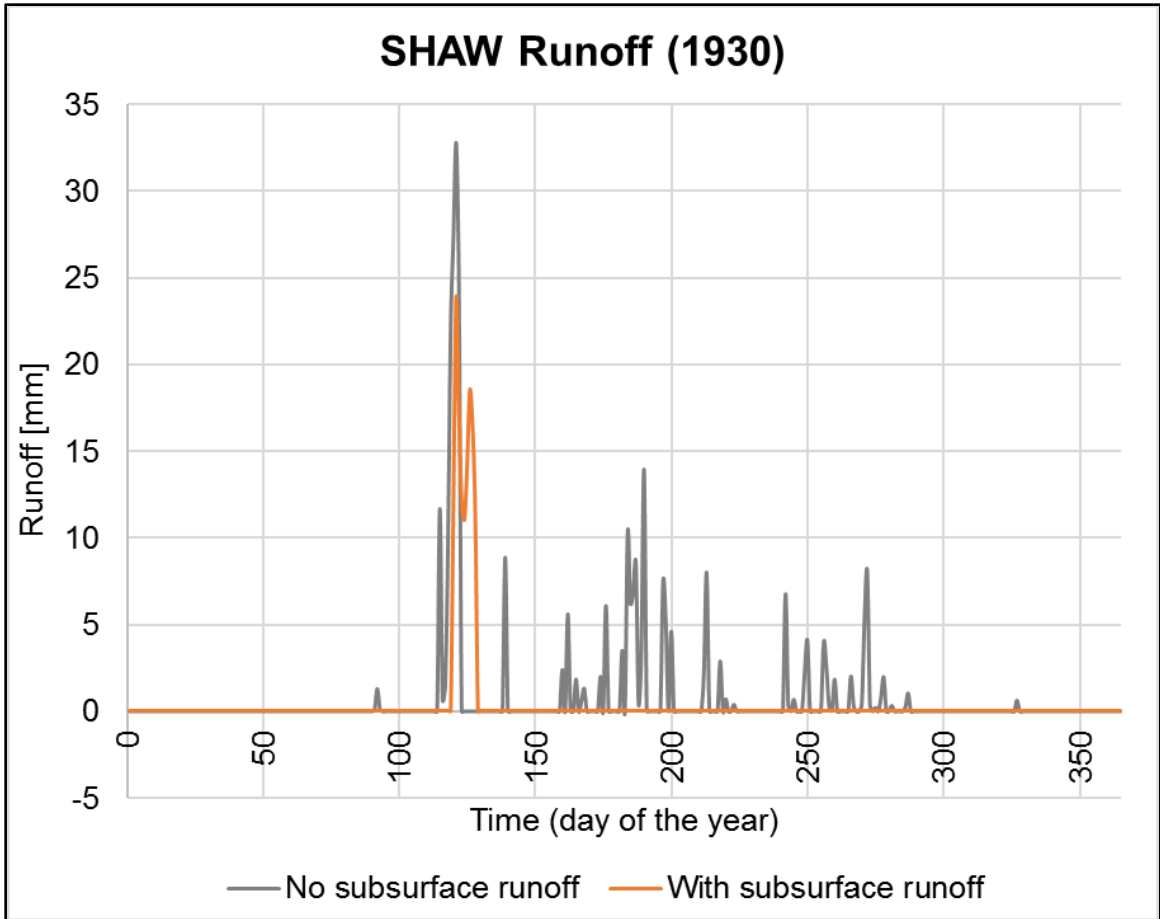
Figure 4-7: The surficial runoff of the first SHAW plateau model that does not include subsurface runoff and the second model that includes subsurface runoff. The 1930 cumulative surficial runoff for the model with no subsurficial runoff is 290 mm/year and with subsurficial runoff is 137.0 mm/year.

The daily SHAW water balance for the permafrost plateau model includes change in snow storage, runoff and evapotranspiration (Figure 3-8). The precipitation contributes to snow storage when the air temperature is below 0 ˚C. Runoff peaks at the same time as snow melt, when the ground surface is still frozen. Evapotranspiration occurs throughout the summer months at approximately 0.5 mm/day and does not happen through the winter months. The cumulative plateau evapotranspiration is approximately 50 mm/year. Measured cumulative evapotranspiration in Scotty Creek is approximately 270 mm/year; the measured value is larger than the modelled because

the measured value includes evapotranspiration from wetlands, unlike this SHAW
plateau model (Hayashi et al. 2004; Quinton and Hayashi 2005). The SHAW wetland
model has a cumulative evapotranspiration of approximately 315 mm/year.
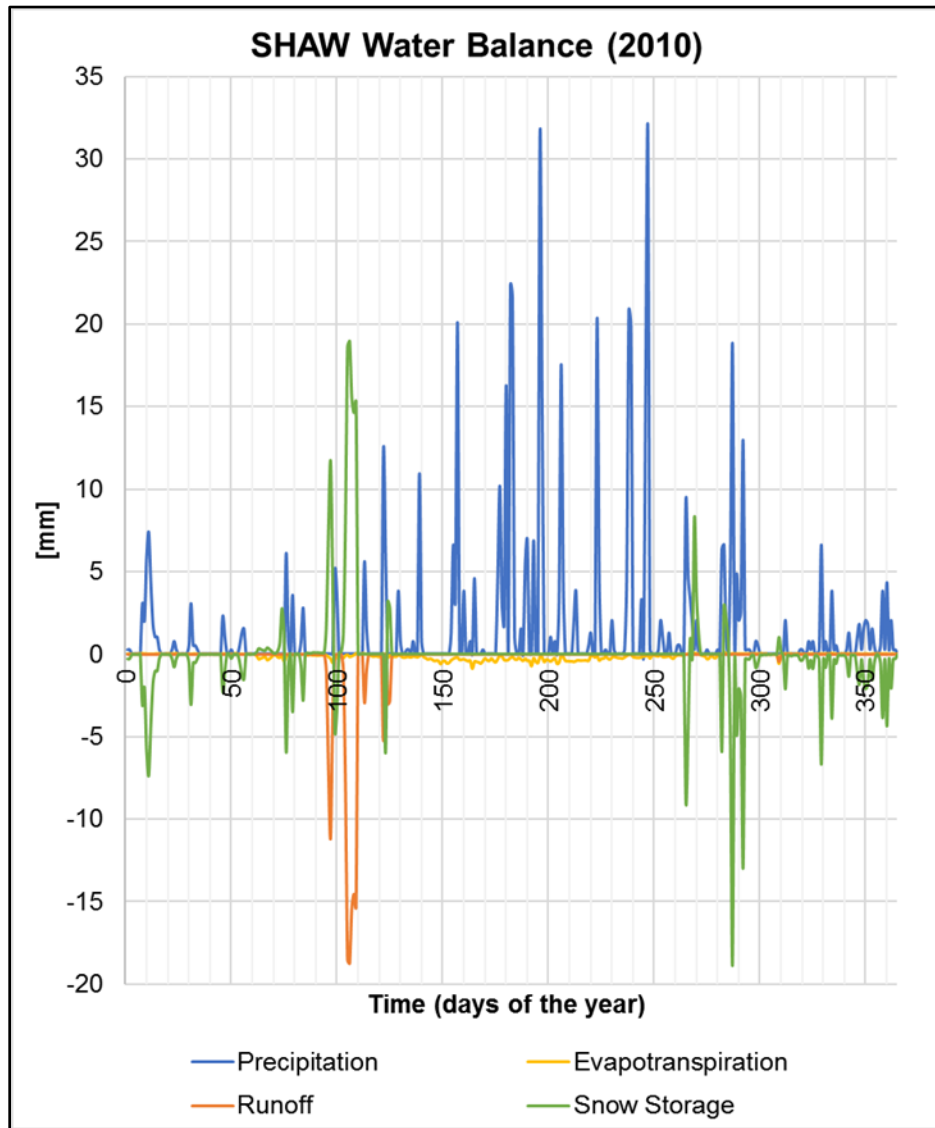
Figure 4-8: The SHAW plateau daily water balance output of 2010 (a typical water year). The
2010 annual total of precipitation is 585.4 mm, evapotranspiration is 50.5 mm and runoff is 129.6
mm.

The daily water balance computed in the SHAW model is used to determine the
daily net surface water transfer that is used as ground surface input for the FEFLOW

model (Figure 3-9). Most water enters the subsurface in the summer and fall when the

ground is thawed and there are large precipitation events. Very little water is transferred

at the ground surface during winter months when the ground is frozen and ice fills pore

space.
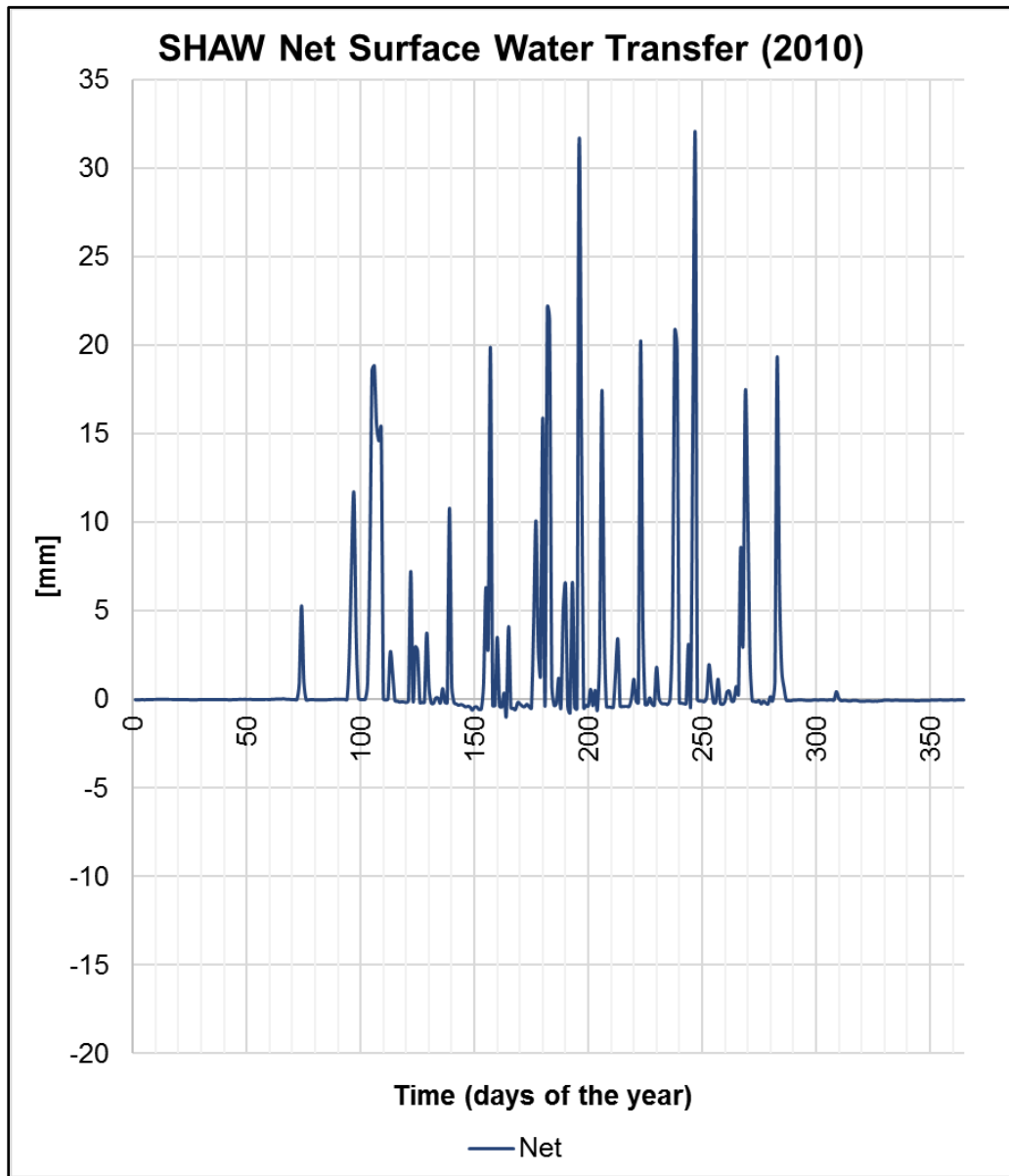
Figure 4-9: The net surface water transfer from the SHAW output water balance of 2010 (a typical water year). The 2010 cumulative net water transfer is 537.0 mm/year.

4.2 FEFLOW

4.2.1 Preliminary testing with hypothetical -1˚C permafrost bulb

Before starting the long 1875 transient run the FEFLOW model was tested over a shorter 2 year time period (2005 to 2007) to determine if the assigned ground properties were properly transporting water and heat (Table 2-4 and Figure 2-6). To develop a permafrost bulb that didn't require a long spin-up period, nodes were selected between 1 m and 16 m below the plateau ground surface and assigned a temperature of -1 ˚C. The remaining nodes were assigned a temperature of 1.5 ˚C. The model was run using daily net water transfer and average monthly temperature SHAW data from 2005 to 2007. The plateau and wetland temperatures were compared to temperatures measured in Scotty Creek and the results are presented and discussed in the following sections 3.2.1.1 and 3.2.1.2.

4.2.1.1 Plateau

The plateau ground temperatures compared well to the measured ground temperatures in the two-year preliminary test run (Figures 3-10 and 3-11). The modelled temperatures lack the daily temperature spikes because the average monthly ground temperature was applied, but they follow the same trend (Figure 3-10 and 3-11). The one-to-one plots of this preliminary test demonstrate how well the trends match with measured values (Figure 3-11). The MAE ranges from 0.06 ˚C at 0.7 m depth to 0.23 ˚C at 0.1 m depth. This test shows that heat is transferring appropriately from the surface thermal boundary condition into the supra-permafrost layer and the assigned ground properties are fitting.
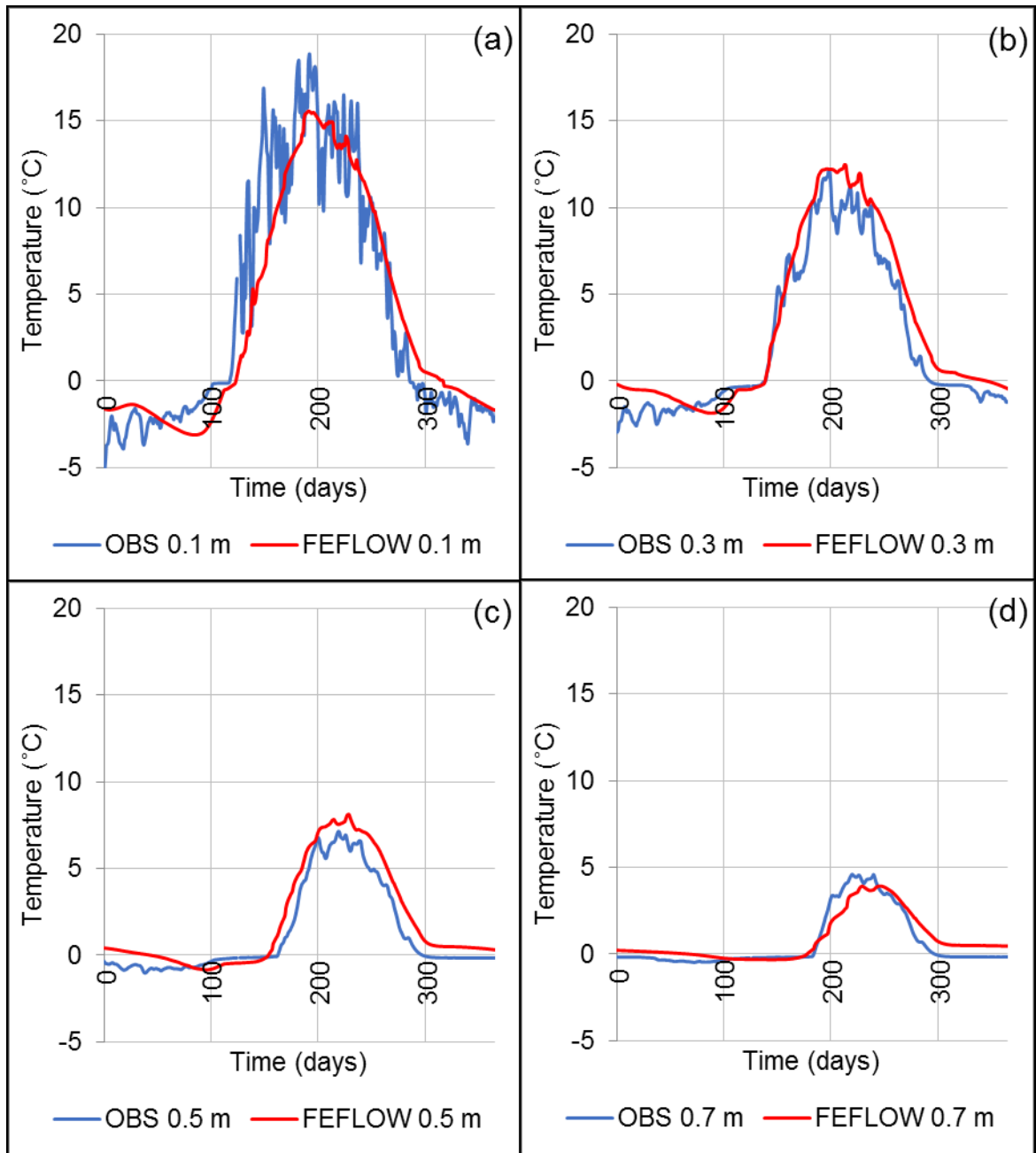
Figure 4-10: The measured versus modelled ('Plateau Middle' on Figure 3-2) plateau ground temperatures at depths (a) 0.1 m; (b) 0.3 m; (c) 0.5 m and (d) 0.7 m. Temperatures were measured on the southern tip of the permafrost plateau. ***The closest FEFLOW nodes are used in (c) and (d)

Figure 4-11: One-to-one plots of the plateau measured and preliminary test ground temperatures displayed in Figure 3-10 at depths 1) 0.1 m, b) 0.3 m, c) 0.5 m and d) 0.7 m. Model statistics are listed below the corresponding plot.

4.2.1.2 Wetland

The wetland calibration was not as close of a match as the plateau, sometimes varying as much as 4 ˚C (Figures 3-12 and 3-13). Wetland measurements were taken at approximate depths of 0.1, 0.5 and 1.3 m in the fen directly west of the plateau (Figure 3-2). At 0.1 m depth in the wetland the FEFLOW model underestimates winter temperatures, overestimates spring temperatures and performs well in the summer and fall months with a MAE ˚C of 0.21 ˚C (Figure 3-12 a). At this shallow depth, this reflects the applied SHAW temperatures (refer to section 3.1.1). A larger variance from measured temperature values and measured trend occurs at 1.3 m depth (MAE of 0.43 ˚C), which is stratigraphically below the floating mat (Figure 2-6 and 3-12 c). At depths of 1.3 m FEFLOW overestimates the temperature in the summer by a maximum of 5 ˚C and underestimates temperatures in the fall by approximately 2 ˚C. The largest FEFLOW underestimation of temperature is approximately 3 ˚C at the onset of fall (225th day of the year; Figure 3-12 c). The trend does not match as well at the depth 1.3 m and this is a sign that heat is not being transported with depth in the wetland accurately (Figures 3-12 c and 3-13 c).
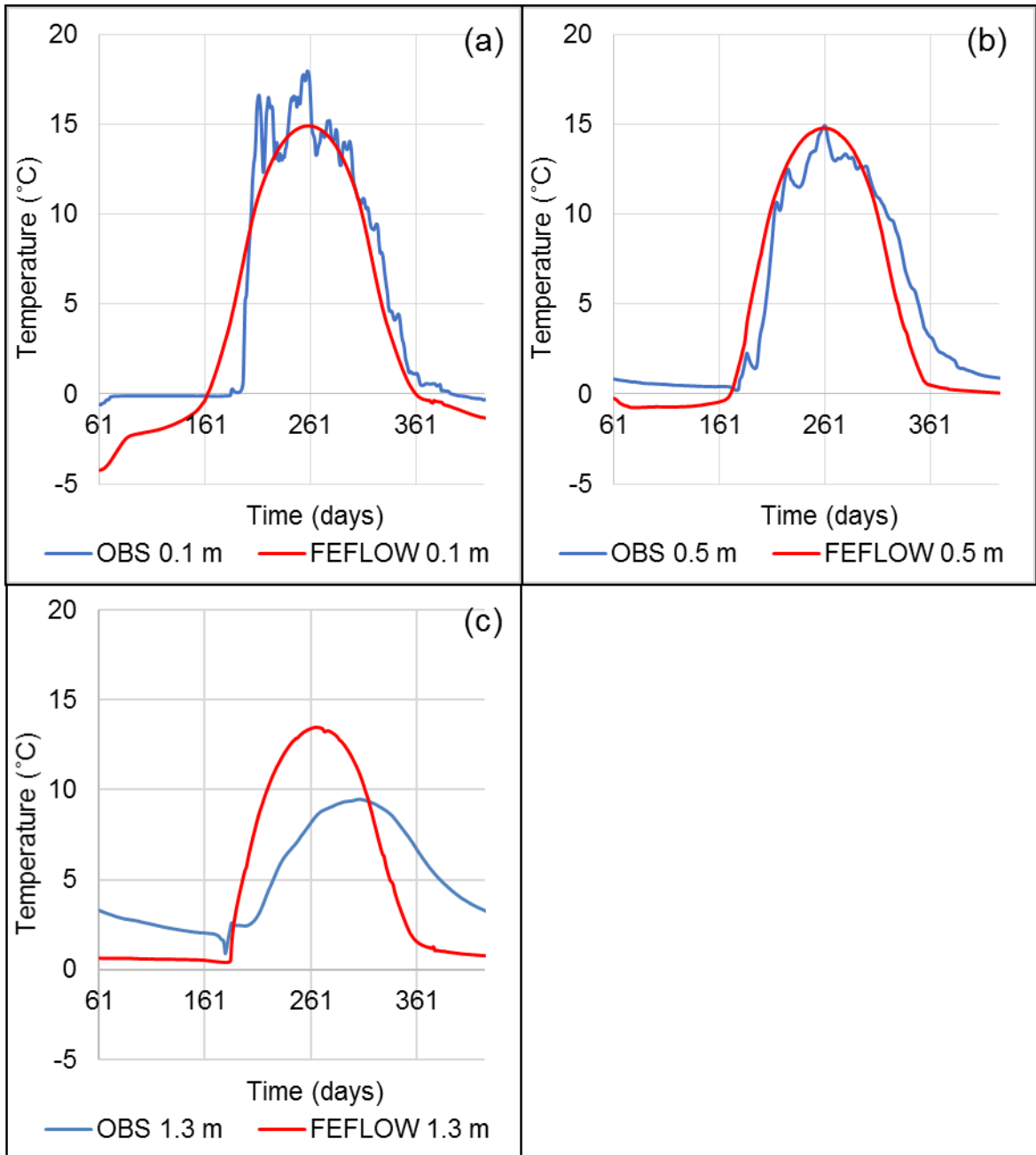
Figure 4-12: The measured versus modelled ('Fen Middle' on Figure 3-2) wetland ground temperatures at depths (a) 0.1 m; (b) 0.5 m and (c) 1.3 m. The temperatures were measured in the fen to the west of the plateau.
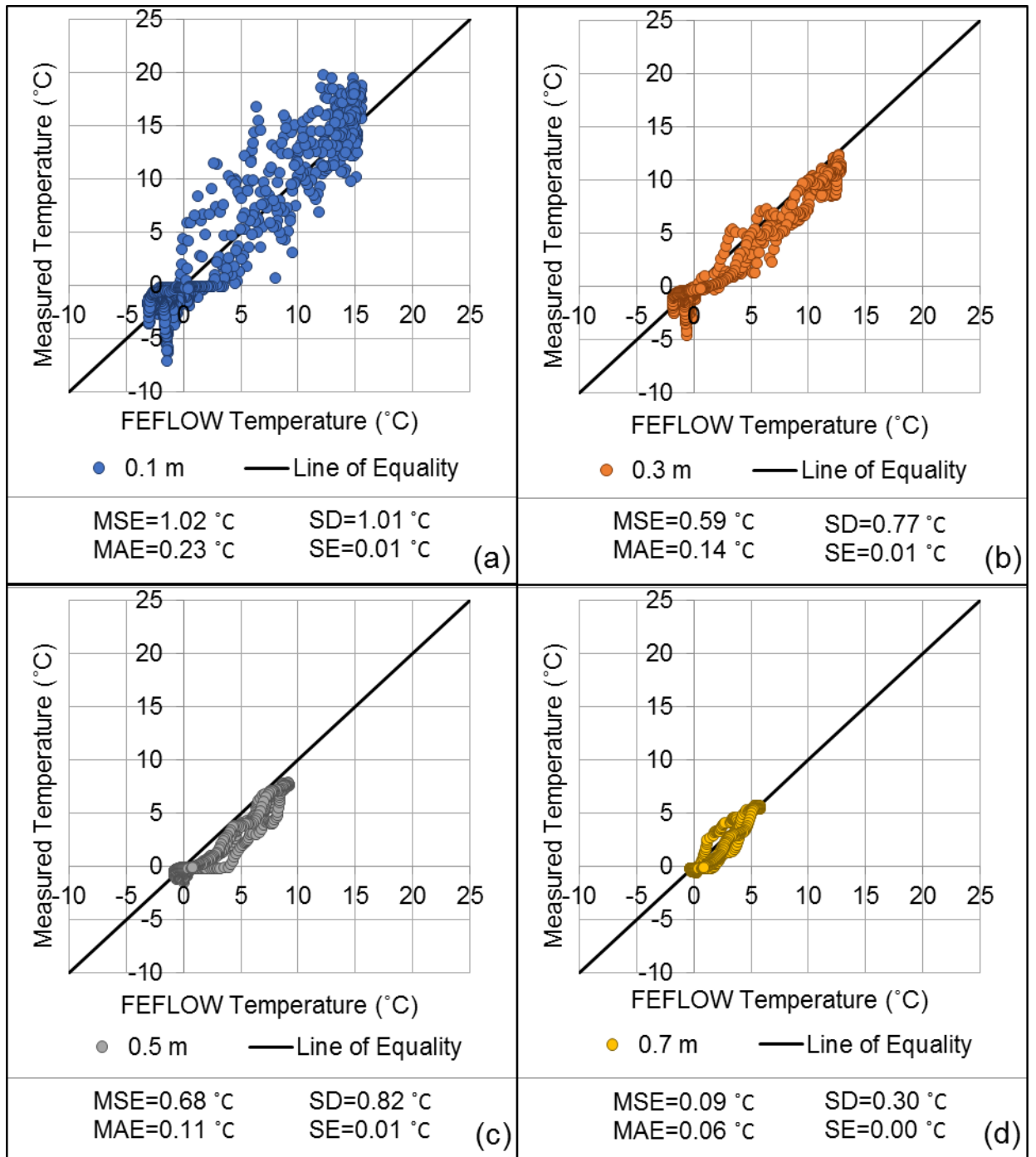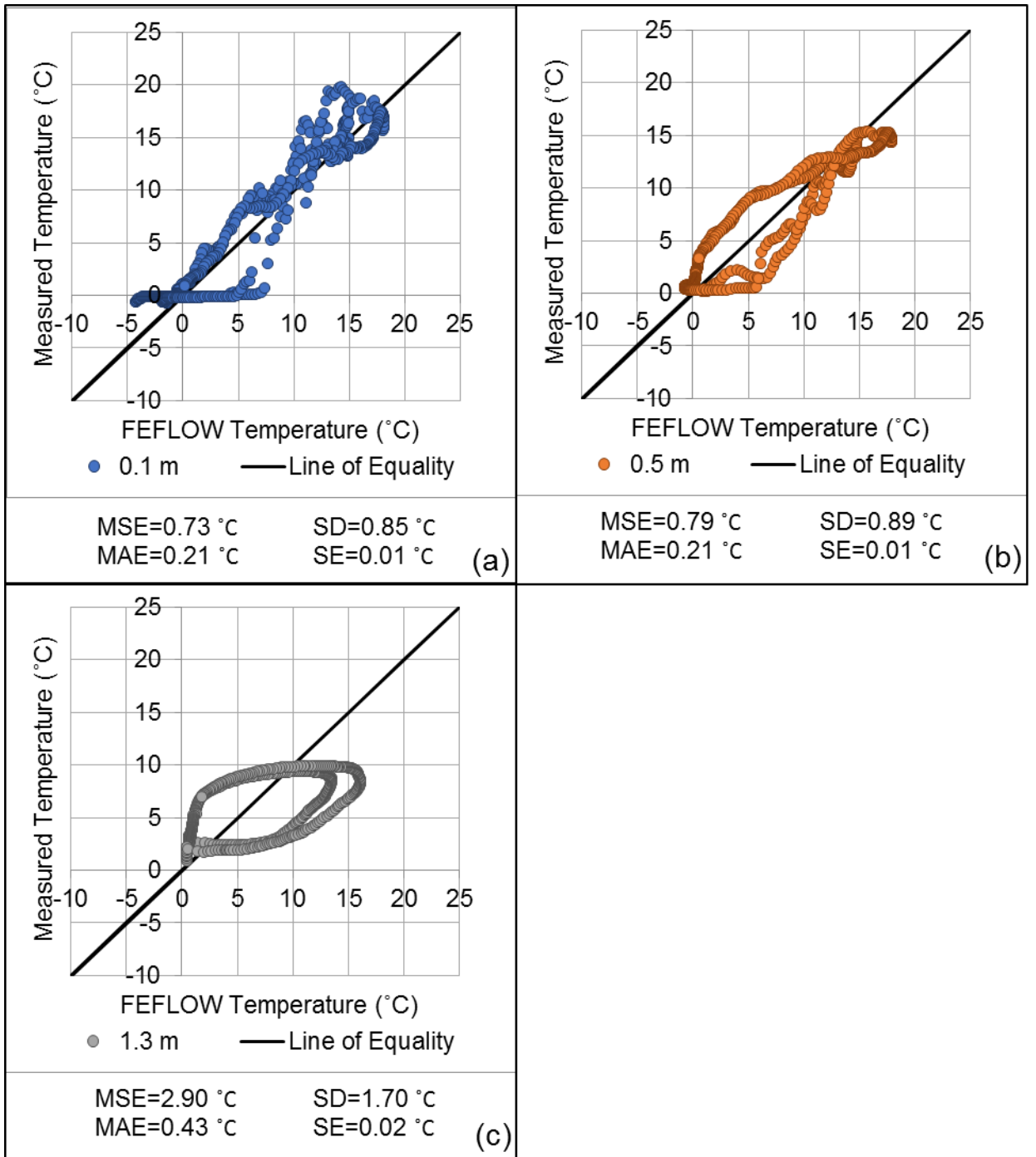
Figure 4-13: One-to-one plots of the wetland measured and preliminary test ground temperatures displayed in Figure 3-10 at depths 1) 0.1 m, b) 0.5 m and c) 1.3 m. Model statistics are listed below the corresponding plot.

A pressure transducer that also records temperature was installed in the same wetland location adjacent to the plateau in 2014. This allowed for accurate depth from wetland surface measurements to be recorded throughout the year with temperature. Measurements show that the surface elevation of the fen fluctuates throughout the year, early summer/spring being the highest and winter being the lowest, with a difference of approximately 0.5 m (Figure 3-14). Fens are technically surface water features; however, they are being represented as completely saturated subsurface features in this FEFLOW model. Because fens are surface water features, their surface elevation moves up and down with the water level. The floating mat moves with the water level relative to the fixed thermistors (Figure 3-14). This process is not represented in FEFLOW due to the stationary model domain and this is likely a cause of temperature discrepancies between 1.3 m measured and FEFLOW modelled wetland temperatures. This difference is especially evident during the spring freshet. During spring, fen water levels peak and there is increased flow as the hydraulic gradient in the region increases, diluting the surface temperature effects. In the FEFLOW model, spring is represented by a larger infiltration, but the surface elevation remains the same and the fen thaws from the surface elevation down. Once thaw reaches the observation point the temperature abruptly rises (Figure 3-12 c). This seasonal temperature damping effect causes overestimated summer temperatures and underestimated winter temperatures, which results in the ovoid pattern in the 1.3 m one-to-one plot (Figure 3-13 c). Another factor that would cause differences between the 1.3 m measured and modelled temperatures, is the development of a larger connected thermal system. At Scotty Creek, this fen is connected to a lake that is not represented in this model.
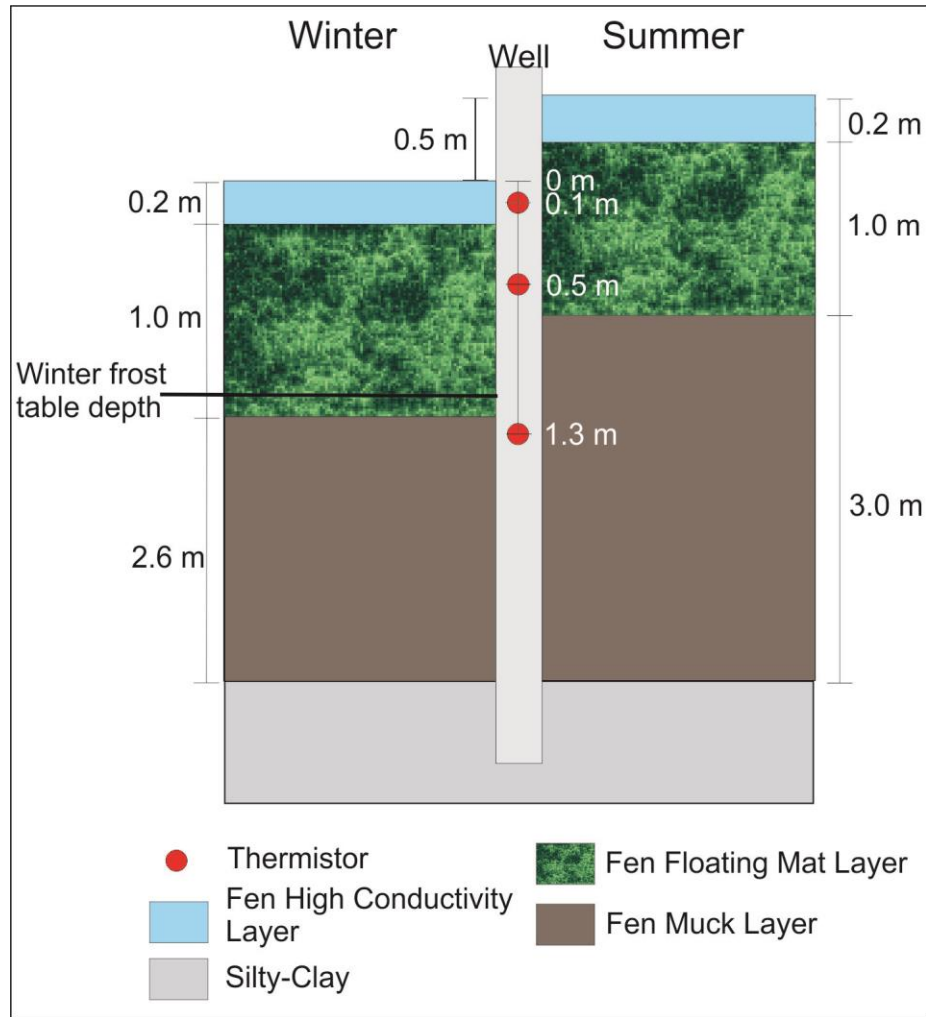
Figure 4-14: A schematic of a static well in the Scotty Creek fen holding thermistors. The schematic demonstrates the relative changes in elevation of the fen layers with low winter water levels and high summer water levels.

4.2.2 Steady state permafrost development

In the steady state model the ground temperatures used to develop the initial permafrost bulb were selected based on a study by Kurylyk et al. (2016). Ground surface temperatures of -2.5 °C and 1.3 °C were applied to the plateau and wetland respectively. A basal temperature of 1.5 °C was applied across the entire base model boundary. The resulting permafrost bulb is displayed in Figure 3-15. The base of the permafrost is rounded, with the deepest portions in the center of the plateau. The 1.3 °C temperatures

applied on the wetlands prevented permafrost from developing shallower than 10 m, but permafrost does underlie some smaller wetland regions between permafrost plateaus due to adjoining adjacent bulbs (Figure 3-17).
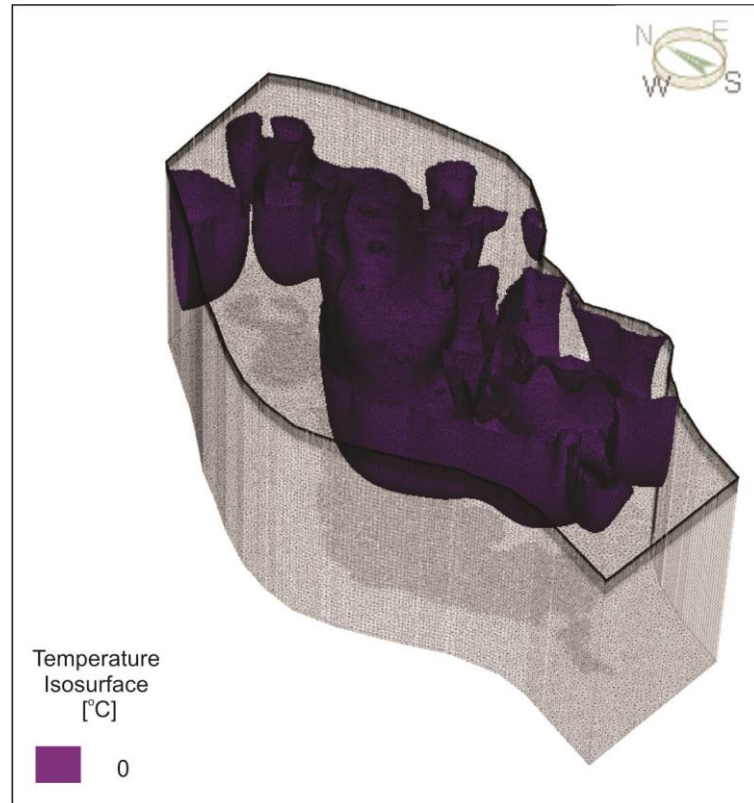
Figure 4-15: A three-dimensional image of the 0 ˚C iso-surface developed in steady state within the model domain.

McClymont et al. (2013) used electrical resistivity tomography (ERT) and ground penetrating radar (GPR) to determine permafrost depth at the southern tip of the plateau (approximately E-F line in Figure 3-16). These tools revealed the permafrost extends to approximately 15 m depth at this location. This compares well to the 16 m depth for the permafrost bulb developed with a steady state ground temperature of -2.5 ˚C applied to the plateau ground surface. To see how sensitive permafrost depth is to surface temperatures, ground temperatures of -1 ˚C and -3 ˚C were applied and compared

(Figure 3-17). The locations of the cross-sections used to display the resulting steady state temperature distributions are displayed in Figure 3-16. Steady state temperatures of -1 °C and -3 °C generated a bulb of approximately 5 m and 20 m depth respectively at the southern tip. Thus the bulb geometry that best matched the measured geometry was developed from steady state ground temperatures of -2.5 °C, agreeing with the study by Kurylyk et al. (2016).
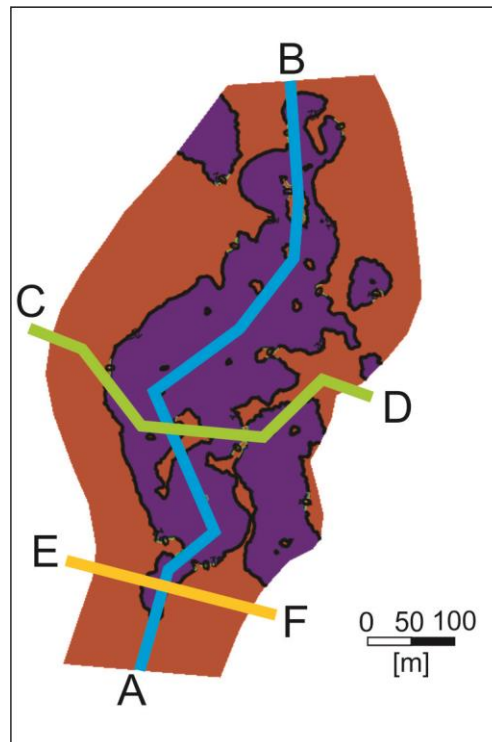
Figure 4-16: Map of the various cross sections used in the following figures.
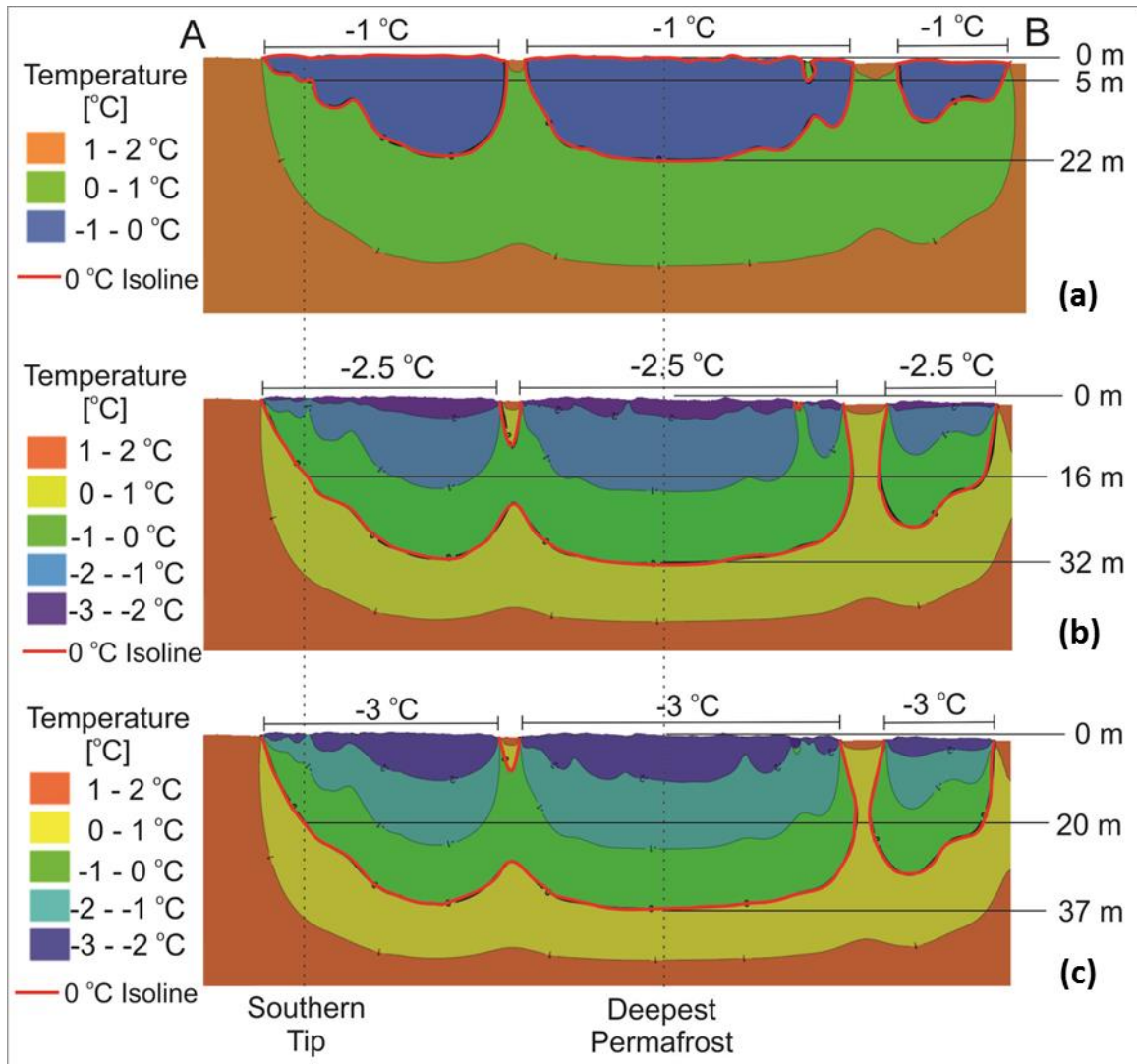
Figure 4-17: Cross sections (Location displayed in Figure 3-15) of steady state temperature profiles with wetland temperatures applied of 1.3 ˚C, a base temperature of 1.5 ˚C and plateau temperatures of (a) -1 ˚C; (b) -2.5 ˚C and (c) -3 ˚C. The depths of the deepest permafrost and depth below the southern tip of the plateau are displayed.

4.2.3 Transient Model Simulations

4.2.3.1   1875-1924 transient model run

After developing a permafrost bulb in steady state (Figure 3-15), the model was run transiently, applying the SHAW model derived plateau and wetland surface temperatures and net surface water transfer (i.e. infiltration). The progression of

permafrost thaw was continually monitored throughout the model run. After

approximately 30 years it became apparent that the permafrost was thawing more

rapidly than anticipated, and the permafrost bulb would not last the entire 140-year

model run to represent the permafrost in 2008 (Figure 1-2). The transient model was

stopped at 50 years (1875-1924) and the results are presented as in Figures 3-18 and 3-

19. The simulation was ended at 50 years because it became clear that continuing with

this model run would not result in an accurate model of the 2000-2015 field instrumented

permafrost plateau.

It is hypothesized that the permafrost melted more rapidly than the permafrost

that existed in 1875 because the plateau, and thus permafrost bulb, was much more

laterally extensive in 1875 (Figure 1-2). The oldest available imagery of the plateau

dates to 1947 (Figure 1-2). Comparing the 1947 and 2008 imagery shows how the

currently modelled region was once surrounded to a much larger degree with permafrost

(Figure 1-2). The current modelling effort had to utilize the current topography and

permafrost distribution as no 1875 data is available. Therefore, the model run from 1875

to 1925 essentially demonstrates what would happen if a plateau of today's geometry

was exposed to the climate of 1875 to 1924 and the results are displayed and discussed below.
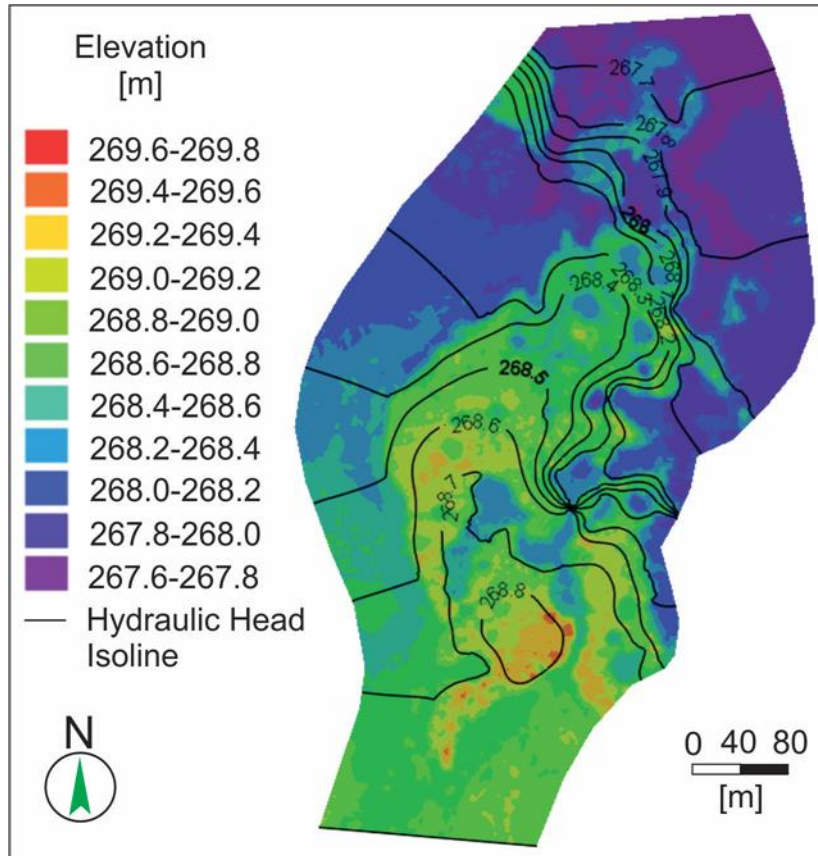
Figure 4-18: The model typical summer hydraulic head distribution.

The summer hydraulic head distribution agreed well with the conceptual model (Figures 2-3 and 3-18). Water flowed into the model at the southern boundary and continued to flow north around the plateau and through the surrounding wetlands. Water also entered the model through the surface boundary during precipitation events. Water that entered the model above the plateau flowed along the supra-permafrost table downgradient into surrounding wetland or into local depressions in the permafrost. The water table was maintained along the surface elevation of the wetlands. The defined hydraulic heads at the northern and southern boundary prevented the water table from

moving up and down as much as it does in Scotty Creek and this is reflected in the fen

temperatures, but had little effect on the plateau.
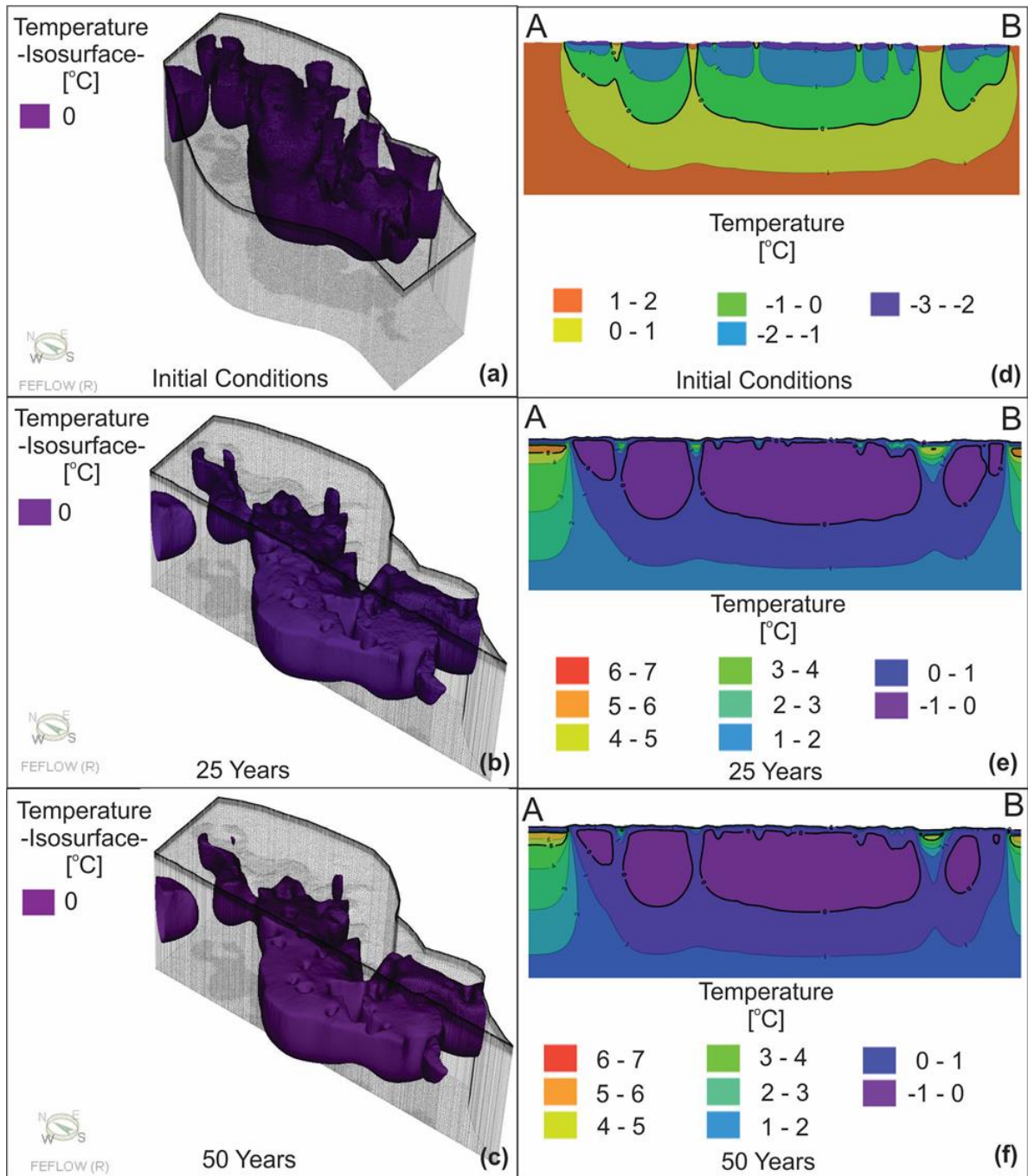
Figure 4-19: The progression of the permafrost thaw over a 50-year model run from initial conditions in 1875 to 1924. A 3-dimensional iso-surface is depicted in a) 1875; b) 1900 and c) 1924. A cross section (refer to Figure 3-16 for location of cross section) is depicted in d) 1875; e) 1900 and f) 1925.
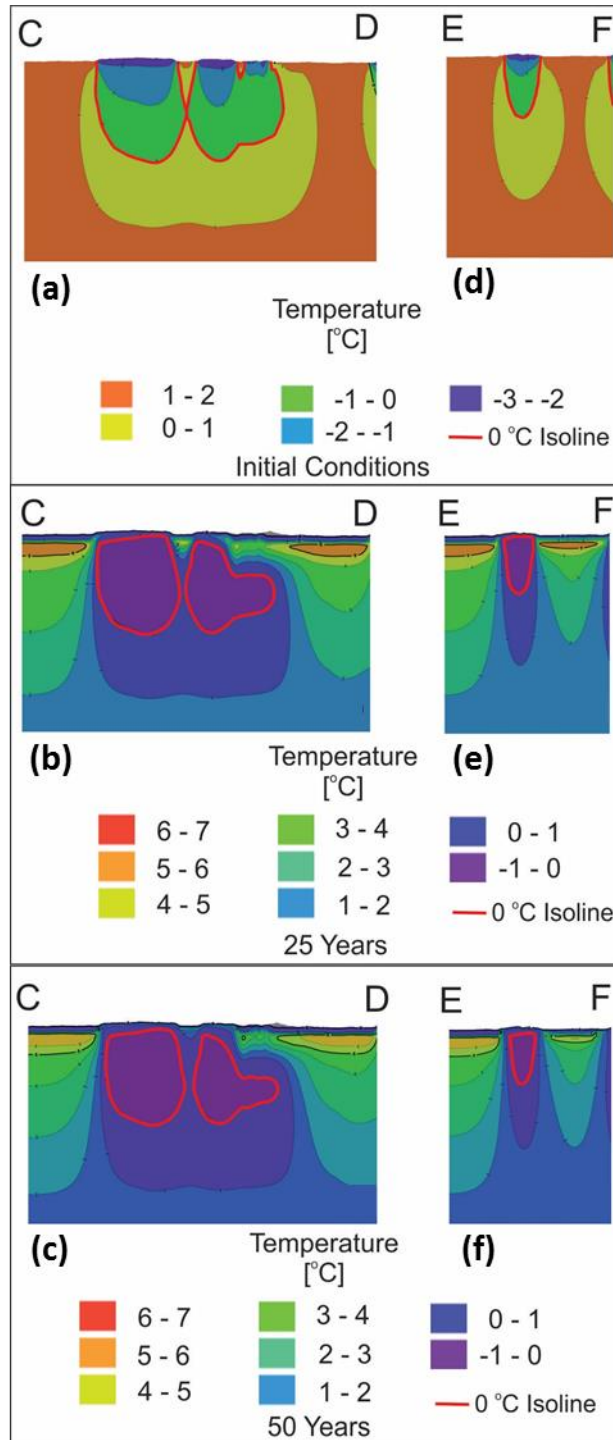
Figure 4-20: Cross sections (refer to Figure 3-16 for cross section location) of the progression of permafrost thaw from initial conditions along the middle of the plateau in a), b) and c) and along the southern tip of the plateau in d), e) and f).

There is a defined spin-up period between the steady state temperatures and transient temperatures. A spin-up period is the time required to bring a transient model from its initial, typically steady-state, conditions to transient conditions. This is demonstrated by the rate of change of the plateau and wetland temperature (Figures 3-21 and 3-23). Based on this model run, the spin-up period takes approximately 2-3 years for the rate of permafrost (depths 4.48 m and 12.88 m below plateau surface) temperature change to approach zero (Figure 3-21). These rates will never reach zero because the permafrost is unstable and thawing due to the warming climate. The rates of temperature change within the permafrost should be near zero as the permafrost temperature measurements in Scotty Creek remain just below zero (approximately -0.2 ˚C) due to the zero-curtain effect during phase change. The average rate of change of permafrost temperature, after the spin-up period of 3 years, at a depth 12.88 m for observation point 'Plateau Middle' is 0.007 ˚C/year (Figures 3-2 and 3-21). The spin-up period of 3 years brings the permafrost temperatures to just below 0˚C (Figure 3-23).
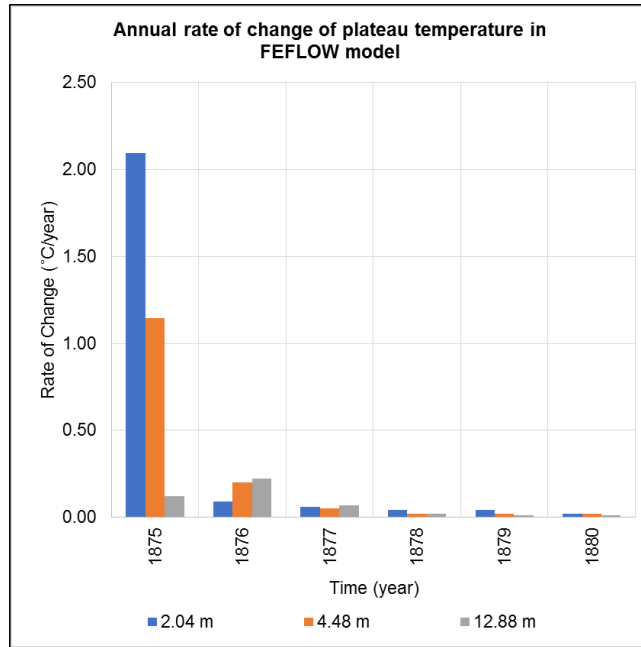
Figure 4-21: The annual rate of change in temperature at different depths at the 'Plateau Middle' (Figure 3-2) observation point location.
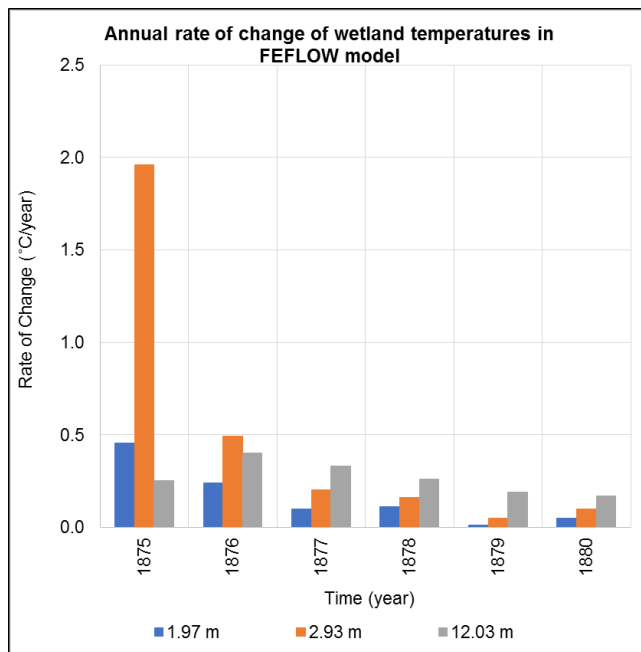
Figure 4-22: The annual rate of change in temperature at different depths at the 'Fen Middle' observation point location (Figure 3-2).
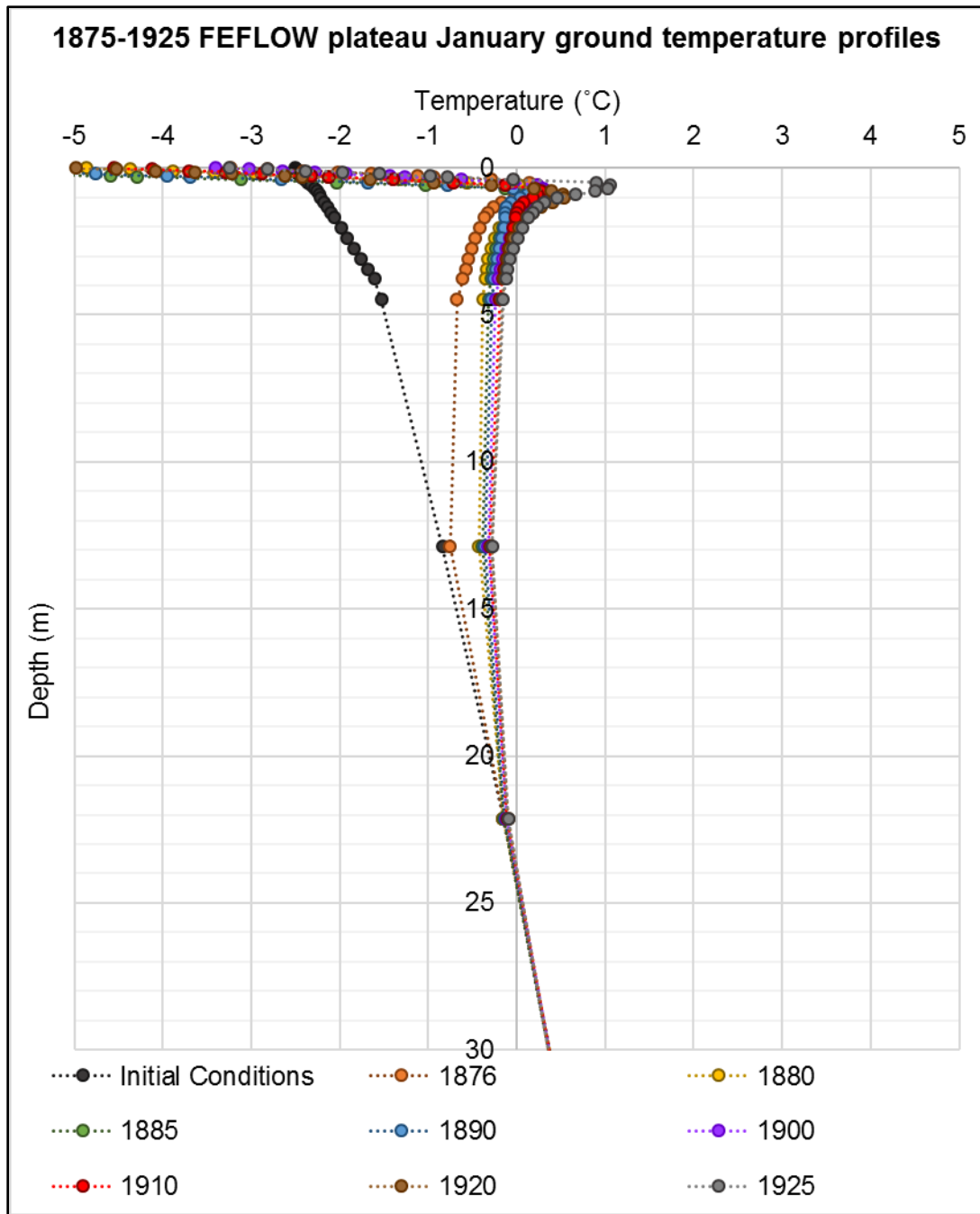
Figure 4-23: Modelled ground temperature profiles through time at the 'Plateau Middle' observation point location (Figure 3-2).

The temperature rates of change in the wetland are more variable than the permafrost following the first year (Figure 3-22). This is because the wetland is not undergoing phase change and is not being affected by the zero-curtain effect like the

permafrost and their temperature changes are more reflective of a changing annual climate. The transient climate caused the wetland temperatures to warm from the initial 1.5 ˚C temperature at the fastest rate in the saturated organic material in the fen, above the silty-clay which starts at approximately 3 m depth (Figures 3-22 and 3-24). The silty-clay warms at a relatively constant rate over the 50-year transient run (Figures 3-22 and 3-23).
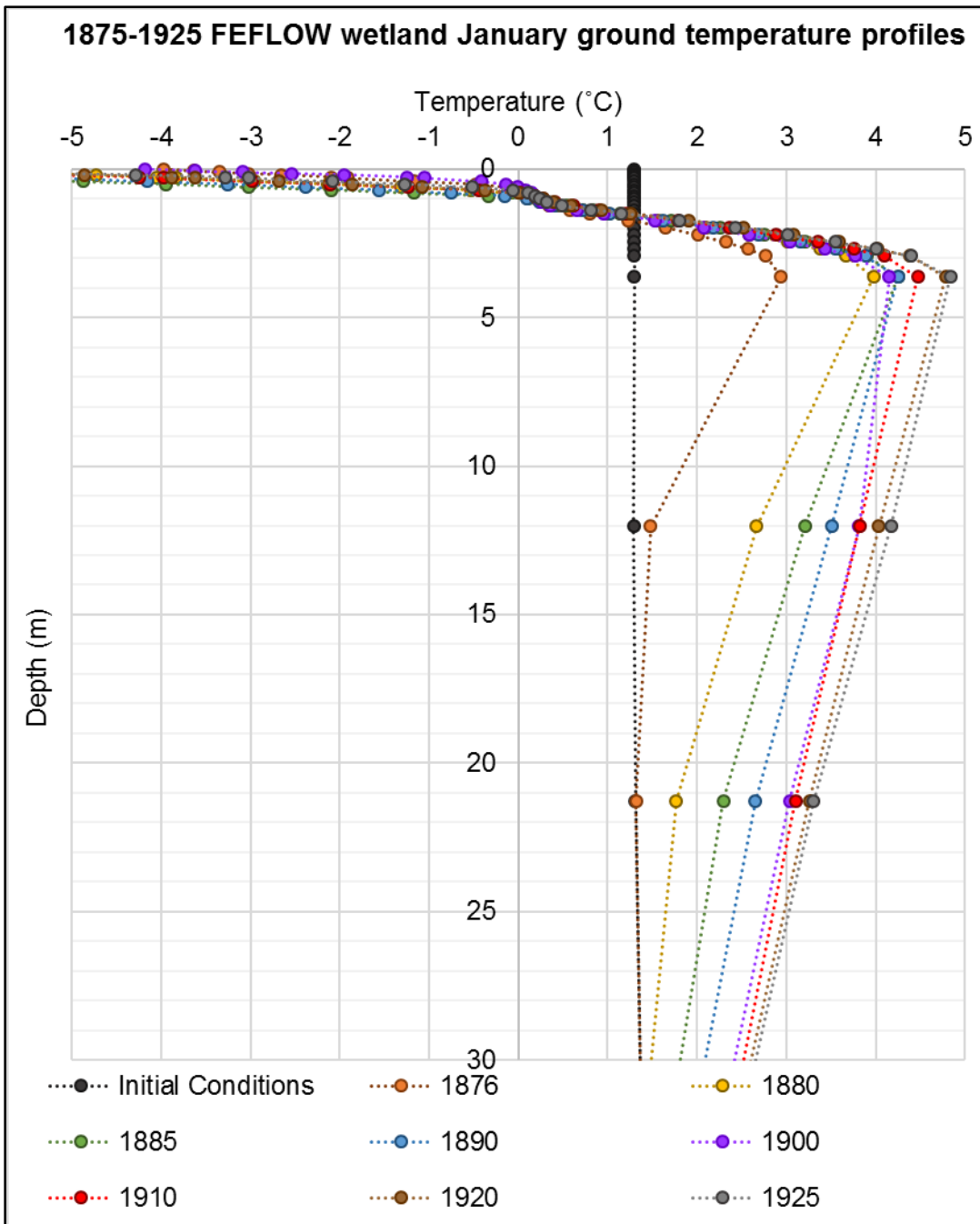
Figure 4-24: Modelled ground temperature profiles through time at the 'Fen Middle' observation point location (Figure 3-2).

The thinnest portions of the permafrost bulb, the north and south points, thawed at the quickest rate (Figure 3-19). The eastern half of the permafrost plateau thawed vertically from the surface more rapidly than the western half (Figure 3-20). The western

portion of the plateau has a relatively smooth higher elevation and the eastern half

consists of many small depressions. Water collects in these small depressions,

generating regions of higher bulk thermal conductivity than the surrounding elevated

drier peat (Equation 2.5 and Table 2-4). This increased bulk thermal conductivity leads

to increased vertical permafrost thaw and talik development. Permafrost with and without

an overlaying talik deepened at rates of approximately 0.04 m/year and 0.1 m/year

respectively (an example of this calculation is located in table A1 in the appendix). These

rates were found by measuring the depth over time at various portions of the plateau

and calculating the average rate of deepening. The horizontal thinning of the plateau

from the eastern side and western side of the plateau were both approximately 0.5

m/year (an example of the calculation is located in table A2 in the appendix). This

confirms that the reason for the eastern portion of the plateau thawing more quickly is

due to vertical thermal effects and not horizontal effects from the adjacent wetlands

(Figure 3-20).

4.2.3.2   1999-2015 transient run

The purpose of this model run is to represent a modern day thawing permafrost

bulb in three-dimensions including topography, the unsaturated zone and the freeze-

thaw processes that occur in the active layer. The first transient run from 1875 to 1924

run demonstrated that a spin-up period of approximately 3 years is required to transition

the model from steady state to transient conditions. To model modern-day permafrost

(2000-2015) the same steady-state permafrost bulb development method of applying -

2.5 °C and 1.3 °C applied over the permafrost and wetlands respectively, is used

followed by the application of 1999-2015 transient SHAW data. These results can be

compared to measurements taken in Scotty Creek (Figures 3-30 and 3-32). However,

again we cannot expect close correlation with field data as the current Scotty Creek

permafrost distribution did not result from warming the current plateau / wetland geomorphic expressions.

The thaw of the permafrost bulb is exhibited in Figures 3-25 and 3-26. By 2015 a talik over the entire plateau of approximately 2 m has developed (Figure 3-28). Field studies have found sporadic taliks on plateaus, but not this extensive. This is a sign that the warm summer temperatures are moving through the supra-permafrost layer and thawing the permafrost too quickly. Temperature depth profiles demonstrate that the most warming is occurring in the peat (upper 4 m), in which the permafrost in the peat has nearly completely thawed by 2015 leaving permafrost only in the silty-clay (Figure 3-28).
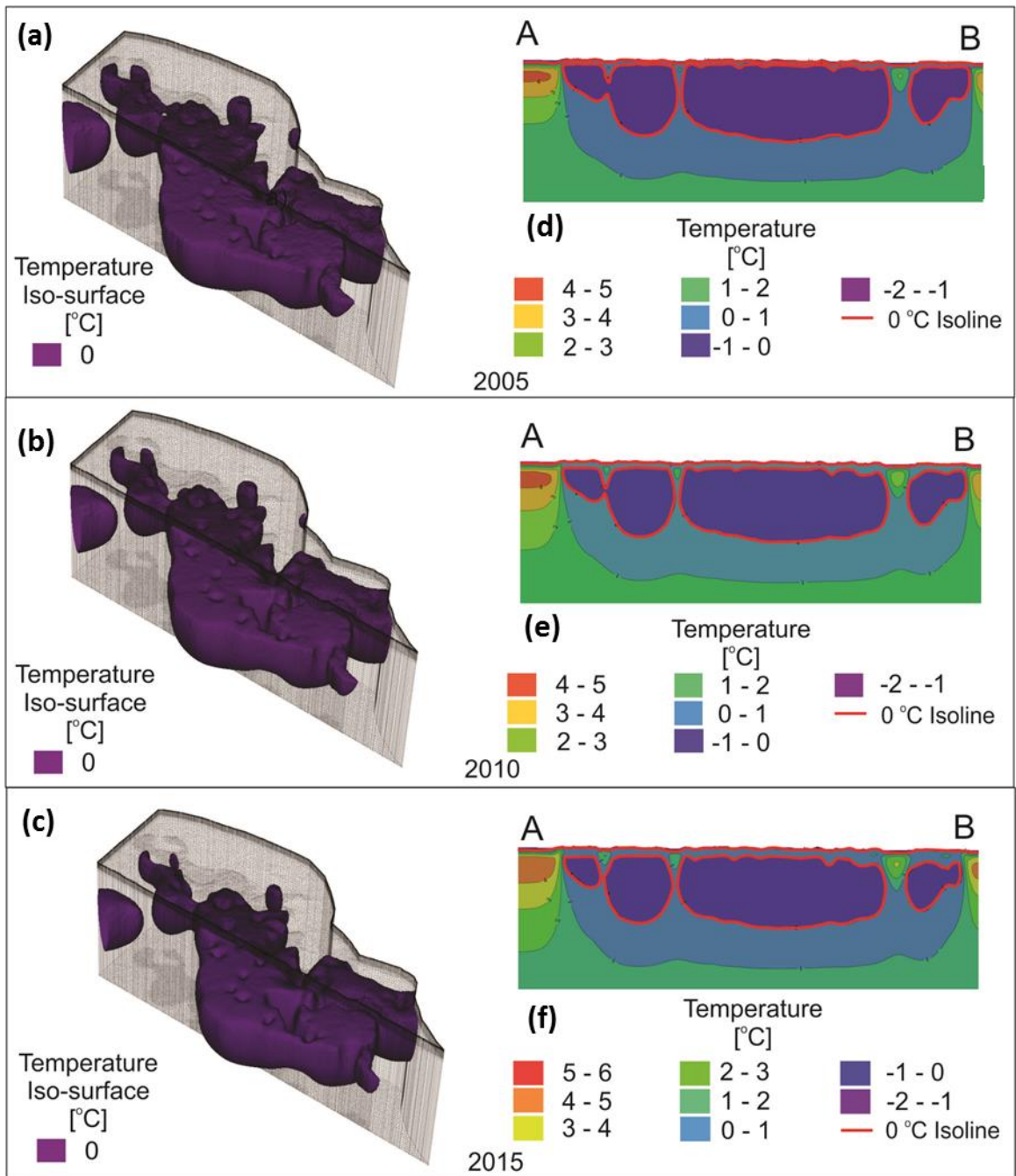
Figure 4-25: The progression of the permafrost thaw over a 15-year model run starting in steady-state initial conditions. A three-dimensional iso-surface in September is depicted in a) 2005; b) 2010 and c) 2015. A cross section in March (refer to Figure 3-16 for location of cross section) is depicted in d) 2005; e) 2010 and f) 2015.
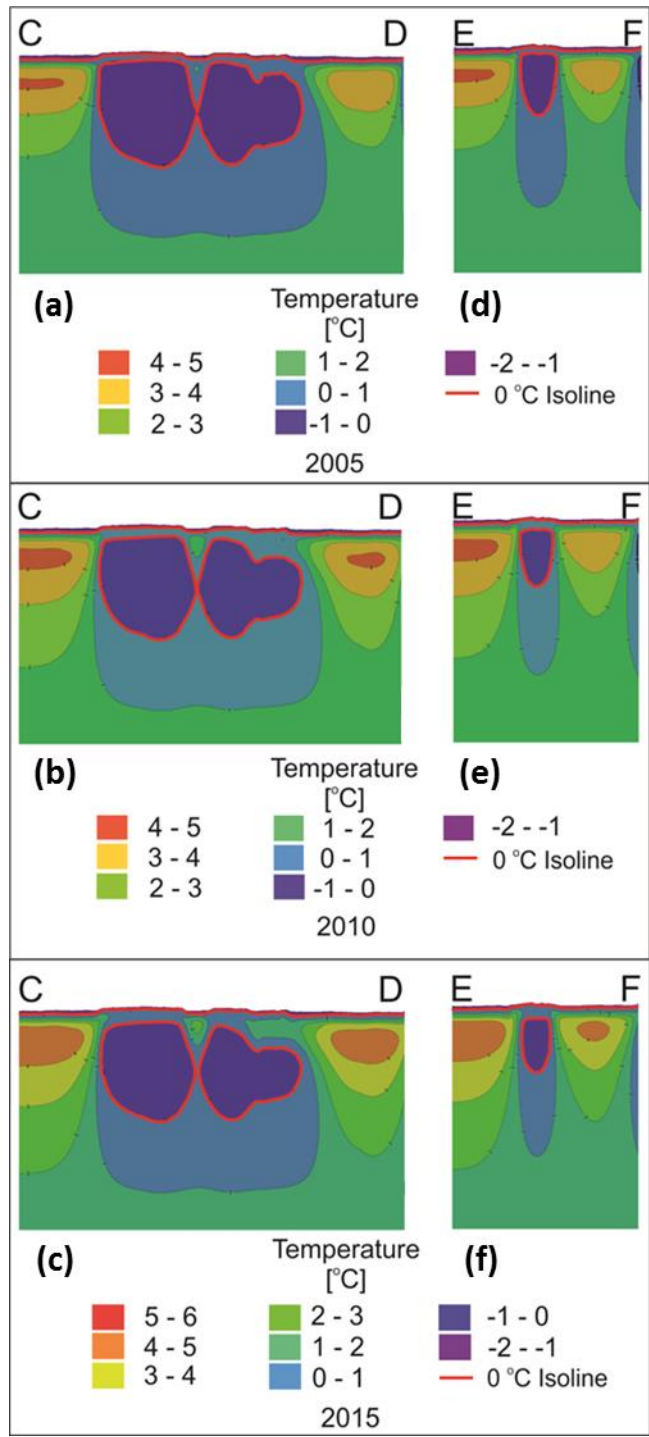
Figure 4-26: March cross sections (refer to Figure 3-16 for cross section location) of the progression of permafrost thaw from steady-state initial conditions to 2015 along the middle of the plateau in a), b) and c) and along the southern tip of the plateau in d) e) and f).

The permafrost annual temperature rates of change in the 1999-2015 transient run is similar to the temperature rates of change in the 1875-1924 run with an average rate of permafrost (12.88 m depth) temperature of 0.0065 ˚C/year (Figure 3-27). The permafrost temperature stabilizes after approximately 3 years and the greatest rate of temperature change occurs at shallower depths below plateau ground surface (0-4 m) (Figure 3-28). Ground temperatures in 2000 are on average approximately 1.5 ˚C warmer than 1875 ground temperatures, which caused increased warming of the 2000 model relative to the 1875 model (Figure 3-1). In the 1875 model run the permafrost thawed to a depth of approximately 2.5 m after 50 years of transient boundary conditions (Figure 3-23). In the 2000 transient model the permafrost thawed to a depth of approximately 3.5 m after only 15 years (Figure 3-28). The 2000-2015 wetland temperature profiles progress in a very similar manner to 1875-1925 temperatures, except about a degree warmer due to the warmer climate conditions (Figures 3-24 and 3-29).
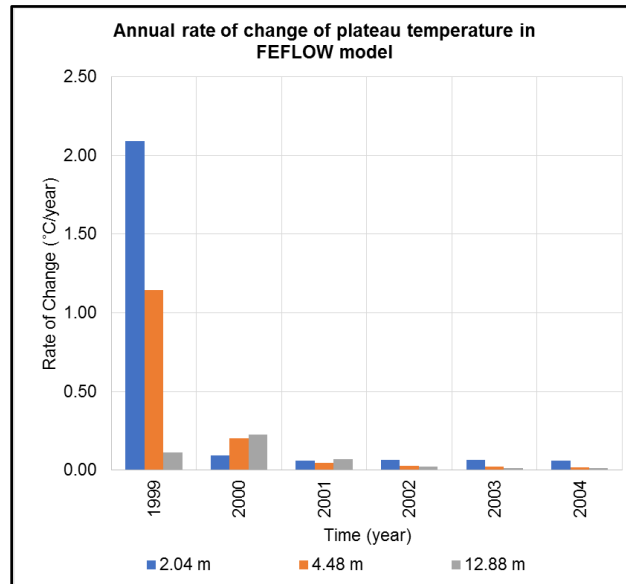
Figure 4-27: The annual rate of change in temperature at different depths at the 'Plateau Middle' (Figure 3-2) observation point location from initial conditions (1999) to 2004.
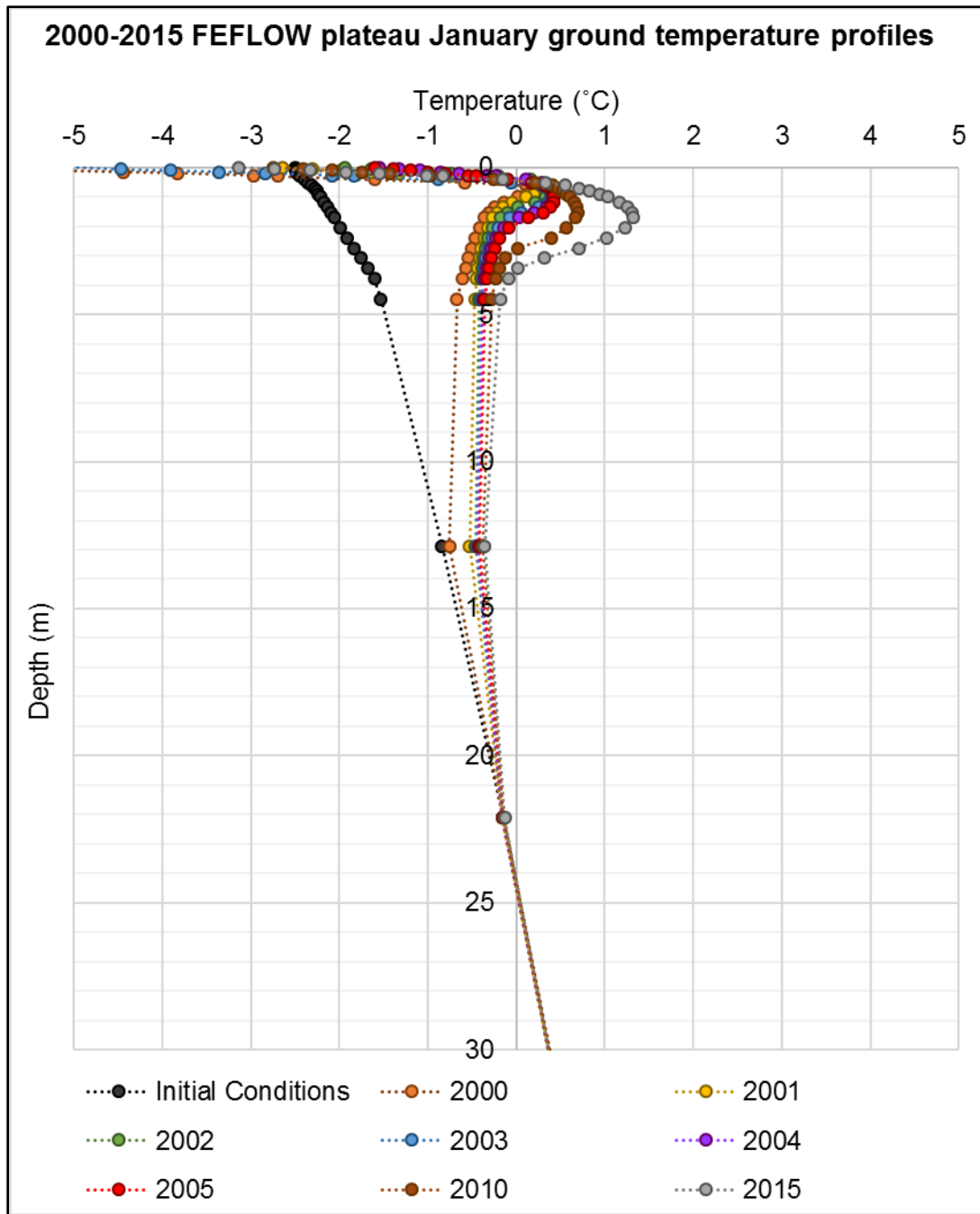
Figure 4-28: Modelled plateau ground temperature profiles through time at the 'Plateau Middle' observation point location from initial conditions (1999) to 2015 (Figure 3-2).
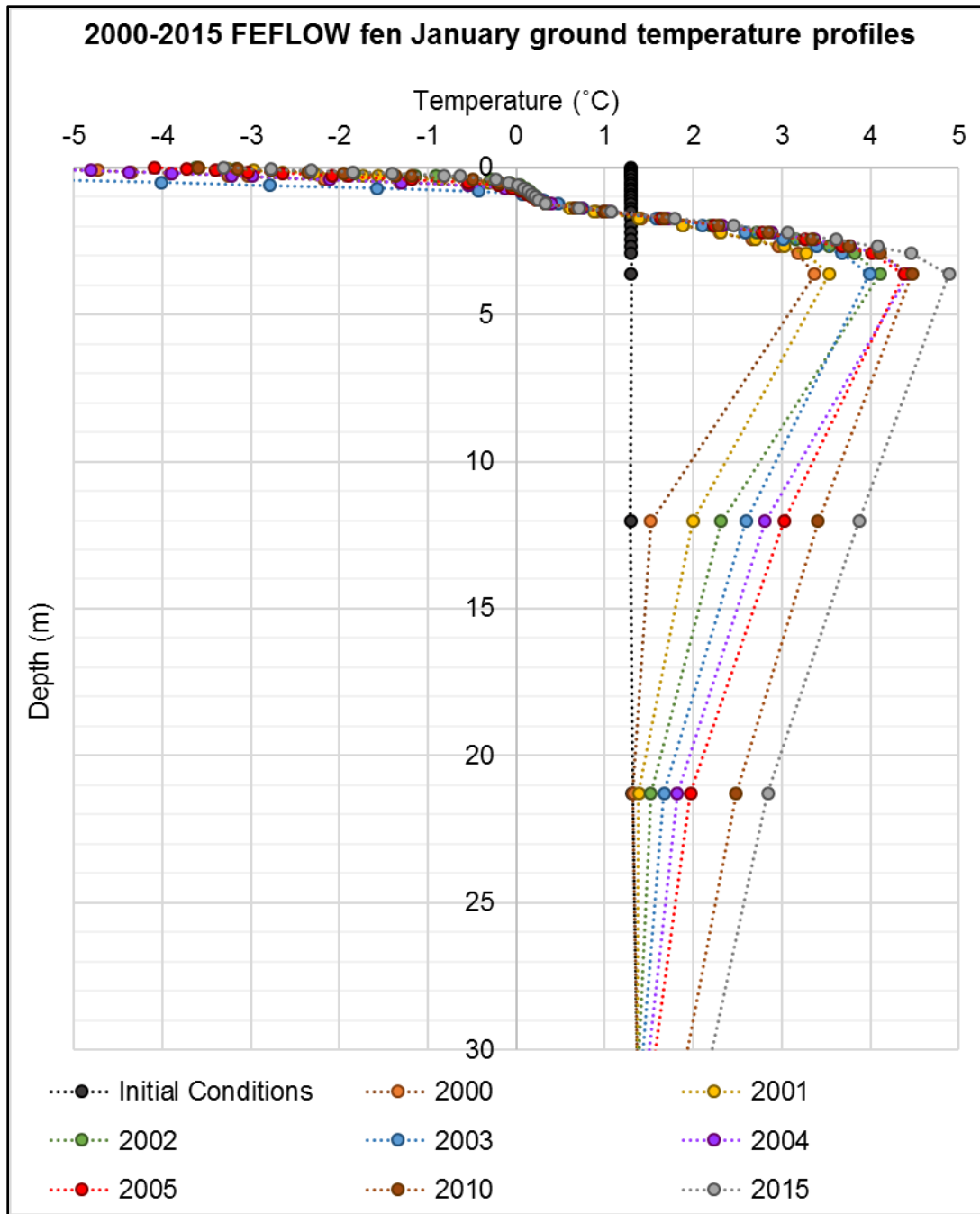
Figure 4-29: Modelled fen ground temperature profiles through time at the 'Fen Middle' observation point location from initial conditions (1999) to 2015 (Figure 3-2).

The Scotty Creek measured and FEFLOW modelled plateau temperatures are displayed below in Figure 3-31. The shallow temperatures at 0.1 m and 0.3 m depth match well to measured data with MAEs of 1.55 °C and 1.70 °C respectively (Figure 3-31

a and b). The temperature match worsens with depth with a MAE of 1.88 ˚C at 0.7 m

(Figure 3-31 d). This decrease in accuracy with depth means that heat is not properly

moving through the supra-permafrost layer. The model results follow the same trend as

the temperatures measured on the plateau and fall / winter temperatures continue to

have a relatively high accuracy with depth. At 0.5 m depth the spring and summer

temperatures are overestimated by approximately 1 ˚C and 3 ˚C respectively. At 0.7 m

depth the spring warming begins approximately 30 days early and summer temperatures

are overestimated by approximately 4 ˚C in the summer (Figures 3-30 and 3-31).
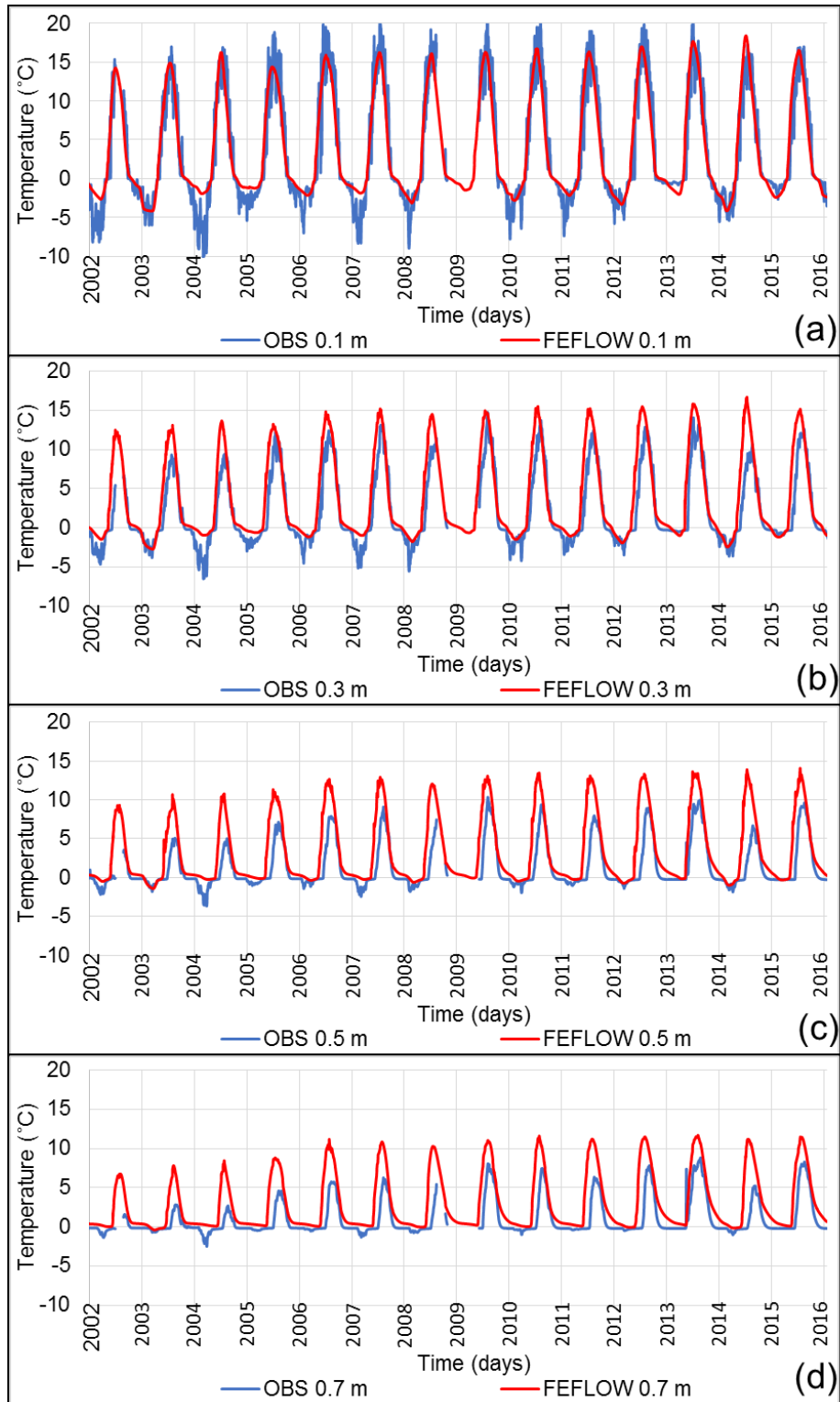
Figure 4-30: Measured and FEFLOW modelled plateau ground temperatures. Ground temperatures were measured at the 'Plateau South' location (Figure 3-2). *** Sensor failure occurred between August 2008 and May 2009.
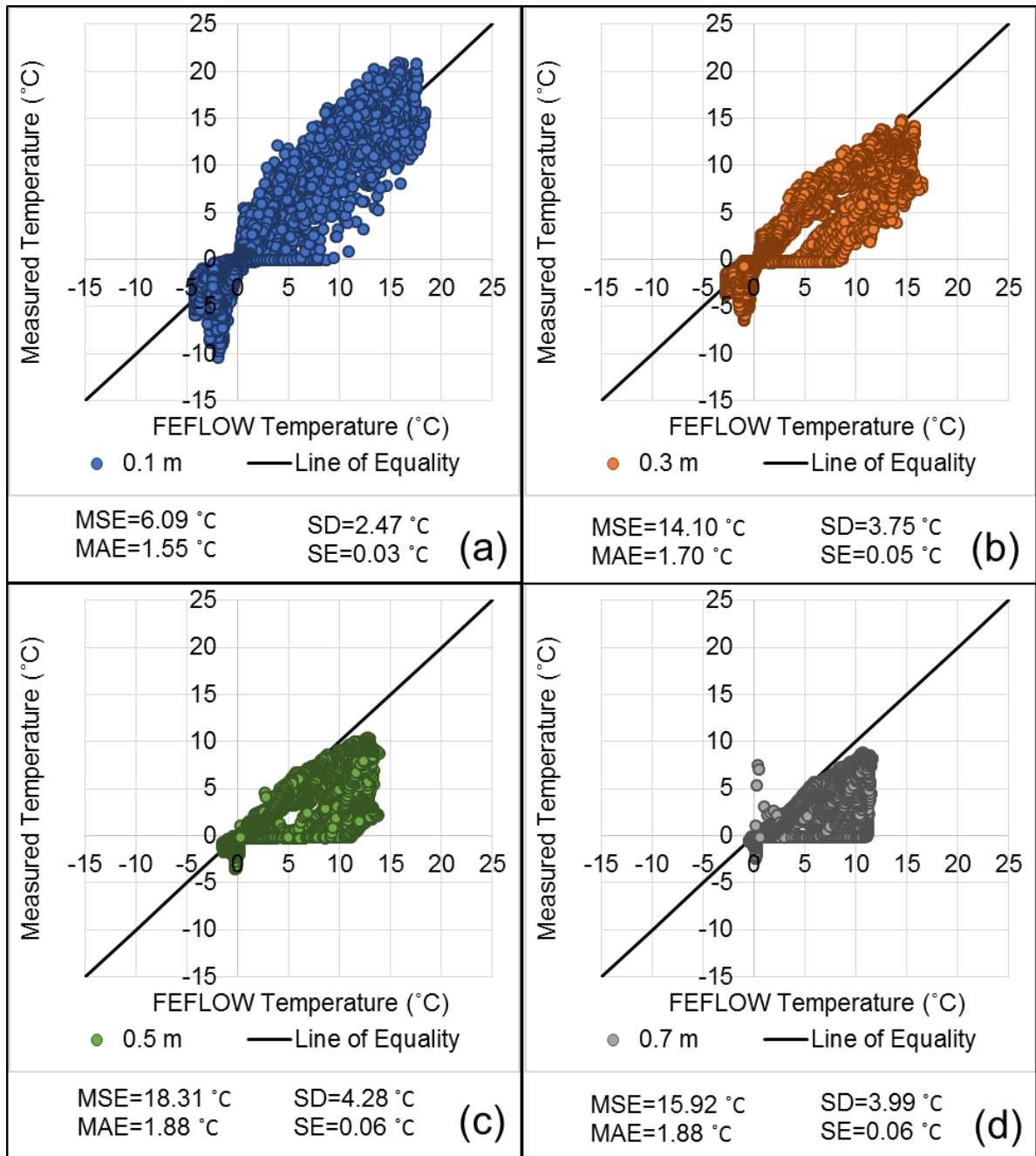
Figure 4-31: One-to-one plots of the plateau measured and modelled (at location 'Plateau South' on Figure 3-2) ground temperatures displayed in Figure 3-30 at depths 1) 0.1 m, b) 0.3 m, c) 0.5 m and d) 0.7 m. Model statistics are listed below the corresponding plot.

Wetland temperature results in the 1999-2015 run are similar to the sensitivity testing results (Section 3.2.1.2; Figure 3-13). The shallow temperatures at 0.1 m and 0.5 m match well with measured temperature data, with MAEs of 0.45 °C and 0.53 °C

respectively. The results at 1.3 m, however, do not as accurately represent the

measured (Figure 3-32). The reason for this discrepancy in modelled versus measured

wetland temperature is explained in section 3.2.1.2.
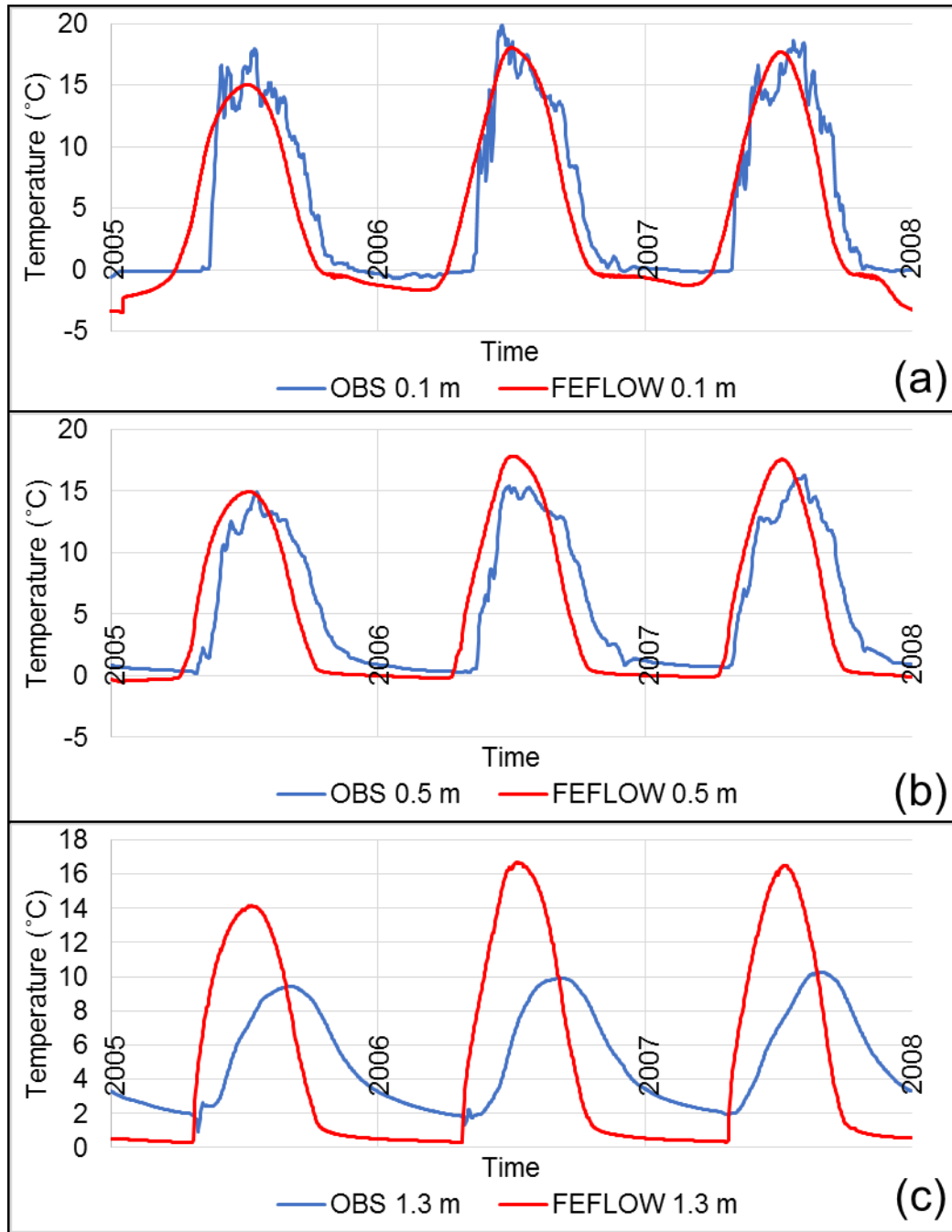
Figure 4-32: Measured and FEFLOW modelled wetland ground temperatures. Ground temperatures were measured at the ''Fen Middle' location (Figure 3-2).
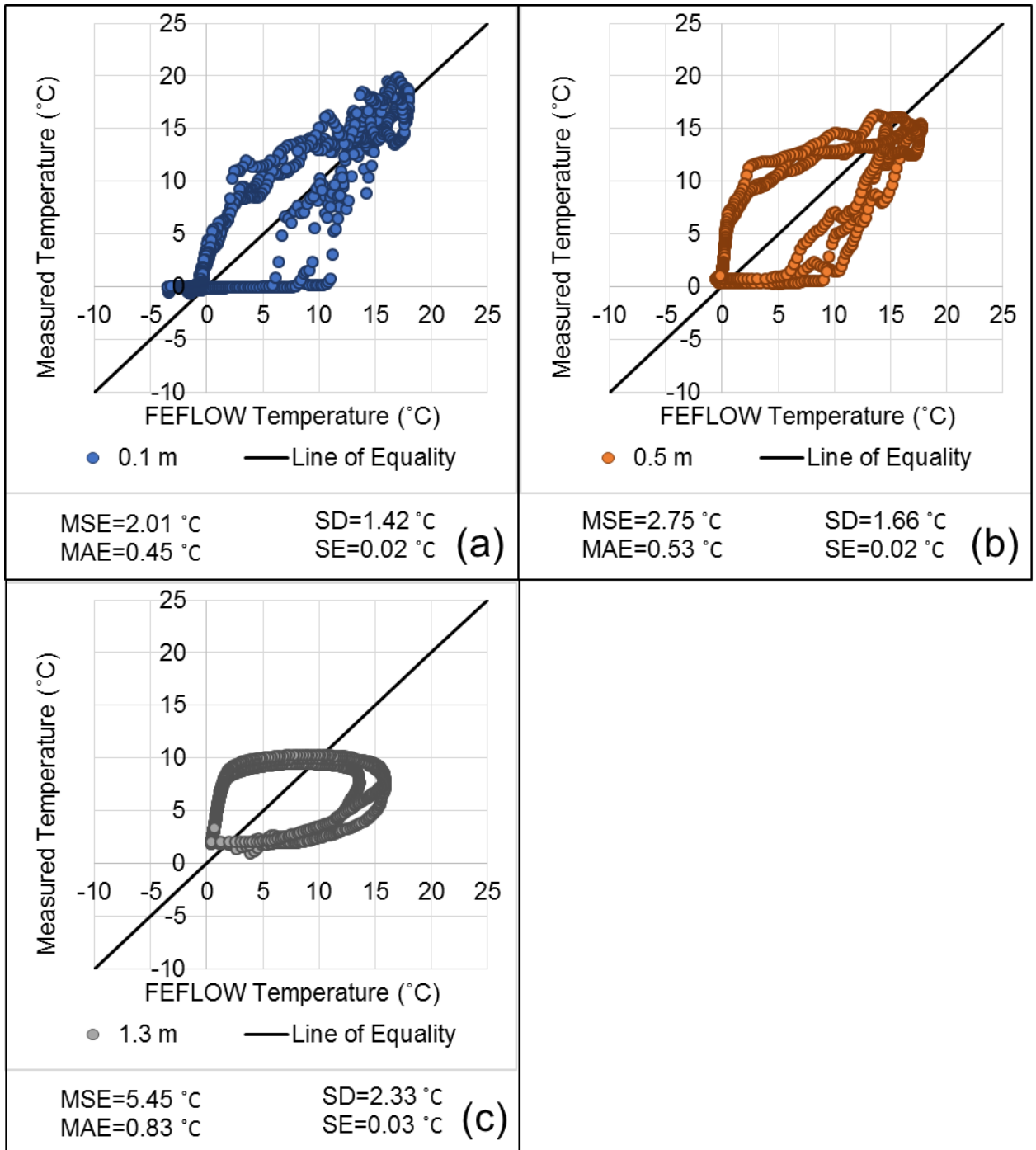
Figure 4-33: One-to-one plots of the wetland measured and modelled (at location 'Fen Middle' on Figure 3-2) ground temperatures at depths a) 0.1 m, b) 0.5 m and c) 1.3 m. Model statistics are listed below the corresponding plot.

Model observation points were selected to develop a cross section of the plateau-wetland complex at surface elevation 3 m depth across the model width (Figure 3-34). The 3 m depth moisture and temperature observation point recordings are displayed in Figure 3-35. The average moisture content of the entire 15 year run for each observation point is presented with a SD bar on each point to demonstrate the relatively small range of moisture content over the 15 year run (Figure 3-35). The observation point temperatures for 2005, 2010 and 2015 are plotted with moisture to demonstrate their relationship (Figure 3-35). These cross sections display that the ground with higher moisture content warms at a faster rate than ground with less moisture due to the differences in the bulk thermal conductivity (Equations 2.5 and 2.6; Figure 3-35). This demonstrates that this three-dimensional FEFLOW permafrost model is representing differential thaw due to differences in moisture content and that moisture is building up in supra-permafrost table depressions.
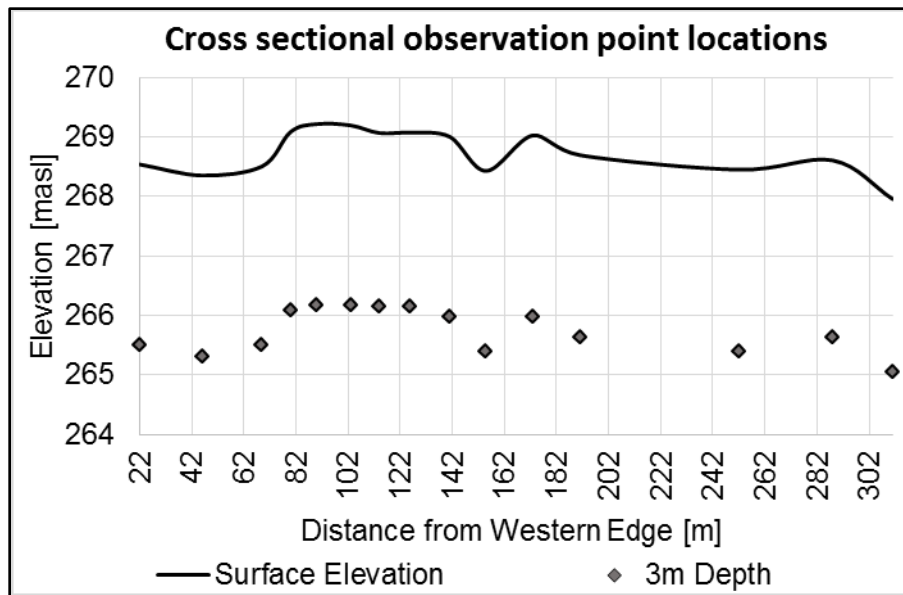
Figure 4-34: The elevations of the surface and 3 m depth observation points ('cross-section observation points' location in Figure 3-2).
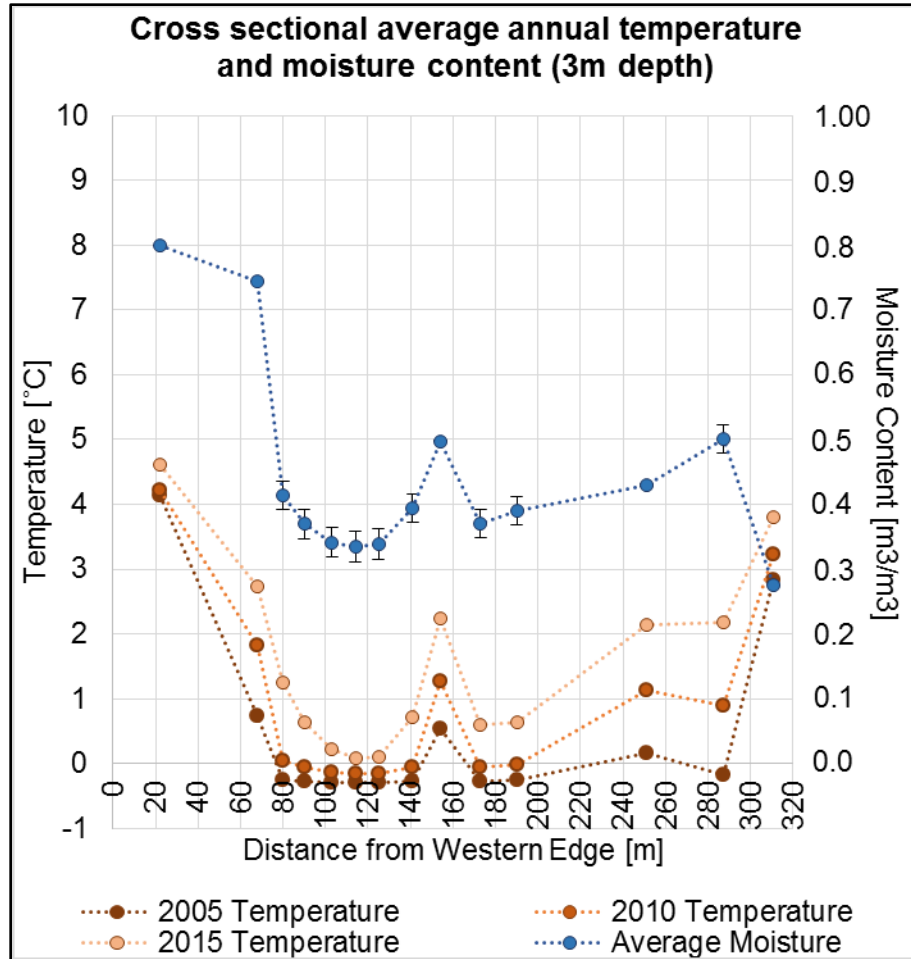
Figure 4-35: The 2000-2015 average moisture content and the 2005, 2010 and 2015 ground temperature of the 'cross-sectional observation points' at 3 m below surface elevation. Moisture content standard deviation is displayed as error bars.

4.2.3.3 "Unsteady-state" initial conditions

Developing a permafrost bulb from the ground surface in steady-state, and using this temperature distribution as initial conditions, as described in Sections 3.2.3.1 and 3.2.3.2, did not yield results as good as the preliminary model testing. In preliminary tests temperatures of -1 °C were assigned to nodes 1 m below the plateau surface down to 16 m. A 5-year (2005-2010) model was run with the same "unsteady-state" initial conditions to compare to the steady state initial condition model results. Ground temperatures of -1 °C were assigned 1 m below plateau surface down to 30 m depth.

This is deeper than the preliminary test permafrost and was selected based on the deepest portion of the plateau created in steady state (Figure 3-17). A temperature of 1.5 °C is applied as the unsteady-state initial conditions for the remaining nodes (Figure 3-36 and 3-37). This method of assigning permafrost does not create a bulbous body of permafrost as steady state conditions do (Figure 3-15). Instead, the permafrost body has equal depth below all points of the plateau, forming a linear base with defined edges (Figures 3-36 and 3-37).

A large difference between the steady-state initial conditions and the unsteady-state initial conditions is that the steady-state permafrost development is forced from the ground surface, thus permafrost is developed right to the ground surface in steady-state. In unsteady-state, freezing temperatures were applied 1 meter below ground surface, leaving an initially thawed portion of overlying ground (supra-permafrost layer). This is a large difference because ice has a thermal conductivity over three times greater than that of water (Table 2-5). Therefore, when transient temperatures are applied to the steady-state conditions heat is transported deeper into the permafrost immediately developing an thick supra-permafrost layer with a talik. As discussed in sections 1.3.1 and 1.3.2, taliks lead to increased thaw rates. When unfrozen space between the ground surface and the supra-permafrost table is given in the initial conditions, the immediate transient thaw does not propagate as deep (Figure 3-39). The temperature rates of change of the model with unsteady-state initial conditions are less than half the rates in the first year of steady-state initial conditions model. This is because the initial freezing temperature is a degree warmer and the permafrost temperature does not change as much to reach temperatures just below 0°C (Figure 3-38).
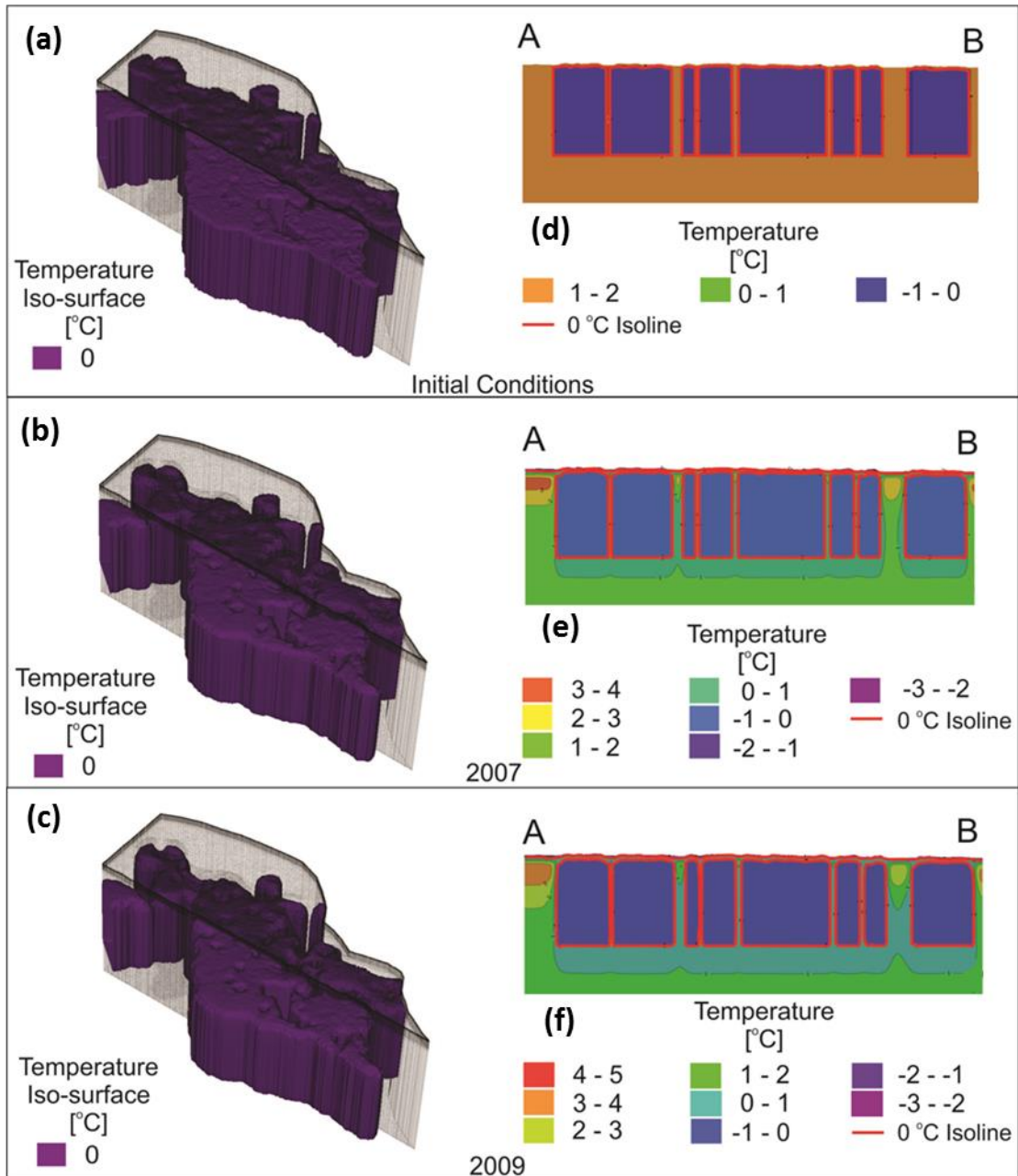
Figure 4-36: The progression of the permafrost thaw over a 5-year model run starting with unsteady-state initial conditions. A three-dimensional display of the 0 ˚C iso-surface is displayed in a) initial conditions, b) September of 2007 and c) September of 2009. A cross section of the model temperature distribution is displayed in d) initial conditions, e) March of 2007 and f) March of 2009 (refer to Figure 3-16 for cross section location).
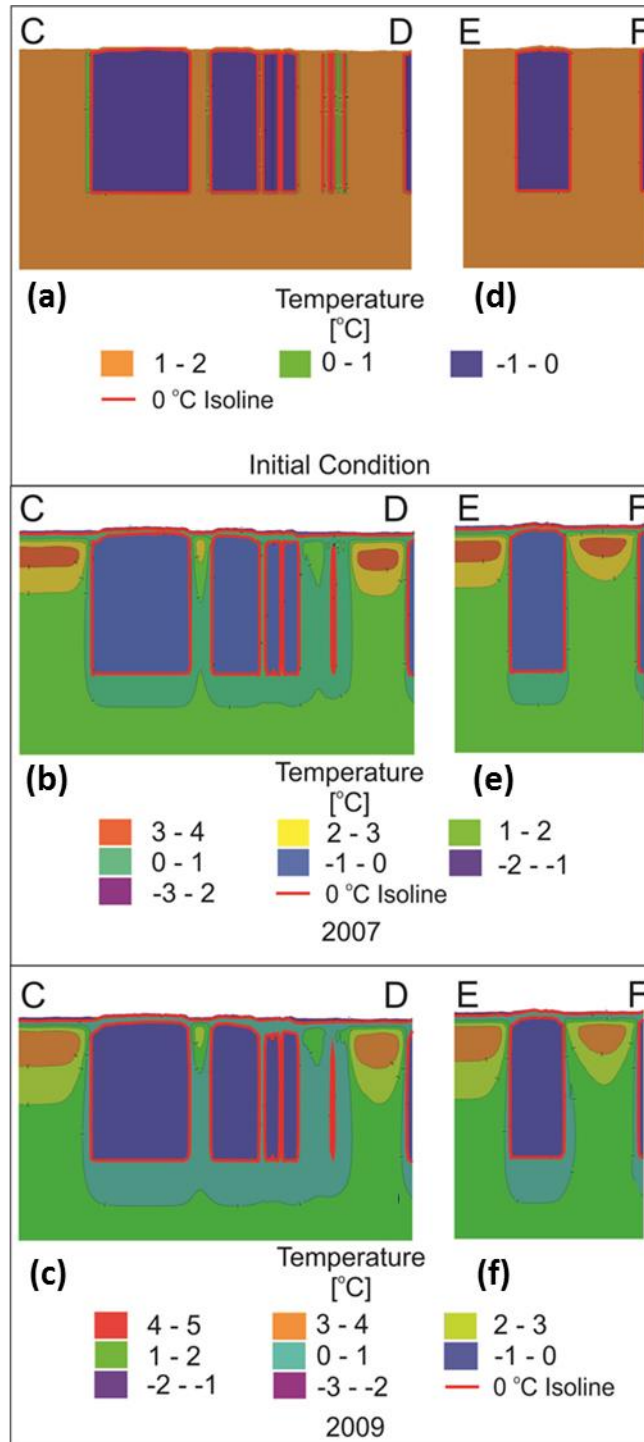
Figure 4-37: March cross sections (refer to Figure 3-16 for cross section location) of the progression of permafrost thaw from unsteady-state initial conditions to 2009 along the middle of the plateau in a), b) and c) and along the southern tip of the plateau in d) e) and f).
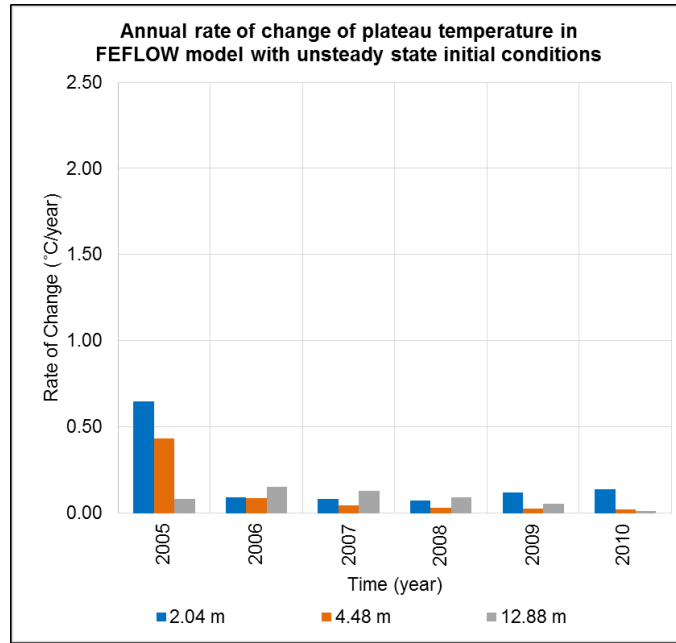
Figure 4-38: The annual rate of change in temperature at different depths at the 'Plateau Middle' observation point location from unsteady-state initial conditions 2005 to 2010 (Figure 3-2).
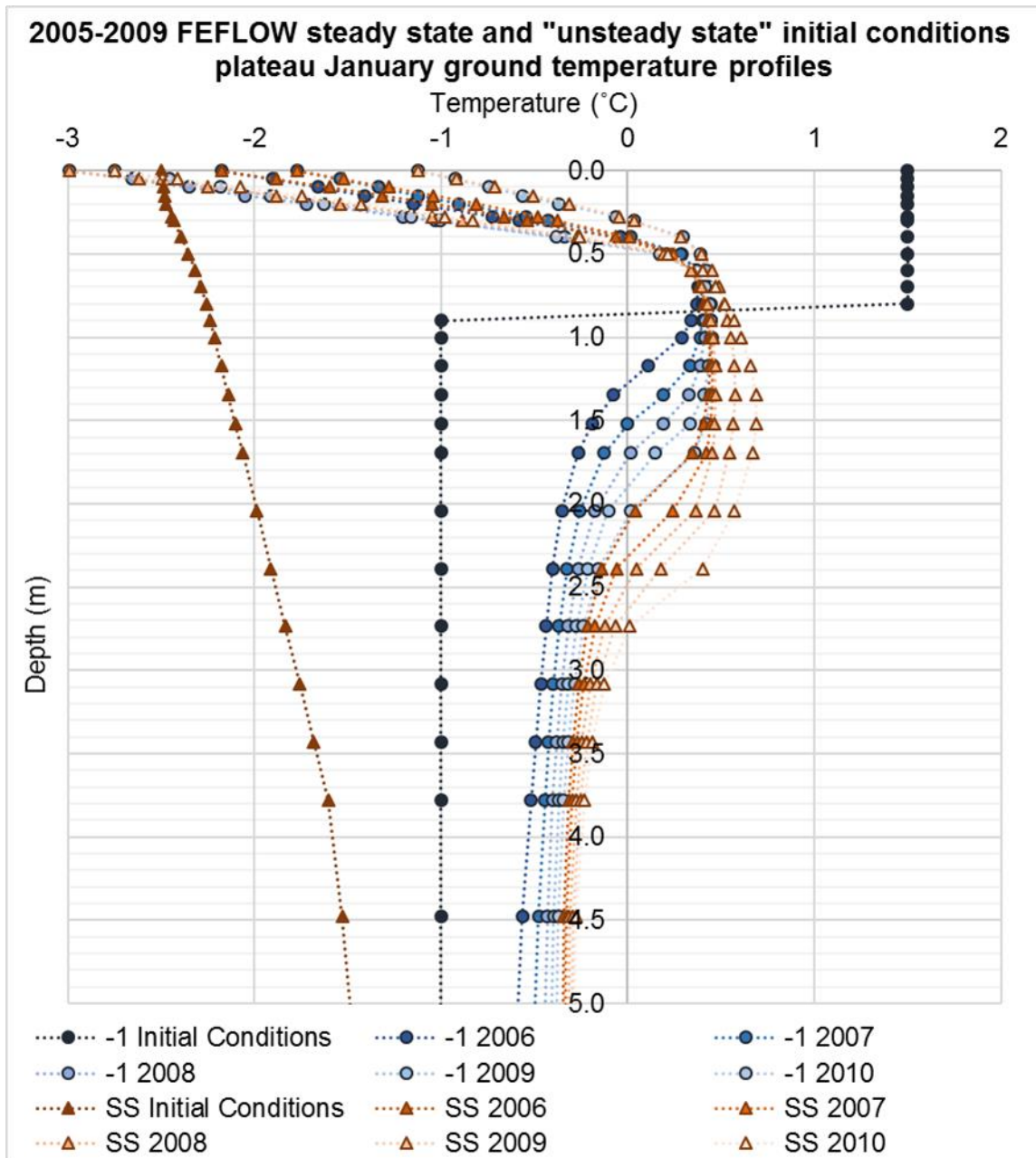
Figure 4-39: Temperature depth profiles of the steady-state and unsteady-state initial condition models in initial conditions, 2005, 2006, 2007, 2008, 2009 and 2010.

Using the unsteady-state initial conditions, in which the permafrost has not been frozen from the ground surface, yielded relatively better plateau temperature results than the steady state initial conditions discussed in Section 3.2.3.2 (Figures 3-40 and 3-41). The MAE ranges from 0.36 ˚C to 0.52 ˚C, which is less than half that of the steady-state

initial condition model results. Deeper plateau model temperatures do not get as warm in the summer months as the steady-state initial condition temperatures did (Figure 3-30 c and d). This means that heat is not moving through the supra-permafrost layer as quickly as the steady-state initial conditions model. The two methods produced similar wetland temperature results with nearly identical MAEs, ranging from 0.46 ˚C at 0.1 m to 0.84 ˚C at 1.3 m depth (Figures 3-42 and 3-43). The initial temperature in the fen was 1.3 ˚C in the steady-state initial conditions and 1.5 ˚C in the unsteady-state initial conditions, therefore, the results are nearly the same.
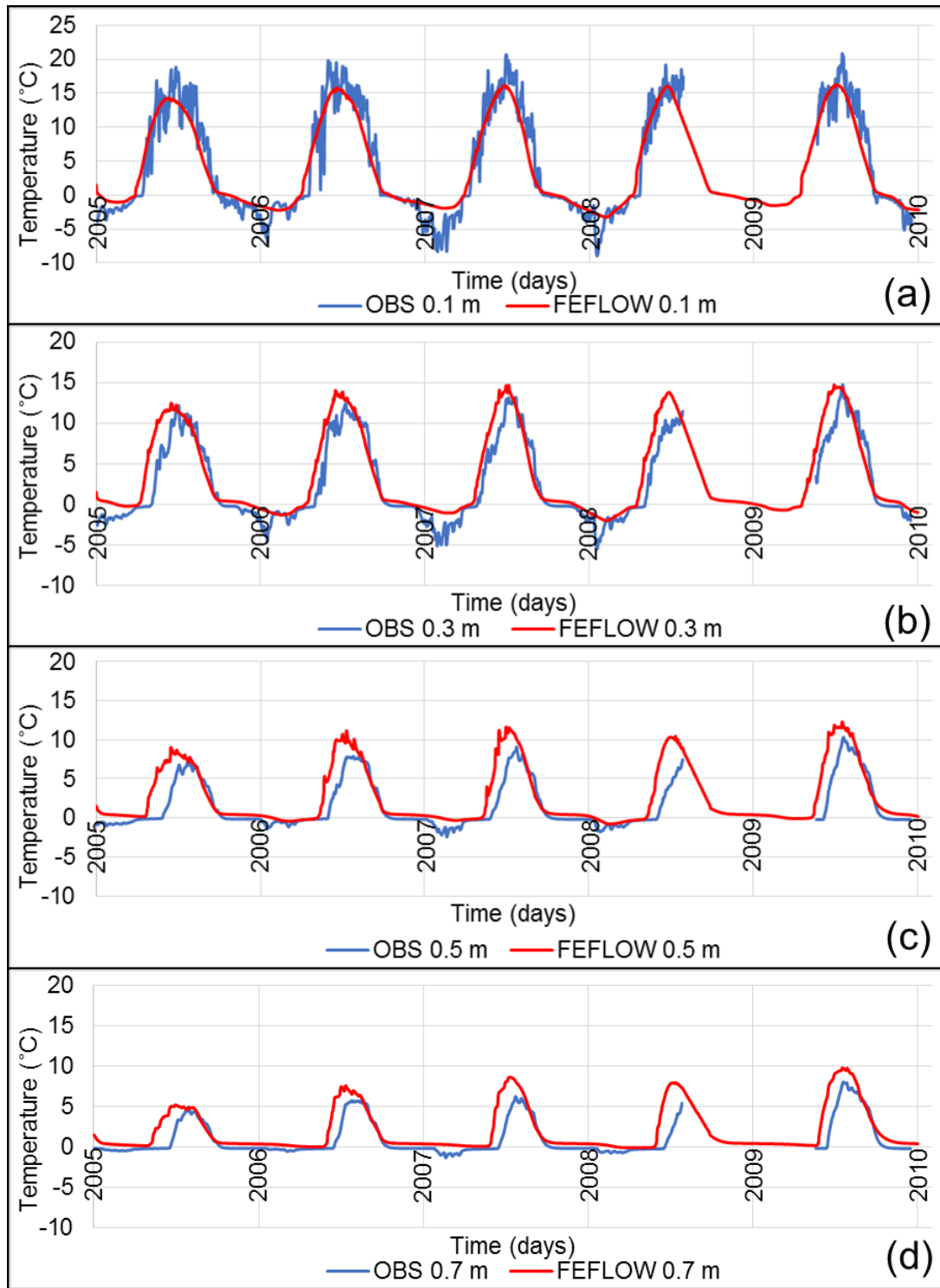
Figure 4-40: Plateau measured and FEFLOW modelled with unsteady-state initial condition ground temperatures with time at depths a) 0.1 m, b) 0.3 m, c) 0.5 m and d) 0.7 m. *** Sensor failure occurred between August 2008 and May 2009.
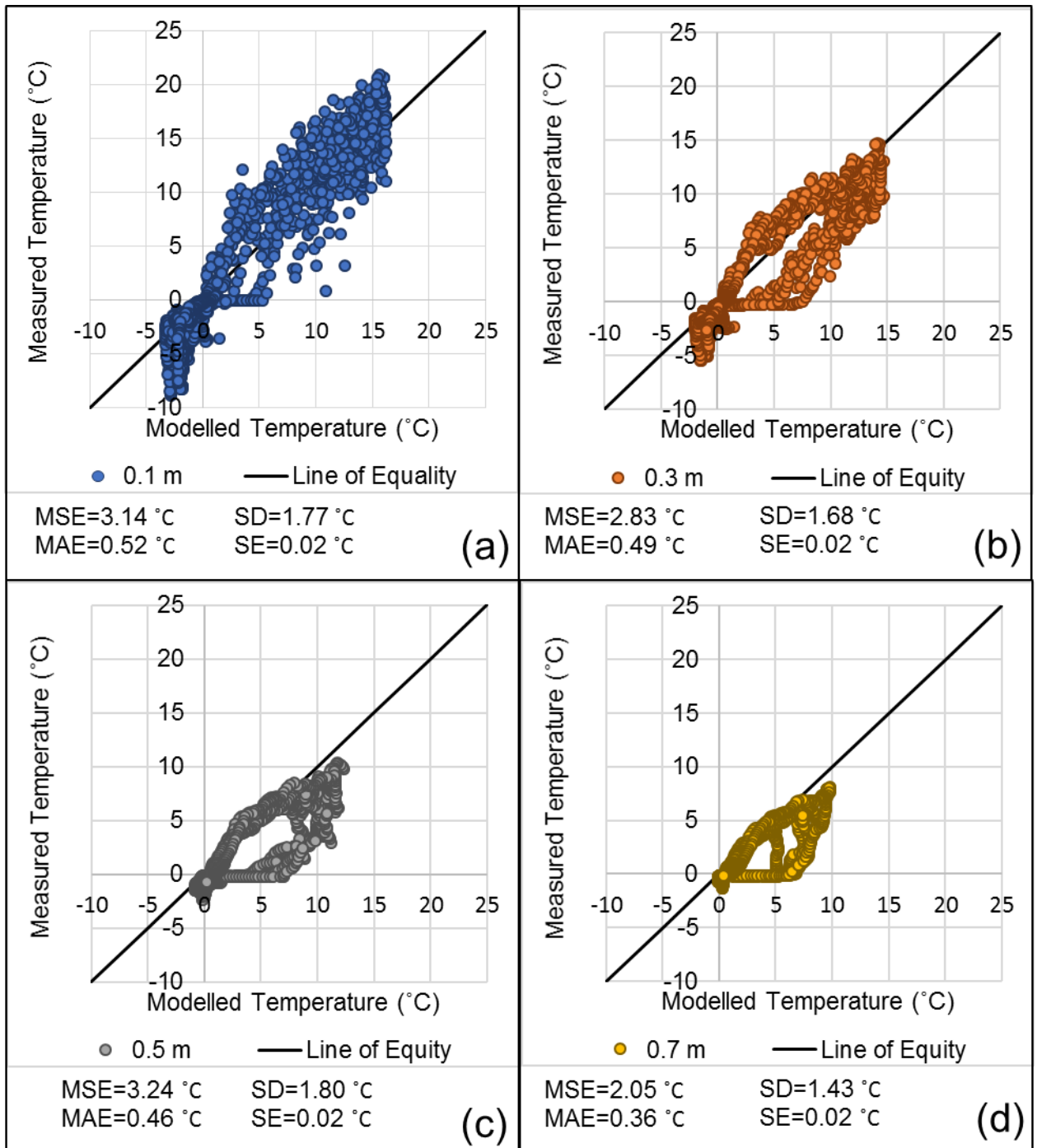
Figure 4-41: One-to-one plots of measured versus FEFLOW modelled plateau temperatures with unsteady-state initial conditions at depths a) 0.1 m, b) 0.3 m, c) 0.5 m and d) 0.7 m. Statistics are displayed below the corresponding plot.
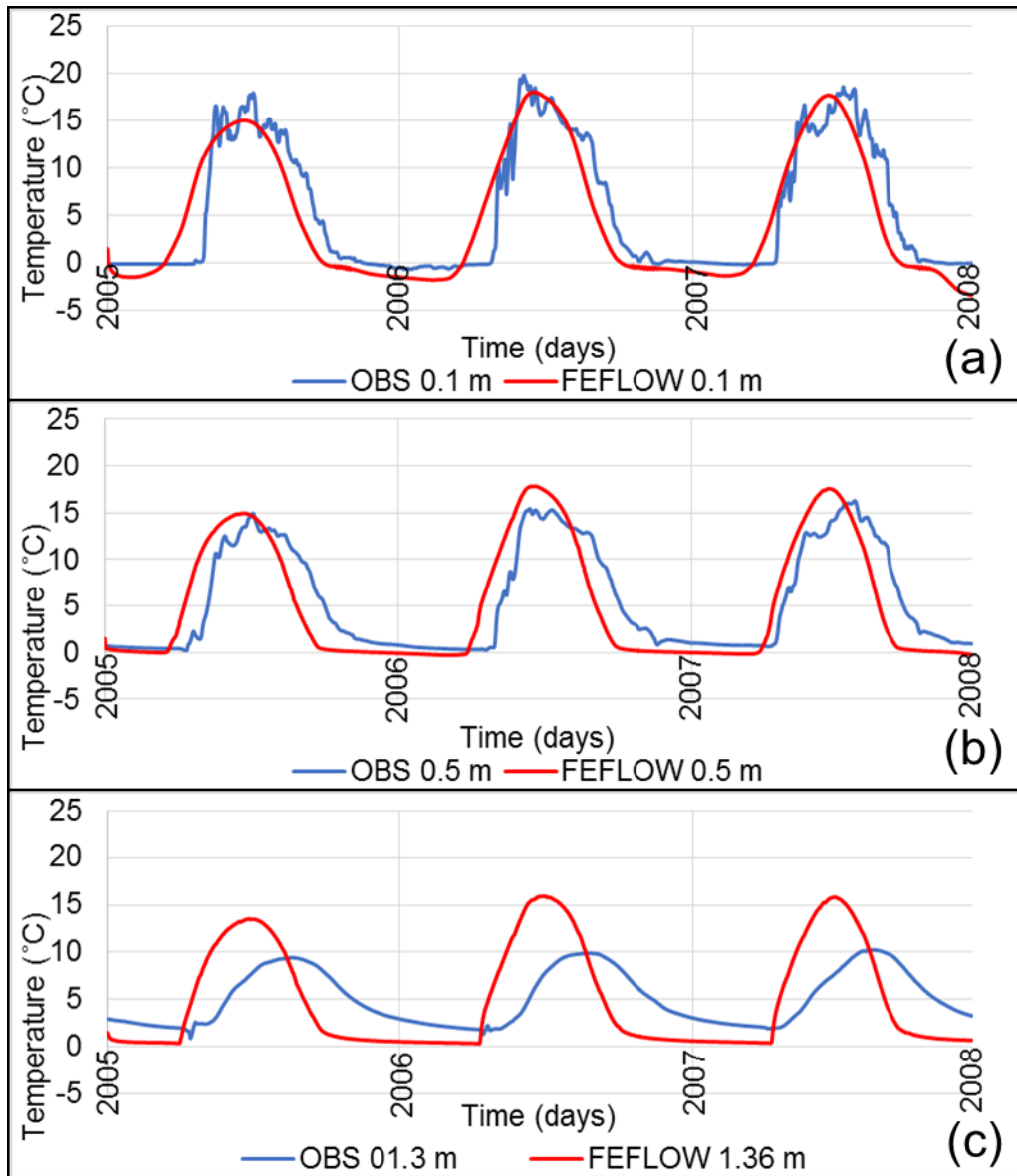
Figure 4-42: Wetland measured and FEFLOW modelled with unsteady-state initial condition ground temperatures with time at a) 0.1 m depth from ground surface, b) 0.5 m and c) 1.3 m. **FEFLOW data was collected from the nearest node.
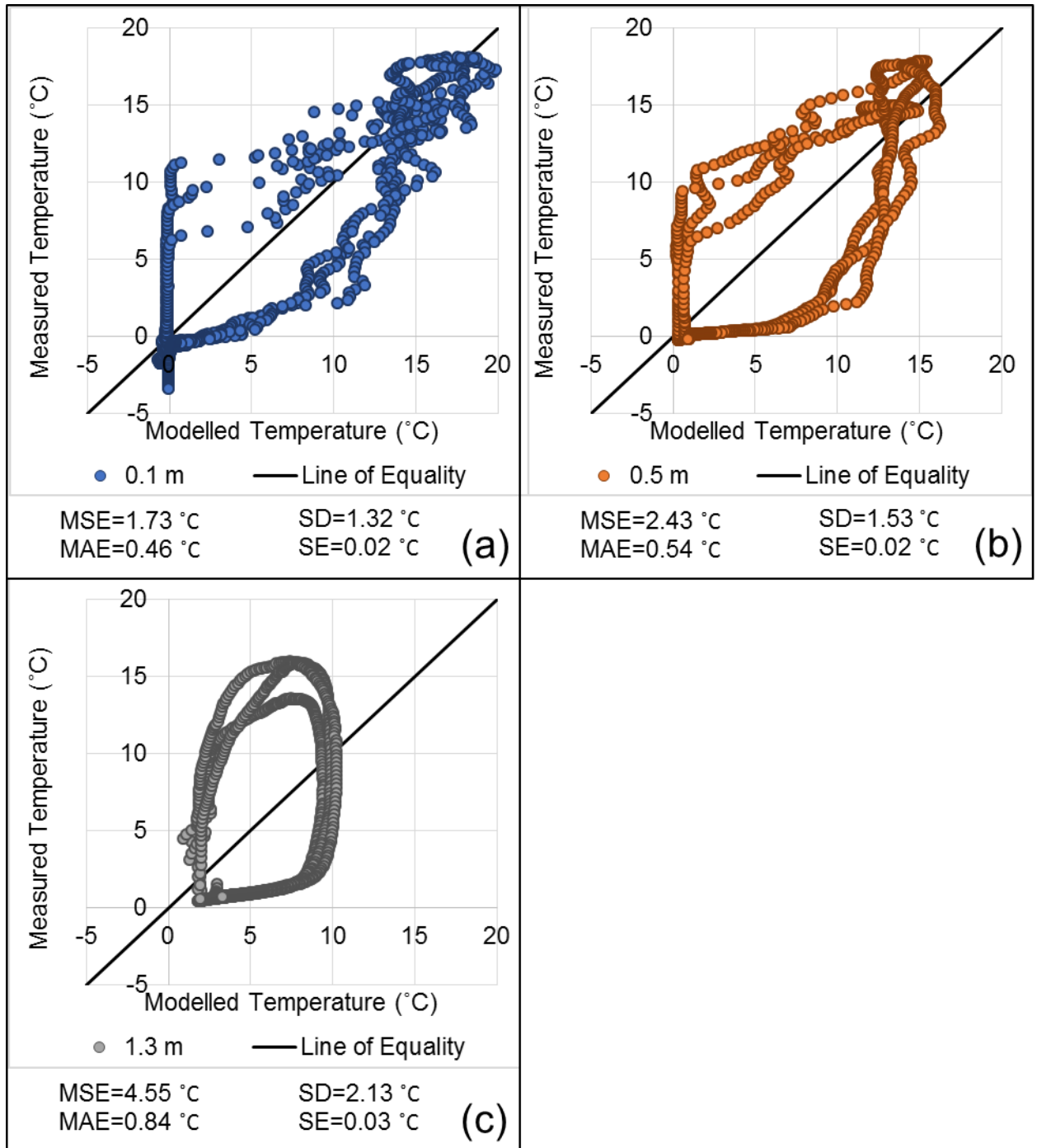
Figure 4-43: One-to-one plots of FEFLOW modelled wetland temperatures with unsteady-state initial conditions at a) 0.1 m depth from ground surface, b) 0.5 m and c) 1.3 m. Error values are displayed below the corresponding depth.

Moisture content with depth, for the steady-state and unsteady-state initial condition models, was compared to determine if a difference in moisture content, and thus bulk thermal conductivity, was the cause of the differences in thermal transport rates (Figure 3-45). In the shallower peat it was found that the steady-state initial condition model had lower moisture content than the "unsteady-state" initial condition model; the opposite effect than what was observed if moisture content was the cause of the thermal transport difference between the two models. Therefore, moisture content of the peat overlying the permafrost can be ruled out as the cause of the difference between these two models.
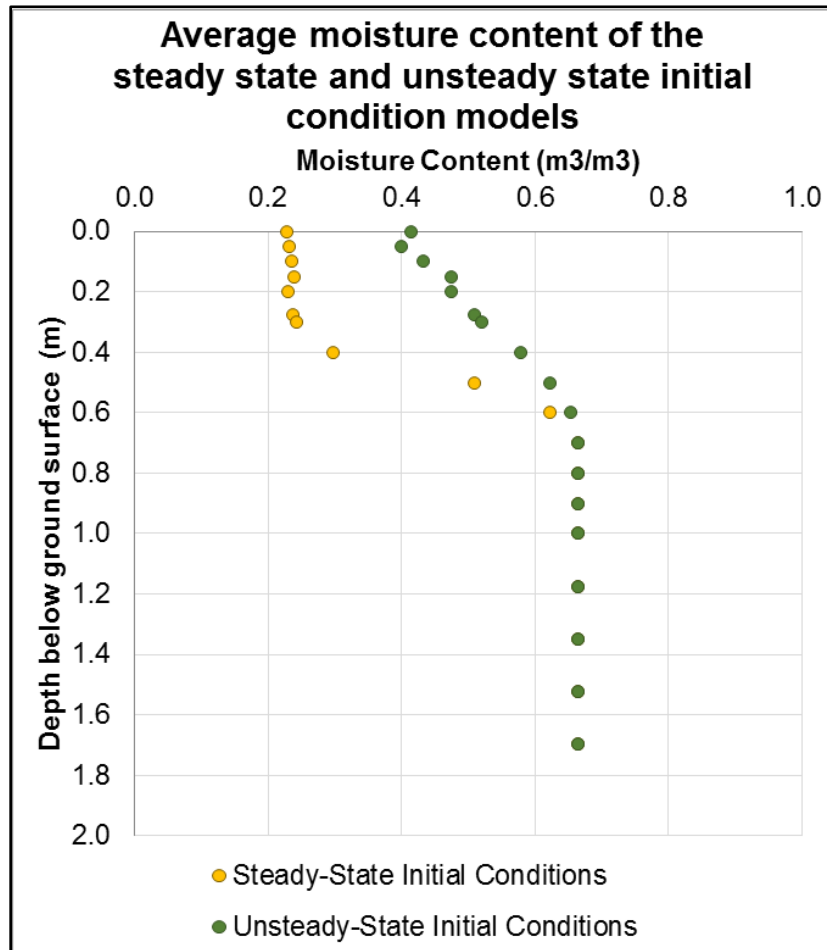
Figure 4-44: The modelled average moisture content for the steady-state and unsteady-state initial condition FEFLOW models.

Another factor that affects the way heat is transported through the peat overlying permafrost, according to Fourier Law of conductive heat transport, is the thermal gradient (Equation 2.5; Figure 3-46). Especially during the summer months, there is a large thermal gradient that develops between the supra-permafrost table (just below 0 ˚C) and the ground surface (summer plateau ground surface temperatures on average 17 ˚C). The distance between the ground surface and the supra-permafrost table has a large effect on the vertical thermal transport through this layer. In the steady-state initial condition model the distance between ground surface and the supra-permafrost table is continuously greater than the unsteady-state initial condition model by nearly 1 m (Figure 3-39). The greater the distance between the ground surface and the supra-permafrost table the smaller the thermal gradient and the smaller the thermal flux (Equation 2.5). In a direct thermal gradient comparison for the plateau upper 1.5 m for the steady-state and unsteady-state initial condition models, the gradient of the unsteady-state initial condition model is approximately 0.8 ˚C/m higher than the steady-state initial condition model (Figure 3-45).
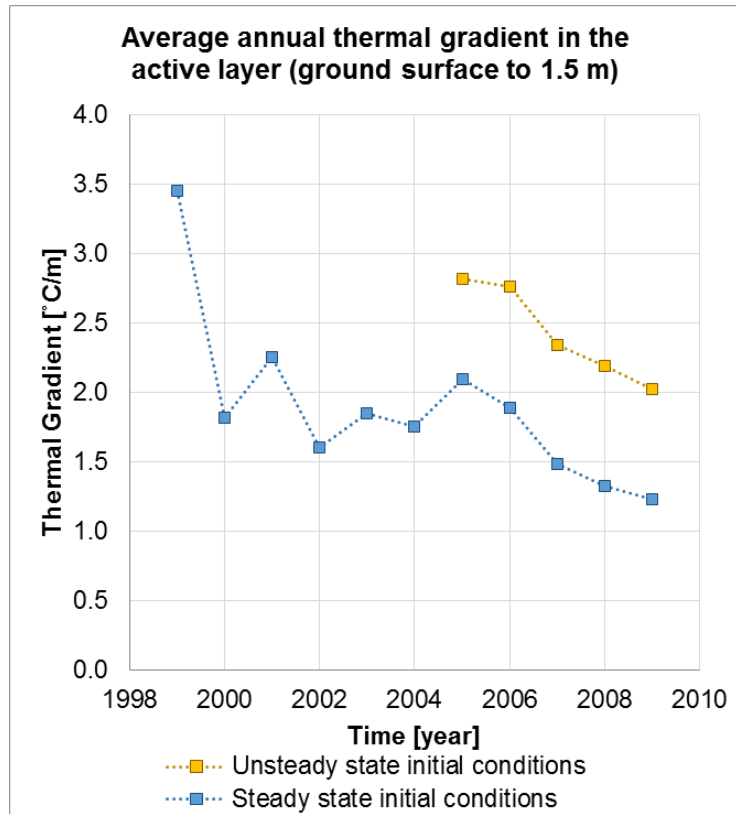
Figure 4-45: The thermal gradient between plateau ground surface and 1.5 m depth for the model with steady-state initial conditions and with unsteady-state initial conditions.

Chapter 5

5   Discussion

5.1   Modelling thermal transport in a plateau-wetland complex

A permafrost plateau-wetland complex is a dynamic thermal transport and hydrogeological flow system. Due to the low hydraulic gradient in the Scotty Creek region (approximately 0.003 m/m), thermal flow is dominated by conduction through water, ice and ground materials. This dynamic system has been developed over hundreds of years under shifting climate regimes. Representing all the processes occurring in this system perfectly is impossible; however, this thesis determined the methods that are critical to building a transient unsteady, thawing permafrost plateau model.

The conceptual model is relatively simple in comparison to the actual continuously fluctuating flow systems (Figure 2-3). The model hydraulic head boundaries are constant in time and do not fluctuate with the annual water cycle. This proved to directly affect the temperatures in the wetlands (Figure 3-12). It was not found that this difference had any effect on the plateau temperatures, though further testing is required for this to be proven. The dominant form of hydrological response in permafrost plateaus, which was represented in this model, is subsurface runoff. The dominant sources of subsurface runoff are snow melt and precipitation, both of which are applied to the ground surface. It was found that the net surface water transfer (i.e. infiltration and evapotranspiration) could be applied in time steps no longer than daily, to properly develop supra-permafrost layer moisture conditions. Average weekly or monthly net

surface water transfer does not allow the ground surface to be exposed to dry periods, which is important for permafrost insulation.

The supra-permafrost layer was found to be the most critical zone of heat transport in the permafrost thaw model because it is through this zone that heat is transferred between the ground surface and the permafrost. To increase the accuracy in this layer, discretization was optimized (Table 2-1). It was found that a nodal spacing as fine as 0.01 m close to the temperature boundary condition was required for the FEFLOW model to properly compute the thermal transport through this zone. Nodal spacing may increase with distance from temperature boundaries. The initial temperature conditions of the supra-permafrost layer proved to have a large effect on the transient ground temperature results, this is discussed further in Section 4.2.

5.2   Finding the perfect "unsteady-state"

As in any model, the initial conditions are a key factor in determining the accuracy of results. The initial conditions of most flow models are steady-state conditions developed from averaged boundary conditions. However, the initial conditions for thawing permafrost cannot be steady-state because the system is transitioning and not in equilibrium. The key to developing the initial conditions of a thawing permafrost model is finding the perfect degree of "unsteady-state" permafrost that transient boundary conditions may be applied to.

A spin-up period refers to a period in which time series are applied as boundary conditions to bring the steady state conditions to a transient temperature distribution. In a permafrost model the spin-up period progresses the permafrost from a continuous bulb into a thawing permafrost bulb with an overlying supra-permafrost layer, and possibly taliks. It was found in this thesis that a spin-up period of approximately 3 years is an

appropriate length of time for a permafrost bulb of approximately 30 m depth to move from the applied steady state temperatures to the modern-day temperatures just below 0 ˚C. It was found that the development of a permafrost bulb in steady state which is then spun-up to modern day conditions, thaws too rapidly during the spin-up period to represent modern-day permafrost thaw. When permafrost is aggraded in steady-state from the plateau ground surface, ice fills the pores of the shallow peat which elevates the bulk thermal conductivity of the media. This increase in bulk thermal conductivity causes rapid thaw to propagate so deep into the permafrost that a talik immediately develops which leads to a further increase in thaw rates.

The perfect "unsteady-state" initial conditions of a transient thaw model include a layer between the supra-permafrost table and the ground surface that is not frozen. This layer acts as a thermal buffer of lower bulk thermal conductivity that maintains shallow permafrost throughout the spin-up period. It was found in this thesis that including an unfrozen buffer layer between the ground surface and the supra-permafrost table yielded better supra-permafrost layer temperature results (Section 3.2.3.3). When shallow permafrost is properly maintained throughout the spin-up period the supra-permafrost layer thermal gradient is more accurately represented and therefore as are supra-permafrost layer ground temperatures. It was found that an applied unfrozen layer of 1 m in the model initial conditions was too thick, as demonstrated by talik development. It is hypothesized that a thinner assigned unfrozen layer between the supra-permafrost table and the ground surface would yield better results.

5.3   Model limitations and uncertainty

Every numerical model has strengths and weaknesses and it is important to recognize limitations to have confidence in the results. Recognizing how a model is a

simplification of a very complex and dynamic system is crucial in order to understand the discrepancies between measured field data and model results. A limitation of this model is the fixed ground surface. Plateau-wetland complex ground surface elevations are evolving as permafrost melts and plateaus collapse into wetlands. The FEFLOW model elevations do no evolve with the permafrost thaw and this affects the thermal transport along the transitioning portions of the plateau. Another transitioning plateau process that is not accurately depicted in this model is "edge effects." Edge effects take place when the permafrost thaws and the ground slumps causing the trees to become waterlogged and die, exposing the ground surface to the same climate effects as the wetlands. The plateau and wetland temperatures are applied over the same plateau and wetland shape respectively over the entire run. Ideally the applied plateau boundary would evolve with the permafrost decay; however, this would require predicting the permafrost plateau geomorphology over time.

Another oversimplification of the model is the constant hydraulic gradient from the southern to the northern boundary of 0.003. Realistically the hydraulic gradient of the region is not constant throughout a year and the hydraulic head moves up and down depending on the water cycle. This should be considered if the model is being used to directly study seasonal effects of groundwater flow on permafrost thaw.

Model boundary locations are challenging to layout in a region without obvious groundwater divides due to such little relief. Because this thesis focused on the thermal transport through a plateau-wetland complex, the boundaries could not come so close to the plateau that they cause thermal dispersion. This forced boundaries to be moved away and cross over adjacent plateaus. The way the boundaries cut through the adjacent plateaus may not perfectly represent no flow boundaries; as flow in permafrost

plateaus is determined by the permafrost table micro-topography which is challenging to decipher from a LiDAR image.

Temperatures of water entering the model, from the surface net water transfer or southern hydraulic head boundaries, enter the model at the same temperature of the node through which it is entering. On the surface boundary this means that water is entering the model at air temperatures, which is a reasonable assumption. At the southern boundary, however, temperatures are dominantly controlled by the vertical thermal gradient wherein reality these temperatures may be affected by a nearby lake. A solution to this problem could be to apply a temperature boundary along the southern edge of the model.

Chapter 6

6   Conclusions and Future Recommendations

6.1   General Conclusions

A three-dimensional model of a permafrost plateau-wetland complex was generated and its strengths and weaknesses have been identified. The goal of this thesis was to identify and test the boundary conditions required to represent transient permafrost thaw in the discontinuous-sporadic permafrost region. It was found that applying appropriate initial conditions is vital to develop an accurate thermal gradient in the supra-permafrost layer, and thus accurate thermal transport from the surface boundary to the supra-permafrost table. Model testing showed that developing a permafrost plateau in steady-state from ground surface freezing temperatures yielded an inaccurate thermal gradient in the supra-permafrost layer, which lead to a more rapid permafrost thaw than observed in the field. Further testing found that an application of "unsteady-state" ground temperature, which include a layer of unfrozen ground between the supra-permafrost table and ground surface, yielded results that more closely matched field conditions.

The flow system developed in the transient model matched well with the conceptual model. However, while this conceptual model is simplified, it still represents the general Scotty Creek surface and groundwater flow systems. Water enters and exits the model at the surface boundary according to a daily net surface water transfer. This boundary condition generates sub surficial flow along the elevated plateaus as well as creates a dry layer of peat during dry periods of the year. Water also enters the model at the southern constant hydraulic head boundary and flows north to the lower hydraulic head boundary. Though in reality these hydraulic heads move up and down with the water cycle, average annual wetland flow was appropriate for the purposes of this

project. If more accurate wetland temperatures and flow rates are required, transient hydraulic head boundaries are recommended.

6.2   Future Work

(1) Further testing of different "unsteady-state" temperature distributions will reveal the optimal initial temperature conditions to run an accurate transient permafrost thaw model. In this project, an initial supra-permafrost layer thickness of 1 m was used, but according to results was too thick.

(2) Further study of wetland characteristics such as hydraulic conductivities would be of great use in plateau-wetland modelling to increase the accuracy of wetland flow and thermal transport. Also, the addition of a transient hydraulic head boundary could improve the accuracy of wetland flow and transport and demonstrate its effect, if any, on permafrost thaw.

(3) The methods of permafrost modelling developed in this thesis could be used to build models to determine the effects of different ground disruptions such as seismic cut lines, developing infrastructure or geothermal energy systems on permafrost.

References

Anderson MP, Woessner WW, Hunt RJ, 2015. Applied Groundwater Modeling, 2nd edition. Elsevier Inc.

Aylsworth JM, Kettles IM, 2000. Distribution of peatlands. In *The Physical Environment of the Mackenzie Valley, Northwest Territories: A Base Line for Assessment of Environmental Change*, Dyke LD, Brooks GR (eds). *Geological Survey of Canada Bulletin* **547**: 49-55.

Beilman DW, Robinson SD, 2003. Peatland permafrost thaw and landform type along a climate gradient. In *Proceedings Eighth International Conference on Permafrost*, Phillips M, Springman SM, Arenson LU (eds), A.A.Balkema: Zurich; Vol. 1: 61–65

Bonnaventure PP, Lamoureux SF, 2013. The active layer: A conceptual review of monitoring, modelling techniques and changes in a warming climate. *Progress in Physical Geography*, **37**(3):352–376. doi: 10.1177/0309133313478314

Burgess MM, Smith SL, 2000. Shallow ground temperatures. In *The Physical Environment of the Mackenzie Valley, Northwest Territories: A Base Line for the Assessment of Environmental Change,* Dyke, L.D., Brooks, G.R. (Eds). *Geological Survey of Canada*, Ottawa, pp. 89-103.

Christensen B, Hayashi M, Quinton WL, 2010. Hydrology of discontinuous permafrost : Effects of permafrost plateau geometry on subsurface drainage. *63rd Canadian Geotechnical Conference and 6th Canadian Permafrost Conference*, pp. 1259–1264

Clausnitzer V, Mirnyy V, 2016. Modeling groundwater and heat flow subject to freezing and thawing. In *Mining Meets Water - Conflicts and Solutions.* pp 1150–1153

Connon R, Devoie É, Hayashi M, Veness T, Quinton W, 2018. The Influence of Shallow Taliks on Permafrost Thaw and Active Layer Dynamics in Subarctic Canada. Journal of Geophysical Research: Earth Surface, **123**: 281–297. doi: 10.1002/2017JF004469

Connon RF, Quinton WL, Craig JR, Hayashi M, 2014. Changing hydrologic connectivity

due to permafrost thaw in the lower Liard River valley, NWT, Canada. *Hydrological Processes* **28**(14):4163–4178. doi: 10.1002/hyp.10206

DHI-WASY, 2016 piFreeze

Dhi-Wasy GmbH, 2010. FEFLOW White Papers Vol. 5

Dobinski W, 2011. Permafrost. *Earth-Science Reviews* **108**(3-4):158–169. doi: 10.1016/j.earscirev.2011.06.007

Donnell JAO, Jorgenson MT, Harden JW, McGuire AD, Kanevskiy MZ, Wickland KP, 2012. The Effects of Permafrost Thaw on Soil Hydrologic, Thermal, and Carbon Dynamics in an Alaskan Peatland. *Ecosystems* 15: 213-229. doi: 10.1007/s10021-011-9504-0

Doven CD, , Riley WJ and Stern A, 2013. Analysis of Permafrost Thermal Dynamics and Response to Climate Change in the CMIP5 Earth System Models. pp. 1877–1900. doi: 10.1175/JCLI-D-12-00228.1

Flerchinger GN, 2000. The Simultaneous Heat and Water (SHAW) Model: User' s Manual

Flerchinger GN, 2017. The Simultaneous Heat and Water (SHAW) Model: Technical documentation

Frampton A, Painter SL, Destouni G, 2013. Permafrost degradation and subsurface-flow changes caused by surface warming trends. *Hydrogeological Journal* 21:271–280. doi: 10.1007/s10040-012-0938-z

Gao J, Xie Z, Wang A, Luo Z, 2016. Numerical simulation based on two-directional freeze and thaw algorithm for thermal diffusion model ∗. **37**(11):1467–1478. doi: 10.1007/s10483-016-2106-8

Garon-Labrecque ME, Leveille-Bourret E, Higgins K, Sonnentag O, 2015. Additions to the boreal flora of the Northwest Territories with a preliminary vascular flora of Scotty creek. *Canadian Field-Naturalist* **129**(4):349–367

Ge S, McKenzie J, Voss C, Wu Q, 2011. Exchange of groundwater and surface-water

mediated by permafrost response to seasonal and long term air temperature variation. *Geophysical Research Letters* **38**(14):1–6. doi: 10.1029/2011GL047911

Grover SPP, Baldock JA, 2013. The link between peat hydrology and decomposition: Beyond von Post. *Journal of Hydrology* **479**:130–138. doi: 10.1016/j.jhydrol.2012.11.049

Hayashi M, 2013. The Cold Vadose Zone: Hydrological and Ecological Significance of Frozen-Soil Processes. *Vadose Zone Journal* 12. doi: 10.2136/vzj2013.03.0064

Hayashi M, Quinton WL, Pietroniro A, Gibson JJ, 2004. Hydrologic functions of wetlands in a discontinuous permafrost basin indicated by isotopic and chemical signatures. *Journal of Hydrology* **296**(1-4):81–97. doi: 10.1016/j.jhydrol.2004.03.020

Heginbottom JA, Dubrevil MA, Harker PT, 1995. Canada Permafrost. In *National Atlas of Canada 5th edition.* Natural Resources Canada: Ottawa

Hinkel KM, Hurd JK, 2006. Permafrost Destabilization and Thermokarst Following Snow Fence Installation, Barrow, Alaska, U.S.A. *Arctic, Antarctic and Alpine Research* **38**(4):530–539. doi: 10.1657/1523-0430(2006)38[530:PDATFS]2.0.CO;2

Iijima Y, Fedorov AN, Park H, Suzuki K, Yabuki H, Maximov TC and Ohata T, 2010. Abrupt increases in soil temperatures following increased precipitation in a permafrost region, central Lena River basin, Russia. *Permafrost and Periglacial Processes* **21**(1):30–41. doi: 10.1002/ppp.662

Johansson E, Gustafsson LG, Berglund S, Lindborg T, Selroos J, Liljedahl LC, Destouni G, 2015. Data evaluation and numerical modeling of hydrological interactions between active layer, lake and talik in a permafrost catchment, Western Greenland. Journal of Hydrology **527**:688–703. doi: 10.1016/j.jhydrol.2015.05.026

Jorgenson MT, Osterkamp TE, 2005. Response of boreal ecosystems to varying modes of permafrost degradation. *Canadian Journal of Forest Resources* **35**:2100–2111. doi: 10.1139/X05-153

Jorgenson MT, Racine CH, Walters JC, Osterkamp TE, 2001. Permafrost degradation and ecological changes associated with a warming climate in central Alaska.

Climatic Change **48**(4):551–579. doi: 10.1023/A:1005667424292

Jorgenson MT, Romanovsky V, Harden J, Shur Y, O'Donnell J, Schuur EA, Kanevskiy M and Marchenko S, 2010. Resilience and vulnerability of permafrost to climate change. *Canadian Journal of Forest Research* **40**(7):1219–1236. doi: 10.1139/X10-061

Kane DL, Hinkel KM, Goering DJ, Hinzman LD, Outcald SI, 2001. Non-conductive heat transfer associated with frozen soils. Global and Planetary Change **29**(3-4):275–292. doi: 10.1016/S0921-8181(01)00095-9

Kurylyk BL, Hayashi M, Quinton WL, McKenzie JM, Voss CI, 2016. Influence of vertical and lateral heat transfer on permafrost thaw, peatland landscape transition, and groundwater flow. *Water Resources Research* **52**(2):1286–1305. doi: 10.1002/2015WR018057

Kurylyk BL, Watanabe K, 2013. The mathematical representation of freezing and thawing processes in variably-saturated, non-deformable soils. *Advances in Water Resources* **60**:160–177. doi: 10.1016/j.advwatres.2013.07.016

Lawrence DM, Slater AG, 2005. A projection of severe near-surface permafrost degradation during the 21st century. *Geophysical Research Letters* **32**(24):1–5. doi: 10.1029/2005GL025080

McClymont AF, Hayashi M, Bentley LR, Christensen BS, 2013. Geophysical imaging and thermal modeling of subsurface morphology and thaw evolution of discontinuous permafrost. *Journal of Geophysical Research: Earth Surface* **118**(3):1826–1837. doi: 10.1002/jgrf.20114

McKenzie JM, Voss CI, Siegel DI, 2007. Groundwater flow with energy transport and water-ice phase change: Numerical simulations, benchmarks, and application to freezing in peat bogs. Advances in Water Resources **30**(4):966–983. doi: 10.1016/j.advwatres.2006.08.008

Meteorological Service of Canada (MSC), 2016. *National climate data archive of Canada.* Environment Canada: Dorval, Quebec, Canada.

Nagare RM, Schincariol RA, Mohammed AA, Quinton WL, Hayashi M, 2013. Measuring saturated hydraulic conductivity and anisotropy of peat by a modified split-container method. *Hydrogeology Journal* **21**(2):515–520. doi: 10.1007/s10040-012-0930-7

Nagare RM, Schincariol RA, Quinton WL, Hayashi M, 2012. Effects of freezing on soil temperature, freezing front propagation and moisture redistribution in peat: Laboratory investigations. *Hydrology and Earth System Science* **16**:501–515. doi: 10.5194/hess-16-501-2012

Noetzli J, Gruber S, Kohl T, Salzmann N, Haeberli W, 2007. Three-dimensional distribution and evolution of permafrost temperatures in idealized high-mountain topography. *Journal of Geophysical Research: Earth Surface* **112**(2):1-14

Osterkamp TE, 2007. The recent warming of permafrost in Alaska. *Global and Planetary Change* **49**(3-4):187–202. doi: 10.1016/j.gloplacha.2005.09.001

Pomeroy JW, Gray DM, Brown T, Hedstrom NR, Quinton WL, Granger RJ, Carey SK, 2007. The cold regions hydrological model: a platform for basing process representation and model structure on physical evidence. *Hydrological Processes* **21**:2650–2667. doi: 10.1002/hyp

Quinton WL, Elliot T, Price JS, Rezanezhad F, Heck R, 2009. Measuring physical and hydraulic properties of peat from X-ray tomography. *Geoderma* **153**(1-2):269–277. doi: 10.1016/j.geoderma.2009.08.010

Quinton WL, Hayashi M, 2005. The Flow and Storage of Water in the Wetland-Dominated Central Mackenzie River Basin: Recent Advances and Future Directions. In *Prediction in Ungauged Basisns: Approaches for Canada's Cold Regions* pp. 45–66

Quinton WL, Hayashi M, Carey SK, 2008. Peat hydraulic conductivity in cold regions and its relation to pore size and geometry. *Hydrological Processes* **22**:2829–2837. doi: 10.1002/hyp

Quinton WL, Hayashi M, Chasmer LE, 2011. Permafrost-thaw-induced land-cover change in the Canadian subarctic: Implications for water resources. *Hydrological Processes* **25**:152–158. doi: 10.1002/hyp.7894

Quinton WL, Hayashi M, Chasmer LE, 2010. Peatland Hydrology of Discontinuous Permafrost in the Northwest Territories : Overview and Synthesis. *Canadian Water Resources Journal* **34**:311–328

Quinton WL, Hayashi M, Pietroniro A, 2003. Connectivity and storage functions of channel fens and flat bogs in northern basins. *Hydrological Processes* **17**(18):3665–3684. doi: 10.1002/hyp.1369

Richards LA, 1931. Capillary conduction of liquids through porous mediums. Journal of Applied Physics **1**(5):318–333. doi: 10.1063/1.1745010

Riseborough D, Shiklomanov N, Etzelmüller B, Gruber S, Marchenko S, 2008. Recent advances in permafrost modelling. *Permafrost Periglacial Processes* pp. 137–156

Sjoberg Y, Coon E, Sannel ABK, Pannetier R, Harp D, Frampton A, Painter SL, Lyon SW, 2016. Thermal effects of groundwater flow through subarctic fens: A case study based on field observations and numerical modeling. *Water Resources Research* **52**:1–16. doi: 10.1002/2015WR017571.Received

Smith LC, Pavelsky TM, MacDonald GM, Shiklomanov AI, Lammers RB, 2007. Rising minimum daily flows in northern Eurasian rivers: A growing influence of groundwater in the high-latitude hydrologic cycle. *Journal of Geophysical Research: Biogeosciences* **112**:1-18 doi: 10.1029/2006JG000327

Smith SL, Burgess MM, Riseborough D, Nixon FM, 2005. Recent trends from Canadian permafrost thermal monitoring network sites. *Permafrost and Periglacial Processes* **16**:19–30. doi: 10.1002/ppp.511

Smith SL, Romanovsky VE, Lewkowicz AG, Burn CR, Allard M, Clow GD, Yoshikawa K, Throop J, 2010. Thermal state of permafrost in North America: A contribution to the international polar year. *Permafrost and Periglacial Processes* **21**(2):117–135. doi: 10.1002/ppp.690

Walvoord MA, Kurylyk BL, 2016. Hydrologic impacts of thawing permafrost - a review. *Vadose Zone Journal* **15**(6):1–20. doi: 10.2136/vzj2016.01.0010

Williams TJ, Pomeroy JW, Janowicz JR, Carey SK, Rasouli K, Quinton WL, 2015. A

radiative-conductive-convective approach to calculate thaw season ground surface temperatures for modelling frost table dynamics. *Hydrological Processes* **29**(18):3954–3965. doi: 10.1002/hyp.10573

Wright N, Hayashi M, Quinton WL, 2009. Spatial and temporal variations in active layer thawing and their implication on runoff generation in peat-covered permafrost terrain. *Water Resources Research* **45**(5):1–13. doi: 10.1029/2008WR006880

Zhang T, Barry RG, Knowles K, Heginbottom JA, Brown J, 1999. Statistics and characteristics of permafrost and ground-ice distribution in the northern hemisphere. *Polar Geography* **23**(2):132–154

Zhang T, Barry RG, Knowles K, Ling F, Armstrong RL, 2003. Distribution of seasonally and perennially frozen ground in the Northern Hemisphere. *Permafrost* pp. 1289–1294

Zhang X, Vincent LA, Hogg WD, Niitsoo A, 2000. Temperature and precipitation trends in Canada during the 20th century. *Atmosphere - Ocean* **38**(3):395–429. doi: 10.1080/07055900.2000.9649654

Zhang Y, Chen W, Cihlar J, 2003. A process-based model for quantifying the impact of climate change on permafrost thermal regimes. *Journal of Geophysical Research* **108**:4695. doi: 10.1029/2002JD003354

Zhang Y, Carey SK, Quinton WL, Janowicz JR, Pomeroy JW, Flerchinger GN, 2010. Comparison of algorithms and parameterisations for infiltration into organic-covered permafrost soils. *Hydrology and Earth System Science* **14**(5):729–750. doi: 10.5194/hess-14-729-2010

Zhang Y, Chen W, Riseborough DW, 2008. Disequilibrium response of permafrost thaw to climate warming in Canada over 1850-2100. *Geophysical Research Letters* **35**(2):2–5. doi: 10.1029/2007GL032117

Appendices

Table A1: An example of the measurements and calculation used to determine the rate of talik and talik-free permafrost table deepening. This was completed for three talik and three non-talik locations.

Time [days]	Permafrost Table Depth -No Talik- [masl]	Rate of Permafrost Table Deepening -No Talik- [m/day]	Permafrost Table Depth -Talik- [masl]	Rate of Permafrost Table Deepening -Talik- [m/day]
31	268.10		268.30	
273	268.00	0.0004	267.90	0.0017
578	267.90	0.0003	267.50	0.0013
912	267.80	0.0003	267.30	0.0006
1277	267.80	0.0000	267.20	0.0003
1642	267.80	0.0000	267.10	0.0003
2008	268.00	-0.0005	267.00	0.0003
2373	268.00	0.0000	267.00	0.0000
2738	267.90	0.0003	267.20	-0.0005
3103	267.90	0.0000	267.00	0.0005
3469	268.00	-0.0003	266.80	0.0005
3834	267.90	0.0003	266.80	0.0000
4200	267.90	0.0000	266.75	0.0001
4565	267.80	0.0003	266.60	0.0004
4931	268.00	-0.0005	266.60	0.0000
5296	268.00	0.0000	266.50	0.0003
5661	268.00	0.0000	266.50	0.0000
6026	267.80	0.0005	266.50	0.0000
6391	267.80	0.0000	266.40	0.0003
6756	267.60	0.0005	266.30	0.0003
7121	267.30	0.0008	266.10	0.0005
7486	267.30	0.0000	266.00	0.0003
7852	267.20	0.0003	265.80	0.0005
8217	267.20	0.0000	265.80	0.0000
8582	267.60	-0.0011	265.70	0.0003
8947	267.50	0.0003	265.70	0.0000
Average:		0.0001		0.0003

Table A2: An example of the measurements and calculation used to determine the rate of horizontal permafrost thinning on the bog and fen side of the plateau. This was completed for three fen side and two bog side locations.

Time [days]	Permafrost Edge Relative Location -Fen Side- [m]	Rate of Permafrost Edge Retreat -Fen Side- [m/day]	Permafrost Edge Relative Location -Bog Side- [m]	Rate of Permafrost Edge Retreat -Bog Side- [m/day]
0	0.00		0.00	
31	0.00	0.0000	0.20	0.0065
273	0.75	0.0031	0.50	0.0012
578	1.50	0.0025	1.00	0.0016
912	3.75	0.0067	1.50	0.0015
1277	4.20	0.0012	2.00	0.0014
1642	5.00	0.0022	2.20	0.0005
2008	5.60	0.0016	3.00	0.0022
2373	5.60	0.0000	3.20	0.0005
2738	6.00	0.0011	3.40	0.0005
3103	6.00	0.0000	3.90	0.0014
3469	6.30	0.0008	4.00	0.0003
3834	6.90	0.0016	4.20	0.0005
4200	7.40	0.0014	4.50	0.0008
4565	7.60	0.0005	5.30	0.0022
4931	8.00	0.0011	5.80	0.0014
5296	8.20	0.0005	5.80	0.0000
5661	8.30	0.0003	5.90	0.0003
6026	8.40	0.0003	6.10	0.0005
6391	8.40	0.0000	7.00	0.0025
6756	8.60	0.0005	9.80	0.0077
7121	10.00	0.0038		
Average:		0.0014		0.0017

Curriculum Vitae

Name: Joelle Langford

Post-secondary   Queen's University
Education and   Kingston, Ontario, Canada
Degrees: 2010-2014 B.Sc.

Related Work   Teaching Assistant
Experience   The University of Western Ontario
2015-2017.

Geotechnical / Hydrogeological Summer Student
EXP Services
2014-2016

Geologist in Training
Matrix Solutions
2018-Current